Appendix A DSC – SRO – 01 The characterization and environments of exoplanet hosts

(Final draft in progress)

A.1 Abstract

MSE will provide spectroscopic characterization at high resolution (R ~ 40000) and high SNR (~100) of the faint end of the PLATO target distribution (m_V ~ 16), for statistical analysis of the properties of planet-hosting stars as a function of stellar and chemical parameters. MSE is able to cover the full ~three-quarters of the PLATO sky (~15000 square degrees) accessible from Maunakea in less than 800 hours. Such a survey will provide homogeneous spectral typing, metallicity estimates and chemical abundances for all PLATO targets at the faint end. Such information will otherwise remain unavailable for most of this important sample. With high velocity accuracy (~100ms^{-1}) and stability, MSE will conduct a monitoring campaign of ~100 square degrees in the PLATO footprint, potentially in the northern long-duration field. This time domain spectroscopic program will directly measure binary fractions away from the Solar Neighbourhood and will allow for a well characterized statistical studies of the prevalence of stellar multiplicity into the regime of hot Jupiters. Such information is important to understand the physical mechanisms governing stellar multiplicity, planet migration and their dependence on host star properties.

DRAFT

A.2 Science Justification

A.3 Key astrophysical observables

A.4 Target selection

A.5 Cadence and temporal characteristics

A.6 Calibration requirements

A.7 Data processing requirements

A.8 Any other issues

Appendix B DSC – SRO – 02 Rare stellar types and the multi-object time-domain

Authors: Kim Venn

B.1 Abstract

The role of MSE for stellar astrophysics is based on three distinct attributes: first, in the collection of spectra for stellar samples of unprecedented size, depth and resolution; second, in the spectral monitoring of time variable sources; third, in accessing stellar populations belonging to Galactic components that are difficult to access with current spectroscopic instruments due to limited aperture and multiplexing. The sheer increase in sample size will create countless opportunities for – and will motivate original science questions in – stellar structure, stellar processes, and local environment. The discovery of significant samples of rare objects through blind surveys, e.g., Li-rich stars, C-rich stars, solar twins and solar analogues, peculiar AGB stars, metal-line white dwarfs, or even potentially first star remnants will have a transformative impact in modeling their phenomena, specifically by allowing for population studies that incorporate accurate completeness corrections and which examine their distribution within the Galaxy. This also extends to increasing the sample sizes of objects in nearby dwarf galaxies, where differences in their environments and histories can provide important constraints for stellar nucleosynthesis, e.g. progenitor mass and metallicity dependent yields from AGB and SNe events. Here, we outline a baseline set of programs and analyses that will provide a transformative legacy for MSE in the broad arena of stellar astrophysics.

DRAFT

B.2 Science Justification

Current and planned surveys at 2 – 4m telescopes will target every stellar population in the Galaxy, providing spectra for 10^5 to $>10^6$ stars, at high and medium resolutions, and have the ability to monitor spectral variation. In addition, the Gaia- ESO survey at the VLT 8m facility can observe small fields of view as deeply as MSE, e.g., globular clusters and the Magellanic Clouds. Many scientific studies of the dominant stellar populations will have been carried out, nevertheless the increased statistical sampling of the MSE could open new avenues of investigation in those populations. There will also be stellar populations that are not easily accessible in the previous surveys, thus the MSE wide-field multi-object programs could have a transformational impact on studies of stars in the outer halo field, the outer disk, and/or the faintest objects in the Bulge. MSE will also have the unique ability to spectroscopically monitor time variable objects, and to support large imaging and possibly astroseismic surveys. We summarize these science cases in this SRO.

The dominant stellar populations that will be observed in significant numbers by the ongoing or planned surveys include those in the Galactic disks, bulge, inner halo, star clusters, and nearby dwarf galaxies. While the MSE will cover nearly a quarter of the Galactic volume and survey ~5 million stars, increasing the sample sizes of these dominant stellar populations could open opportunities for and original science questions related to stellar structure, stellar processes, and/or local environment. Furthermore the discovery of new examples of rare objects through blind surveys, e.g., Li-rich stars, C-rich stars, solar twins and solar analogues, peculiar AGB stars, metal-line white dwarfs, or even potentially first star remnants (e.g., Rameriz et al. 2010, Liu et

al. 2014, Carollo et al. 2014, Datson et al. 2014, Venn et al. 2014, Koester et al. 2014, Aoki et al. 2014) can have a transformative impact in modeling their phenomena. This extends to increasing the sample sizes of objects in the nearby dwarf galaxies, where differences in their environments and histories can provide important constraints for stellar nucleosynthesis, e.g. progenitor mass and metallicity dependent yields from AGB and SN events (e.g., Shetrone et al. 2003, Venn et al. 2004, Herwig 2005, Heger & Woosley 2010, Nomoto et al. 2013, Frebel et al. 2014, Schneider et al. 2014).

The stellar populations that will be difficult to access in the previous spectroscopic surveys include those in the outer halo, outer disk, and faint stars in the bulge. The MSE high resolution (HR, R > 20,000) spectroscopic modes can provide high precision in stellar parameters, radial velocities, rotational velocities, chemical abundances, and isotopic ratios, which are often needed for detailed stellar modeling and observational testing. *In the outer halo*, HR spectra of unique stars (e.g., chemically peculiar stars, remnants of first stars, RR Lyrae stars, and halo dwarfs) could provide new information for stellar nucleosynthetic yields, stellar pulsation theory, and ages for halo white dwarfs (e.g., Ivans et al. 2003, Aoki et al. 2013, 2014, Yong et al. 2013, Cohen et al. 2013, Drake et al. 2013, Kilic et al. 2005, Kalirai 2012). *In the outer disk*, young metal-poor stars found in star forming regions can be compared to the typical outer disk field stars, providing valuable information on the outer disk star formation environment (e.g., Friel et al. 2010, Frinchaboy et al. 2013, Carrero et al. 2015). *In the Galactic bulge*, stars tend to be more metal-rich than in the solar neighbourhood and likely to have formed early, thus HR spectroscopy of the faint stars (dwarfs, and those in high extinction regions) could provide unique constraints for stellar nucleosynthesis, stellar interiors, and stellar atmospheres at higher metallicities, in higher density environments, and with unique chemical compositions (e.g., Fulbright et al. 2006, 2007, Bensby et al. 2010, 2011, Garcia Perez et al. 2013, Johnson et al. 2014). These populations are present in DSC-SRO-03 on Galactic Archaeology, but we include them here as well to highlight that HR observations would also impact Stellar Astrophysics.

DRAFT

Repeat observations in a spectroscopic survey can also be used to detect time variability phenomena. The ongoing and planned spectroscopic surveys already have this ability, though only the SDSS-APOGEE survey appears to use multiple observations to reach their SNR requirements, and have spaced those to also enable the search for variability (e.g., Deshpande et al. 2013). Nevertheless, the timing for MSE could make it unique if it is used to support the planned large photometric, asteroseismic, and other survey projects. In an era of large imaging surveys (e.g., Pan-STARRS, DEC, Skymapper, and Euclid), transit/asteroseimology/variability programs (e.g., LSST, TESS, and PLATO), and the Gaia proper motion survey, then all-sky spectroscopy provides radial velocities for full 6D phase space, accurate temperatures and metallicities for exoplanet hosts, and simple follow-up on new objects. With some thought to the cadence of the MSE observations, then it could play an important *supportive* role in time domain stellar spectroscopy. Spectral monitoring of transients, transit-selected planetary host candidates, binary stars, pulsating and/or eclipsing variables, and also supernovae, could all lead to transformational science in Stellar Astrophysics.

B.3 Key astrophysical observables

B.3.1 Survey components

B.3.2 Measureable quantities

The key measurements for studying stellar astrophysics are well-defined spectral line features for accurate stellar parameter (temperature, gravity, metallicity, rotational velocities, magnetic fields strengths, etc.) chemical abundances, and radial velocities or transient events. Therefore, most stellar astrophysics science requires high- resolution spectroscopy for precise determinations (except in the case of white dwarfs where pressure broadening makes R > 2000 unnecessary). SNR and wavelength range can also play important roles. These are described further here:

- *Resolution and SNR*: High-resolution work is necessary to deblend critical atomic lines, determine precision rotational and radial velocities, and calculate accurate chemical abundances. At R=20,000 (R=40,000), synthetic spectra show that lines are deblended at ~0.2 A (0.1 A), rotational and radial velocities to better than ~0.2 km/s (0.1 km/s) through cross-correlation of many lines (>100), and chemical abundances with Δ log(X/Fe) < 0.15 dex (0.1 dex), when SNR > 30. This precision is necessary for most science cases that involve detailed stellar studies (e.g., Tolstoy et al. 2009, Carretta et al. 2009, Hunter et al. 2009, Brandt & Huang 2015). As an independent example, the CFHT/GYES document also showed that R = 20 000 yields [Fe/H], [alpha/Fe], and 5 – 10 additional elements, whereas R > 40 000 provides higher precision and more chemical elements (Bonifacio et al. 2010). A higher-resolution mode is used for analyses of neutron capture elements (where deblending the few available lines is more critical), and in more metal-rich stars and cool stars where blending is an increasing problem. This could be important in studying exoplanet hosts, which tend to be cooler, metal-rich stars (Buchhave et al. 2012, 2014, Rameriz et al. 2014, Wang & Fischer 2015). This high precision is also useful when studying the radial velocities of binary stars, and subsequently determining orbits and masses.
- *Wavelength range*: Most stellar spectroscopy has been carried out from 390 – 900 nm due to atmospheric throughput and the sensitivity of the available detectors (from photographic film to CCDs). Therefore, most stellar astrophysics, including stellar atmospheric models and precision atomic data, has been developed for this wavelength range. Pushing to bluer wavelengths has opened new science cases e.g., neutron-capture elements (Os, Dy, Er, U, Th) for cosmochronology, and Be and OH lines for studies of stellar evolution, all of which occur between 310 – 390 nm (Hill et al. 2002, Francois et al. 2007, Boesgaard et al. 2011, Roederer et al. 2012, Pasquini et al. 2014). Pushing to near-IR wavelengths has recently been improved by the APOGEE survey (1.5 – 1.7 microns), where atomic data and stellar models can now provide precision abundances for OH, CH, CO, CN bands, as well as new spectral lines of common elements (Meszaros et al. 2012, Smith et al. 2013, Lamb et al. 2015). Additional spectral lines always improve precision by reducing random errors and permitting new investigations of systematic errors. A preference would be to push towards bluer

DRAFT

wavelengths (≤ 370 nm) for more neutron-capture elements.

- *Wavelength stability*: Only time domain spectroscopy requires exquisite wavelength stability. The current gold standard is the ESO HARPS spectrograph, which has provided ~1 m/s radial velocity precision for nearly a decade. It uses two 1" fibers (object + sky or ThAr), feeding an optical spectrograph (378 – 691 nm) contained in a vacuum vessel to avoid spectral drift due to temperature or air pressure variations. While the HARPS resolution (R=115 000) is much higher than that considered for MSE, mechanical stability at any resolution is a benefit in stellar multiplicity, variability, and exoplanetary system research.

B.4 Target selection

Target selection for an all-sky survey naturally benefits from broad-band imaging surveys. In the next decade, several (some public) imaging surveys are planned: Pan-STARRS, DEC, Skymapper, LSST and Euclid. All of these have multi-wavelength photometry, permitting initial estimates at stellar parameters, and some have multiple-epoch observing for selecting transients, binary stars, pulsating stars, etc., and with a priori light curves. The limiting magnitudes (e.g., V ~ 24 in Pan-STARRS) in all are below those necessary for target selection for spectroscopy (V ~ 19, for SNR > 30), and the photometric precision does not need to be extremely accurate for target selection (e.g., ΔV ~ 0.01 as in Pan-STARRS is excellent). Even the Gaia limiting magnitude (g~20) is within reach of the MSE high-resolution survey, if lower SNR is acceptable. The 2MASS and WISE satellite databases are also useful resources for longer-wavelength photometry of brighter stellar sources (e.g., 2MASS includes over 250 million point sources with high SNR and H≤15). U-band photometry will be available after *Luau* (CFHT large program, granted in 2014, P.I.s McConnachie & Ibata) before MSE becomes available, helping to identify hot and metal-poor stars. Narrow band photometry (e.g., CFHT CaH&K filter photometry through the *Pristine* program, granted time in 2015, P.I. Starkenburg) can also help fine-tuned target selection for metal-poor stars.

DRAFT

B.5 Cadence and temporal characteristics

The MSE all-sky survey will likely require multiple 1 hour exposures of individual targets to reach the SNR requirements, therefore if we consider the observing cadence of these observations then it may be possible to use these spectra to search for and characterize variability. The specific cadence is not currently clear though, e.g., RR Lyrae variables have periods < 1 day, Cepheid periods range from weeks to years, giant planet orbits are typically weeks to years as well, and CEMP-s stars have orbital periods that are approximately a year (Lucatello et al. 2005), thus, the specific time frame cannot be determined without knowing the science case. On the other hand, if fields are to be re-observed over 1 – 2 years, then planning multiple observations with *log*(time) displacements is one way to avoid aliasing period determinations. As one example, the SDSS/MARVELS program uses a baseline cadence of 33 visits over 18 months; 15 visits are concentrated within a two-month period to resolve short period variations, 5 more observations are spread over the first year, and two observation per month in the second year to resolve longer periods, phases, and amplitudes (Ge et al. 2008, Lee et al. 2011). Serendipitous discoveries of variable stars (binaries and stellar multiplicity, pulsating stars, eclipsing, and

eruptive stars) are expected, possibly even in the 100s per night from the LSST survey alone (after its first year where much higher rates are expected, Ridgway et al. 2014). Other time-critical observations, such as transients, are best served as PI science programs.

B.6 Calibration requirements

With observations of ~5 million stars, then standardized data taking and data reduction will be necessary of the spectra, including wavelength calibrations, flat fielding, and sky subtraction. Flux calibrations for detailed spectral energy distributions are not essential, however spectra of several rapidly rotating hot stars taken at a variety of air masses each night will be necessary to remove telluric features. In terms of the data reduction and calibration requirements, there are no significant differences between the MSE stellar spectra and other current and planned spectroscopic surveys at the 2 – 4m telescopes or the Gaia-ESO survey. Those surveys are currently developing exquisite data reduction tools and pipelines (e.g., Sacco et al. 2014), and therefore the MSE should adopt these and/or similar tools for its high-resolution stellar spectra reductions.

B.7 Data processing requirements

Starting from 1-dimensional, reduced and sky-subtracted spectra (discussed above), then it is necessary to identify and measure spectral lines. This stage can be improved by line fitting software (e.g., DAOSpec, Stetson & Pancino 2008) and curated line lists (e.g., VALD, Heiter et al. 2008). Data analysis that involves stellar parameters and chemical abundances then requires some sort of model atmospheres analysis. The ongoing and planned spectroscopic surveys currently use grids of stellar spectra for a χ^2-fitting or more sophisticated fitting algorithms (e.g., Lee et al. 2011, Allende Prieto et al. 2015; also, principle components analysis by Ting et al. 2012, optimized pattern recognition by Kordopatis et al. 2011, etc.). This is sufficient for the vast majority of stellar observations, however the results are limited by the grid edges and available calibrations. Further data analysis tools would be helpful for Stellar Astrophysics, e.g., simultaneous errors analysis, co- addition of repeated spectral observations or tools for basic variability analyses. Cross-listing the stellar spectral results with other surveys, such as the large imaging and photometry surveys or the GAIA proper motions, could provide quick kinematic information for targets, or lead to preliminary light curves for variables. The analysis of stellar spectra can be easily misled within a simplified pipeline and grid analysis, e.g., for chemically peculiar stars not represented in the grid or emission line objects, thus raw data, science grade reduced data, and pipeline products would all be desirable.

DRAFT

B.8 Any other issues

None

Appendix C DSC – SRO – 03 Milky Way archaeology and *in situ* chemical tagging of the outer Galaxy

Authors: Carine Babusiaux

C.1 Abstract

MSE will carry out the ultimate spectroscopic follow up of the Gaia mission. No other planned or proposed survey will be able to chemical tag stars at the outskirts of the Milky Way and down to the faintest Gaia stars. Our view of the Milky Way will be completely revisited imminently with the first release of the Gaia data. MSE is designed to have all the key elements to be the essential spectroscopic tool for Galactic Archaeology in the post-Gaia area, able to probe the Galaxy through chemical and dynamical studies of individual stars across all Galactic components at all radii in the Galaxy, and through absorption line studies of the intervening interstellar medium. We highlight here the main questions that we currently know MSE will uniquely be able to answer as well as the essential elements for its implementation. This includes extensive discussion of trades between spectral resolution and wavelength coverage to maximize MSE's utility to efficiently probe chemical space.

C.2 Science Justification

DRAFT

C.2.1 The Interstellar Medium

MSE will be the only instrument able to observe at high resolution millions of objects with known distance, allowing an outstanding step forward in the knowledge of the galactic ISM.

Note that ANY spectral observation of Galactic and extragalactic targets contains information on the GISM through the absorption features that are imprinted by intervening matter and through the reddening (or differential absorption). On the other hand, specific observations and surveys can be conducted with MSE to make unprecedented progresses in GISM mapping and understanding.

C.2.1.2 The third dimension to the Galactic ISM

Paradoxically the Milky Way ISM is extremely well mapped in 2D at many wavelengths but extremely poorly mapped in 3D due to the absence of information on the distance to the inter-stellar matter generating the emission. MSE can bring the distancelimited observations required to produce realistic 3D density and velocity distributions of the GISM, gas and dust. Such a construction will make full profit of the foreseen Gaia parallax measurements. Those maps will be an invaluable general tool in many fields (radiation and particle propagation, foreground, background, environment identification...).

C.2.1.3 Potential carriers of the Diffuse Interstellar Bands (DIBs)

Through measurements and distance and ISM-phase assignment of the hundreds of diffuse bands detectable in the optical, MSE will bring new constraints on the species that are

responsible for the DIBs and their conditions of formation.

C.2.1.4 The multi-phase structure of the Galactic ISM

Accessing absorption by different tracers will give the tools to model the physical, dynamical and chemical properties of the molecular, diffuse and ionized GISM phases and their space distributions in relation with stellar winds and SNR hot cavities, allowing to understand the interplay between the phases, and the role of radiation, energetic particles, magnetic field, etc.

C.2.1.5 The ISM history in relation with the stellar history

The detailed structure of the ISM will be compared for the first time with a detailed Galactic archaeology information also provided by MSE, allowing to better understand the stellar formation- ISM feedback mechanisms and the combined star-ISM evolutionary processes in all regions of the Milky Way, including bulge, halo and thin-thick disk.

C.2.2 The Stellar Halo

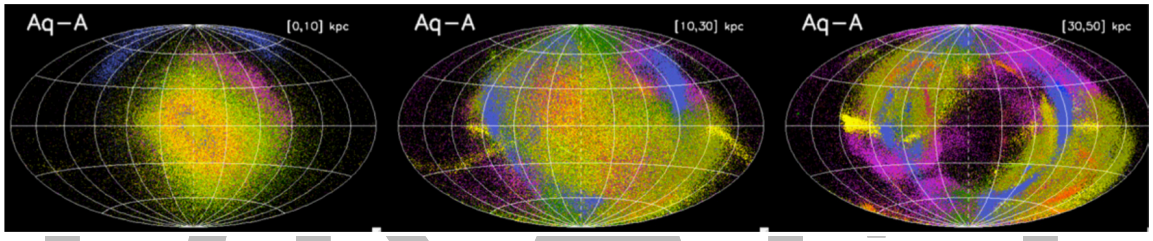

Figure 1: Fig 1 of Helmi et al. (2011): Distribution of field RGB stars on the sky at various distances from the Sun for the stellar halo of the simulation Aq-A. The different colours correspond to stars originating in different progenitors. According to those simulations, the different progenitors cannot be distinguished between 10 and 30 kpc in photometric surveys. Velocities and chemical abundances are needed.

Within the Λ Cold Dark Matter (ΛCDM) framework, stellar haloes around galaxies formed by disrupted satellite galaxies are a natural outcome of the hierarchical build-up of structures. Observationally, there is evidence that the Milky Ways stellar halo contains plenty of substructure. There are also evidences for different formation mechanisms to be at play in the stellar halo of the Milky Way, with an inner and outer component having significantly different structure, metallicity and kinematic properties (e.g. Carollo et al. 2007). Kinematics and chemistry of the Galactic halo up to its virial radius will provide us with strong constraints on the formation and evolution of our Galaxy.

C.2.2.1 The outer halo

Chemical-tagging of local halo stars has shown that very low metallicities halo stars are compatible with having been assembled out of disrupted systems like the classical dSphs and the UFDs, while the more metal-rich halo stars needs to have formed in an environment with higher initial SFR (e.g. Tolstoy et al. (2009), Nissen & Schuster (2010)). But chemical properties of local halo stars that pass near the Sun are not necessarily representative of the whole of the

halo. Moreover high resolution spectroscopy of a large statistics of widely spread halo stars will allow to chemically tag individual accreted progenitors and study in detail their kinematic footprint and spatial spread, allowing us to recover their accretion history. Observing the halo requires a wide field of view. The planned halo surveys on 4-m telescopes will start a first exploration of the in-situ halo, but they cannot reach beyond 50 kpc. MSE will therefore be the only instrument available allowing to explore the chemical abundances of halo red giant branch stars all the way to the MW virial radius.

C.2.2.2 In-situ versus accreted stars in the inner halo

At large distances, the mixing time-scales for Galactic fragments are long, and today, the ancient substructure can be discernible with all-sky surveys as spatial over-densities. However the inner halo (within 10-30 kpc) is better mixed (see Fig. 1): the fraction locked in spatially coherent over-densities (within 40 kpc) does not exceed 20% (Deason et al. 2011). Additional phase- space measurements and chemical abundances are therefore needed to untangle the remnants of old accretion events. For this one needs a large portion of the sky to be probed and enough stars of each progenitor to statistically detect it. MSE is the perfect instrument for this: at 10 kpc, MSE will be able to chemically tag halo dwarfs which are much more numerous than the giants currently targeted (at lower resolution) by 4-m surveys. MSE will therefore not only be able to definitely quantify the portion of halo in-situ stars versus accreted ones but also measure potential gradient in the in-situ population and record the chemical imprint of the accreted progenitor formation history.

DRAFT

C.2.2.3 The first stars

The unprecedented size and quality of the stellar spectroscopic dataset of MSE will enable a detailed analysis of the metal-weak tail of the halo metallicity distribution function (MDF). This key observable has a direct bearing on models for the formation of the first stars, and on the dark baryonic content of galaxies. The first stars to be formed after the Big Bang were formed with the primordial chemical composition: i.e., hydrogen and helium, plus traces of lithium. A protogalactic cloud consisting of such a gas may have had difficulty in providing cooling mechanisms efficient enough to allow the formation of low-mass stars. Several theories on star formation postulate the existence of a critical metallicity below which only extremely massive stars can form. Other theories invoke fragmentation to produce low-mass stars at any metallicity. The implication for the baryonic content of galaxies is direct: if the first generation of massive stars that reionized the universe formed along with low-mass stars, a large fraction of these would now be present as old, cool white dwarfs. On the other hand, a small fraction of these (essentially those of mass less than 0.8 $M_{\odot}$) would still shining today and could be observed. If there is a critical metallicity, then the metal-weak tail of the MDF ought to show a sharp drop at this value. For very metal-poor stars, the metallicity must be determined from high-resolution spectra since the metallic lines become too weak. MSE Galactic Archaeology Survey would represent close to the final word on this key issue. If ultra-metal-poor halo stars do indeed exist, then this extraordinary dataset would allow a complete characterization of the halo MDF down to [Fe/H]~-7.

C.2.3 The Galactic Disk

C.2.3.1 Detailed chemical tagging

In order to follow the sequence of events involved in the formation of the Galactic disk, the ancient individual star-forming aggregates need to be re-assembled. Since the disk formed dissipatively and evolved dynamically, much of the dynamical information is lost. However, locked away within the stars, the chemical information survives the disks dissipative history. The aim of chemical tagging is to re-construct ancient star-forming aggregates and see how they were spread in galactocentric radius by radial migrations. The fact that stars are born in aggregates numbering hundreds to thousands of stars is supported by many observations and theoretical hydrodynamical simulations. First test of chemical tagging has been made on old open clusters which survived dispersion and are therefore ideal probes for testing the historic conditions within a cluster (De Silva et al. 2009). The GALAH survey will develop and extensively test chemical tagging techniques. MSE thanks to its high resolution is the only planned instrument able to expand chemical tagging down to the faintest Gaia stars and up to the end of the Galactic disc.

C.2.3.2 The outer disk

In the last years, extragalactic observations have revealed all the complexity of the outer regions of galaxy disks: truncated/anti-truncated surface brightness profiles , breaks in metallicity profiles , U-shaped age profiles , complex SFR . The origin of all these characteristics is still largely debated. They may be the result of dynamical processes, such as radial migration or heating of satellites, or the result of in-situ star formation, and related to the accretion history of the Milky Way. For the Milky Way, its outer regions are still largely unknown.

DRAFT

MSE is the most adapted instrument for this science. 4-m surveys will not be able to reach beyond ~ 10 kpc from the Sun. On the opposite MSE will be able to go beyond the end of the outer disk. It will quantify its boundary and substructures at those distances where one needs spectroscopic parallax as a Gaia complement. It will provide a detailed chemical description of the outer disk, measuring its degree of inhomogeneity and allowing a reconstruction of its accretion history. MSE will also trace a large fraction of the outer disk depth with dwarfs and subgiants leading to the most detailed age study of the outer disk, tracing its formation history and its link with the inner disk one, in particular in view of the inside-out formation scenario and radial migration.

C.2.3.3 The disc dynamics

MSE would be crucial to map the 3 dimensional velocity field beyond the extended solar neighbourhood. A detailed 3 dimensional map of the velocity field contains not only information the the mass distribution of the Galaxy, it also holds the signatures of the ongoing perturbations of the disc, such as the spiral arms or the central bar and their back reaction. It allows to measure the various pattern speeds at play in the Galaxy and the location of their resonances. The large scale structure of the ISM that MSE will provide at the same time (see Section 2.1) can be compared to the map of the potential perturbations to give additional constraints on the

structure and evolution of the disc. In order to gain knowledge on the perturbations, a spatial resolution on each axis of less than ~50 pc is needed on the constructed 3D maps. Such a resolution requires a large number of stars to be observed over large patches on the sky which makes MSE the best suited candidate to achieve such a project.

C.2.4 The Galactic bulge

The inner regions of the Milky Way keep trace of the early phases of formation of the Galaxy, and of its subsequent evolution. The recent progress in the bulge studies are due to the first large scale high-resolution surveys being able to reach bulge giants. However no high resolution survey is able to reach the bulge dwarfs yet and none are planned. Considering the different structures that high resolution high signal to noise data discovered in our solar neighbourhood (e.g. Fig. 2), we can be sure that the discovery power of a large scale high resolution MSE bulge program will be un-precedented. Targeting the bulge dwarfs will enable to have access to the ages and the high-resolution will provide a range of elements produced by nuclear processes that have distinct time-scales and locations (i.e., SN II, SN Ia, AGB stars). In this way, it will be possible to understand the star formation history that occurred before, and during, the formation of the bulge.

The main competitor of MSE for the bulge science case will be MOONS@VLT. MOONS will observe in the near-infrared over a small field of view, and will therefore be particularly efficient for the bulge most crowded and extincted regions. MSE will observe in the optical and will therefore be more limited in distance due to the extinction, but it will stay complementary to Gaia down to its faintest magnitude limit. Observing in the bulge in the optical has some important advantages: there are more chemical elements available, in particular the crucially diagnostic heavy n-capture elements, and it is in particular more adapted to the study of the metal-poor stars. Moreover the resolution of MOONS will be of only 20 000. MSE is therefore be the only planned instrument able to do chemical tagging of the bulge down to the faintest Gaia stars.

DRAFT

C.2.4.1 The bulge star formation history

The bulge is too far to use Gaia astrometry to derive ages in the bulge. For this one relies entirely on spectroscopy. The higher the precision on the atmospheric parameters the higher the precision on the ages, in particular for the old populations. MSE is the only high-resolution spectrograph that can reach the bulge turn-off which is at V~ 20 in Baade's Window and H~ 17.5, therefore too faint for MOONS.

C.2.4.2 Linking the inner galactic substructures to the outer Galaxy

The detailed abundance distribution of the bulge and its outskirts, and its comparison with those obtained for the halo and the disk studies, will enable to quantify the link between them and ultimately the continuity/ discontinuity between these populations. The bulge is highly populated and different populations dominate at different longitude/latitudes. Reconstructing the distribution of its chemistry, kinematics and age profiles therefore requires high statistics over a large area, up to "high" latitudes ($|b| > 10-20^{\circ}$). Isolating substructures and being able to

claim continuity or discontinuity, requires not only high statistics, but also high resolution, high S/N spectra.

C.2.4.3 Searching for primordial populations

It is possible that the bulge contains the remains of the most ancient mergers that shaped the core of our Galaxy. Because stars in the inner most centre of the Milky Way are expected to be kinematically well mixed, only chemical abundances would allow to find their different origins.

We know from the structure and kinematics of the bulge that the Milky Way is a barred system presenting a boxy/peanut shape resulting from a secular evolution of the disk. However there are also indications of the presence of a primordial structure too within the inner galactic regions, but its relative mass and link with the local old structures, which are expected to have their maximum density in the bulge area, are fully open. This is an important unknown, because it would affect our understanding of the early evolution of the inner Galaxy. Stellar kinematics alone cannot answer this question because a small classical bulge is rapidly spun up by the torque of the bar/bulge, and its kinematics become indistinguishable from those of the main bar/bulge itself. We depend on detailed chemical studies for many elements in order to identify the presence of a separate primordial bulge component and distinguish or link it with the structures we know at our solar neighbourhood, in particular the thick disk and the inner halo.

DRAFT

Simulations show that the first stars to have formed in our Galaxy are likely to be found today in the bulge region. They are expected to be in the bulge region but are not part of the bulge itself. They formed in small over-densities in the early universe before the Galaxy itself had formed, and were subsequently accreted by the Galaxy. Medium-resolution surveys are starting to identify population of metal-poor stars in the bulge region with metallicities as low as [Fe/H] = -3. These are candidates for the first stars. Detailed high resolution studies of these stars are needed to determine whether they are chemically different from the stars of the inner halo which are also expected to be found in this region.

C.2.5 Chemical tagging versus Chemical labelling

The outer layers of the star atmospheres, accessible to spectroscopic studies, keep a fair representation of the mixture of elements present in the gas cloud out of which they formed. By determining those element mixtures, it is possible to “tag” stars with similar abundance patterns. Combining those tags with distances, kinematics and age information, it is possible to piece together the history of the Milky Way.

To detect distinct abundance patterns between population, one needs high-resolution high-signal-to-noise spectra. The two distinct abundance patterns of the thin and thick disc as well as the distinction between the high and low-α halo populations have been found using such high quality data. As can be seen from Fig. 2, the differences in the abundance trends of those structures are around 0.1-0.2 dex. Surveys reaching abundances precisions ~ 0.1 dex will be able to “label such structures, e.g. assign to each survey star a probability of belonging to one or the other population and then statistically study their properties. However, to detect new sub-structures, one needs a higher precision. The lower the number of stars in the structure (e.g.

halo streams, cluster dislocation), the higher the precision on the abundances should be to detect them (see Fig. 8).

C.2.6 The ultimate Gaia follow-up

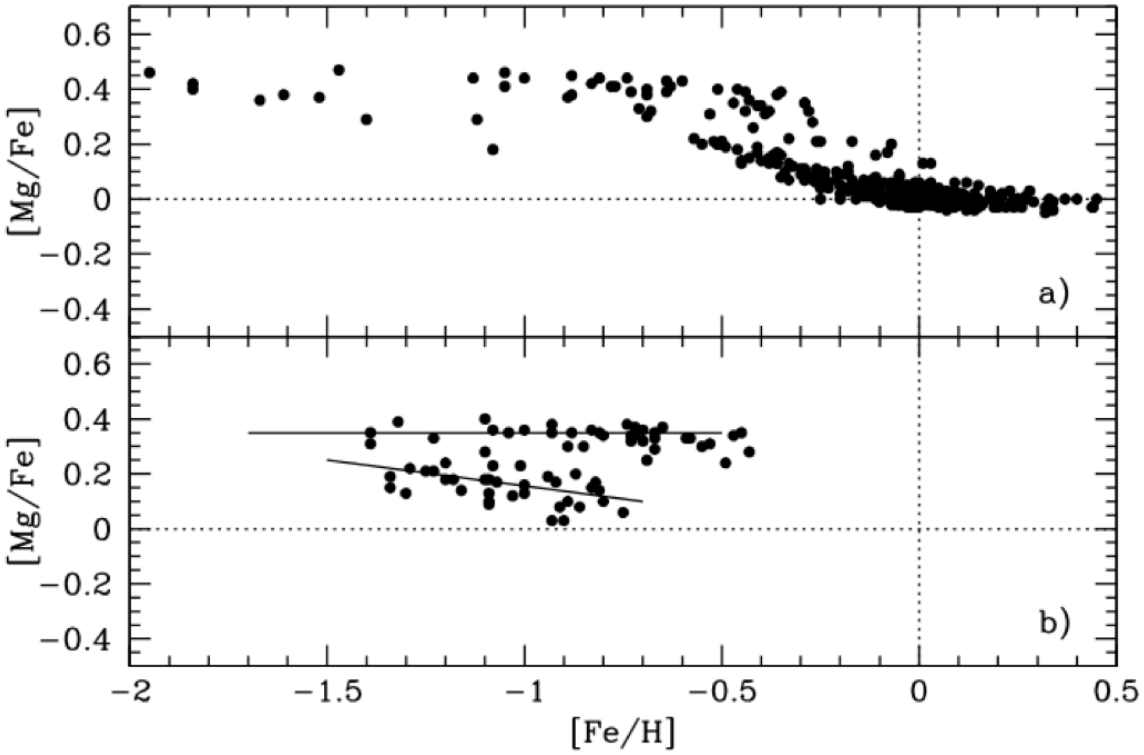

Figure 2: Fig 1 of Lindegren & Feltzing (2013). Fe and Mg abundances for stars in the so- lar neighbourhood. a) Fuhrmann data showing the two distinct thin and thick disc sequences (Fuhrmann 2011). b) the two high and low-α halo star sequences identified by Nissen & Schuster (2010). Those chemically different structures have been found using high SNR, high resolution (R>40,000) spectra. 4-m surveys with R=20,000 will use this knowledge to "tag" those structures according to those findings. The high SNR, high resolution MSE survey will allow to discover new sub-structures.

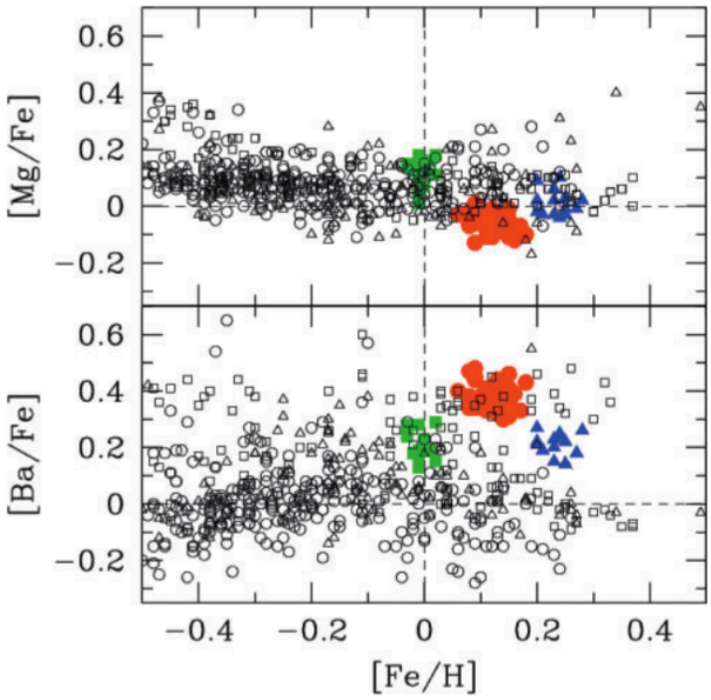

DRAFT

Figure 3: Fig 3 of De Silva et al. (2009). A test of chemical tagging done on the moving group HR1614 (blue triangles) compared to the Hyades (red circles) and the Collinder 261 (green squares) Open Clusters, together with field stars (open black symbols). Note that this study is beyond the reach of R=20,000 surveys.

Our vision of the Milky Way as described above will change in the coming years, in particular in the post-Gaia area in which MSE will start its operation. We may learn that the Galaxy is not an equilibrium figure and that the different components are not that easily separated. Migration/scattering or cataclysmic event (bar onset, merger) has blurred out the different components with cosmic time, at least at some level. This is why we are discussing here about “tagging“ (allowing to distinguish detailed SFH differences and streams) and not just ”labelling“ a finite set of stellar populations.

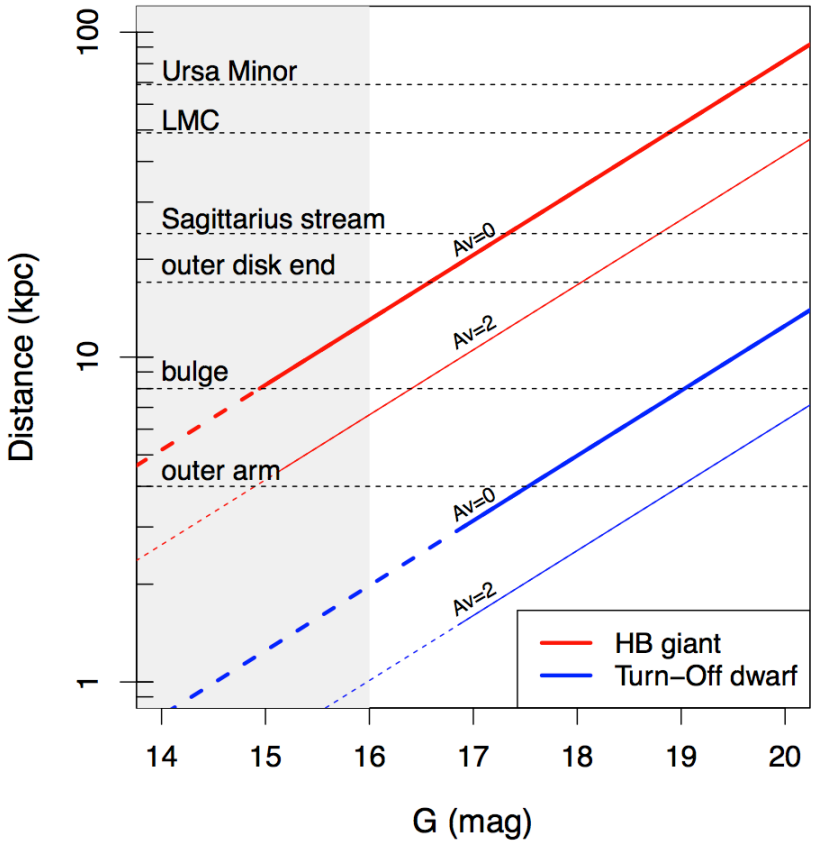

Figure 4: Distances and main galactic structures (and some satellites for illustration) probed by the MSE Galactic Archaeology Survey for two different tracers. The Turn-Off dwarfs (in blue) probe the structure age distribution; cooler (fainter) dwarfs provide the full age and abundances distribution as they did not evolve from the main sequence. The Horizontal Branch giants (in red)probe greater distances and derive the distribution function of the various Milky Way sub- structures, streams and companions. The red giant branch tip stars (not represented here) reach beyond the Milky Way virial radius. The dotted line represent the distance - magnitude range where Gaia parallax accuracies should reach 20%. The solid line therefore need spectroscopic distances from MSE to complement Gaia. The shaded grey area corresponds to the magnitude range covered by the 4-m HR surveys. The extinction shifts the red and blue lines to the right as illustrated with the Av=2 mag presented here.

For all those science cases the observation of a very large number of stars is crucial as we need to dissect the Milky Way along a very wide range of parameters and trace rare objects such as first stars.

MSE is the only instrument planned able to observe in high-resolution millions of the faintest Gaia stars. The scientific outstanding differences between the planned 4-m surveys and MSE just by the increase of the mirror size are highlighted in Fig. 4. An increase in resolution compared to the planned surveys WEAVE/4MOST/MOONS operating at R=20 000 would make the jump of MSE not only in magnitude but also in the parameter space probed by increasing the number of r and s-process elements and allowing accurate spectroscopic age determinations. Going to resolutions even higher than MSE would be interesting in particular for specialised isotopic studies but could be limited to a small number of stars and could even be planned as an upgrade

of MSE (see White Paper & SRO by Aruna Goswami).

MSE will operate after the final release of the Gaia data, during LSST operation, and will be built on the experience of other wide-field spectroscopic surveys. It will therefore have all the ingredients at end to give an answer to all our current and future questions about the composition, formation and evolution of the Milky Way.

De Silva G.M., Freeman K.C., Bland-Hawthorn J., Apr. 2009, PASA, 26, 11
Erspamer D., North P., Feb. 2003, A&A, 398, 1121
Feltzing S., Jun. 2015, ArXiv e-prints
Fuhrmann K., Jul. 2011, MNRAS, 414, 2893
Helmi A., Cooper A.P., White S.D.M., et al., May 2011, ApJ, 733, L7
Lindegren L., Feltzing S., May 2013, A&A, 553, A94
Nissen P.E., Schuster W.J., Feb. 2010, A&A, 511, L10
Smiljanic R., Korn A.J., Bergemann M., et al., Oct. 2014, A&A, 570, A122
Tolstoy E., Hill V., Tosi M., Sep. 2009, ARA&A, 47, 371

C.3 Key astrophysical observables

C.3.1 Key measurement of the source spectrum

Vr, v sin i, Teff, logg, micro-turbulence, [Fe/H], [α/Fe], r and s-process elements (see Fig. 6), ISM absorption lines EW.

DRAFT

As the total wavelength coverage will be limited it is important to ensure that enough gravity and temperature sensitive spectral features are available in the wavelength region, that a maximum of r and s-process elements are present and that metal-poor stars will still have some interesting lines that can be observed. Summary on wavelength coverage trade-off for other surveys can be found in Feltzing (2015) with it's illustrative figure 3 reported in Fig. 5.

A spectral region was selected for the Feasibility Study under the R=20 000 resolution hypothesis (Fig. 6). A new dedicated study is needed to find a new baseline for a shorten wavelength coverage induced by the increase in resolution.

Detailed key measurements for general GISM mapping: In order to build 3D ISM maps with high spatial resolution and at large distance the main measurements are those of the gaseous lines and bands that are easily extracted and allow the best estimate of evolution with distance of the ISM matter. Note that a strict proportionality between the column density of H and the tracer is not required for mapping, what is used is the spatial gradient. For nearby targets, information can be extracted from the "classical" and strong lines: NaI (589.0-589.6nm), CaII (393.4-396.8nm), CaI (422.7nm) for the gas and from the reddening for the dust. The strongest diffuse bands 578.0, 579.7, 628.4, 619.6, 661.4 nm are also the most appropriate. While the strong lines can still be used above the Plane or in directions here clouds are distributed in velocities, weaker lines more appropriate for large optical depths (to avoid saturation) are NaI (330nm doublet) and KI (769.9nm), and the weaker diffuse bands (numerous and distributed above 430 nm).

Detailed key measurements for ISM phase studies: While the ionized and diffuse atomic ISM fraction is best traced in the optical, the molecular and dense atomic phase phase is best traced

when access to the blue is provided. Molecular clouds are detected with CH(430nm), CH+ (423nm) , CN (387nm) and also metallic lines such as TiII (323,324, 338nm), TiI (363nm), FeI (386nm), MnI, NiI, AlI (394nm). Alternatively the molecular phase can be probed with the infrared bands of C2 around 878 nm.

C.3.2 Accuracy of those measurements

V_r < 1 km/s would match Gaia transverse velocity accuracy (see Fig. 17 of the Feasibility Study). This will allow in particular to disentangle velocity substructures at various locations within the Galactic disc to gain access to the physical parameters of the disc and its perturbations. These substructures are typically a few km/s across.

Atmospheric parameters (Teff, logg, micro-turbulence, vsini, [Fe/H]) as accurate and as uncorrelated as possible: those determine the accuracy of the abundances and are used to derive spectroscopic distances and ages. An error of 0.1 dex in logg for a turn-off star leads to a spectroscopic distance error of 10%. An error of 0.1 dex in logg and 100 K in Teff for a turn-off star leads to a spectroscopic age error of 30%.

Concerning the abundances, we want to identify populations separated by less than 0.2 dex (see Fig. 2). We therefore need [X/Fe] < 0.1 dex. The higher the precision, the finest will be the separation between populations on a widest range of metallicity. As a example, Nissen & Schuster (2010) obtained a relative precision of <0.04 dex for [α/Fe] with a resolution R>40000 and SNR>150 on metal-poor dwarfs.

DRAFT

C.3.3 Information extraction

Vr and v sin i by cross-correlation with templates, atmospheric parameters via maximum likelihood with stellar templates, EW measurements.

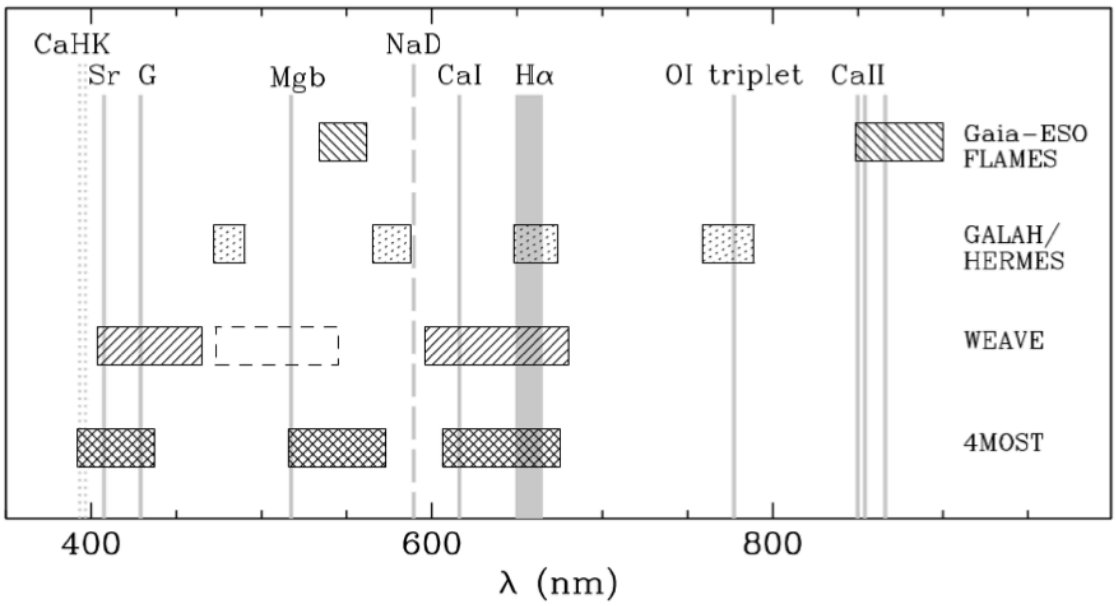

Figure 5: Figure from Feltzing (2015): Wavelength coverage in the optical for a number of current and future survey instruments with high resolving power.

DRAFT

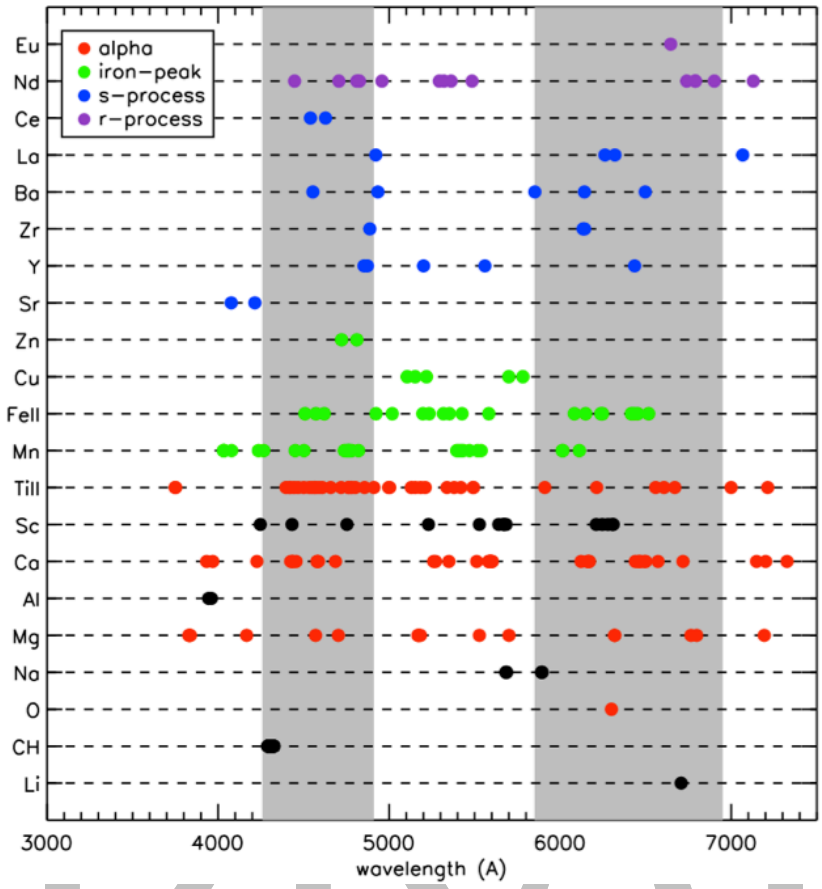

DRAFT

Figure 6: Figure from the Science Feasibility Study. Schematic representation of the spectral diagnostics available for various elements in the Galactic Archaeology Survey. These diagnostics are based on a synthetic metal-poor red giant spectrum; the available diagnostics will of course depend on the exact stellar target. Individual elements have been colour coded according to primary formation route: i.e., alpha, iron-peak, s- and r-process elements. The grey regions show the blue and red windows proposed for the HR mode.

Successful measurement depends on:

- high spectral resolution. Line blending, in particular in metal-rich stars, makes it difficult to perform accurate measurements of weak lines of most of the n-capture elements at R=20000, pushing towards higher resolution. To reach [X/Fe] < 0.1 dex, we actually need R=40000. For the ISM studies, the higher the resolution the better to isolate the ISM lines from the stellar ones and resolve the radial velocities of the different clouds that participate to the global ISM line profile. A resolution R 40,000 has already been proven to allow this disentangling and a cloud-by-cloud analysis.
- high signal-to-noise ratio (>25)
- large wavelength coverage (needed not only to get abundances of several interesting elements but also to have less correlated atmospheric parameters)
- stable wavelength calibration
- good sky absorption / emission removal. Sky emission in particular affects the main lines

of the ISM (e.g. NaI emission). Fibers must be devoted to this in sufficient number to allow a proper treatment. Sky absorption correction can be done through atmospheric transmission modelling that has considerably progressed in the last years.

- multi-epoch measurements to detect binarity

C.4 Target selection

A key point for the target selection of a Galactic Archaeology survey is the homogeneity and reproducibility of its target selection. The target selection should be simple and constant enough through time so that it can be easily reproduced and modelled for a proper study of completeness and target selection bias.

C.4.1 Source of astrometry and photometry

Gaia should be able to provide all targets for high resolution mode of MSE as it will be complete up to G = 20 and will have a magnitude limit G > 20.3.

Other photometric surveys that could be used include Pan-STARRS 3π, Subaru/HSC, LSST, Euclid.

C.4.2 Target luminosity

DRAFT

See discussion below on the trade-off between numerous (faint) stars and brighter stars but with higher resolution and/or SNR. Main targets for the HR survey will be Gaia stars (G < 20) without already available follow-up from 4-m surveys (G > 16).

The highest resolution and SNR is needed for stars for which one can derive accurately their distances to be able to study their origin through their 6D phase-space position. Note that the higher the logg accuracy, the higher the accuracy on spectrometric distances will be. At G = 17 a Gaia turn-off star will have a Gaia parallax accuracy of $\sigma\pi/\pi$ = 20% at 3 kpc. At larger distances, dwarfs will have to rely on spectroscopic distances. Dwarfs and sub-giants for which we can derive age estimates will be primary targets. At G=20 a turn-off star can reach 12.5 kpc (without extinction) allowing to study the outer disk. Standard candles such as stars from the horizontal branch and red giant branch tip can reach the outer parts of the Milky Way (80 kpc at G=20 for horizontal branch stars and 315 kpc for red giant branch tip without extinction). G > 16 is needed to reach the bulge red clump stars in low extinction regions such as Baade's Window. To study the bulge turn-off stars and derive spectroscopic ages, G=20 is needed.

Gaia will provide spectrophotometric estimates of stellar parameters as well as variability information, enabling a detailed (while still simple and uniform) target selection including standard candles.

C.4.3 Source density

See Fig. 7. At G=20 the sky density at the Galactic Poles is around 1500 stars/deg2, meaning largely enough targets to be observed with SNR>20 in less than 1h with 800 fibres according to the Feasibility Study numbers.

The highest density is in the Bulge, with more than 3 million stars/deg2 with G< 20 in Baade's Window so the fibres need to be small to avoid all the fibres to be contaminated by light from other sources. The bulge therefore also needs to be observed with a very good seeing.

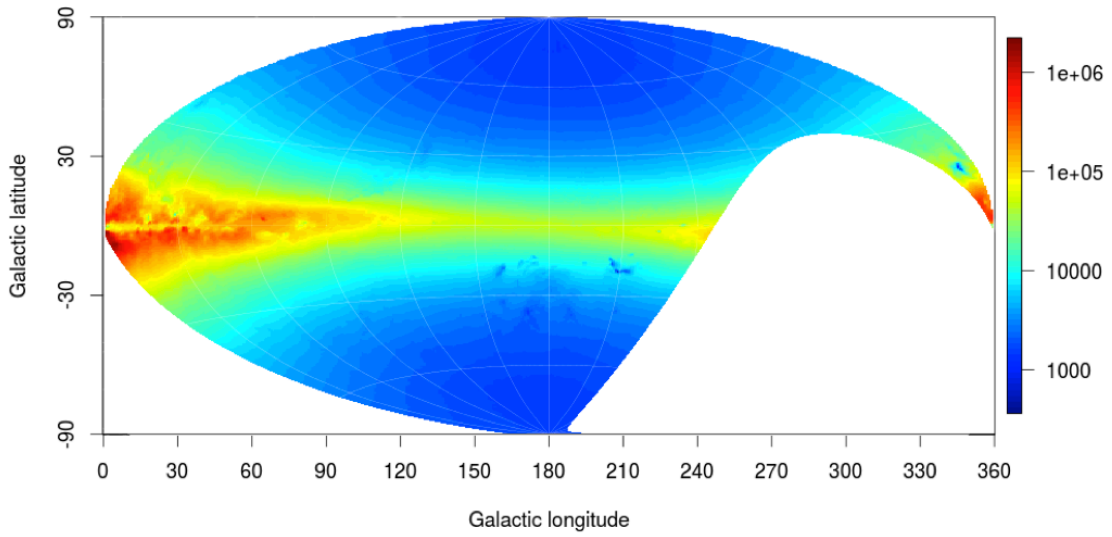

Figure 7: Sky density (per deg2) up to G=20 visible from MSE (δ > −30◦), aitoff projection. Input data credit: Gaia DPAC CU2.

DRAFT

C.4.4 Total number of science targets required

See Lindegren & Feltzing (2013) for a discus- sion of the trade-off between high precision on abundances and high number of stars. According to their model (see also their hypothesis), to distinguish 2 populations separated by 0.1 dex with an accuracy on the abundances of 0.05 dex one needs, as a lower limit, N=3000 stars (Fig. 8). We want here to study different (or not!) populations: thin disc (young and old, inner and outer), thick disc, halo (inner and outer), bulge (primordial and secular). We will want also to study the variations of those populations within the Milky Way (e.g. abundance gradients) to study their formation mechanisms (e.g.. inside-out formation, radial migration...). We therefore want to study various "bins" in 3D position, age, metallicity and velocities. The good news is that those parameters are correlated. But we don't yet understand very well the dynamical state of the Milky Way and therefore what the best 6D phase-space "bins" should be in particular, and those request a very large amount of stars to be probed. Gaia in combination with MSE will make all the difference on this question. We can therefore hope that several million stars should indeed allow to disentangle the main formation scenarios.

C.4.5 Spatial coverage

A large and uniform sky coverage is needed in particular for the detection of halo streams and for a full 3D mapping of the GISM.

C.5 Cadence and temporal characteristics

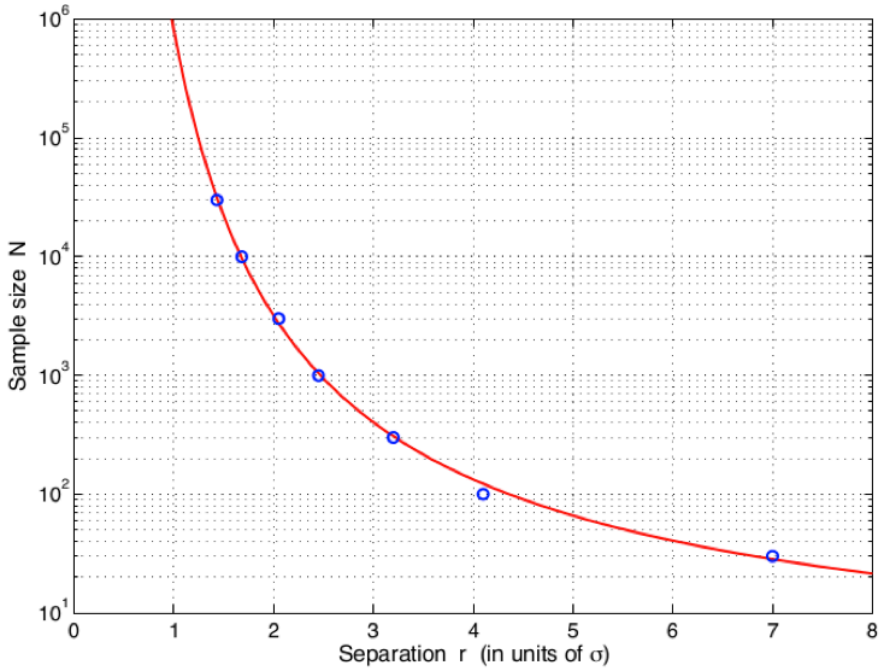

Figure 8: Fig 4 of Lindegren & Feltzing (2013). Minimum sample size needed to distinguish two equal Gaussian populations, as a function of the separation of the population mean in units of the standard deviation of each population.

DRAFT

Repeat observations are required to detect binarity. They also allow observation of variable stars (15' max to accommodate delta scuti stars, which are about half of the variable stars that will be observed by Gaia), to accommodate transient follow-up1 and eventually to observe more bright stars (bright stars need less integration time and could be swapped from one OB to the next). Repeat observations at different epochs also allow a better handling of regions polluted by sky emission and absorption thanks to the variation of its radial velocities versus the target star and its foreground ISM.

Note that binarity detection is not only interesting by itself (see the SRO on stellar astrophysics), but is also needed as their non-detection can bias both the abundances determinations and the radial velocity dispersion. Erspamer & North (2003) tried to estimate the effects on the chemical abundances of a wrong continuum placement due to undetected duplicity and showed for example that for a V sin(i) of 10 km/s the bias can reach 0.1 dex. Concerning radial velocities, the effect of the un-detected binary orbital velocity on top of their systemic velocity can increase by about 9 km/s the velocity dispersion of the population they belong to.

C.6 Calibration Requirements

- Wavelength calibration accuracy and stability: high requirement. Both for multi-epoch observation (needed for multiplicity assessment) and for abundances determined by

differential analysis (see next section).

- Sky subtraction and Telluric absorption model accuracy: high requirement. Reached either with respectively sky and early-type stars observations and/or by sky emission and telluric absorption models
- Flux calibration: not a design driver.

Atmospheric parameters calibration will require observation of calibration stars. In particular a set of stars observed at different resolution modes will be needed to ensure a consistent output. Observations of clusters are very efficient for those kind of calibrations.

C.7 Data processing

1. Wavelength calibration, sky subtraction, telluric absorption model.
2. Spectra normalisation, Vr and V sini measurement, stellar atmosphere parameters determination (the best being those 3 done at the same time by a maximum-likelihood technique).
3. Binarity assessment.
4. EW measures or adjustment of line profile to stellar model: abundances determinations

The very large sample of stars studied by MSE will also allow the usage of large scale differential analysis. Indeed the accuracy of elemental abundances depends on a number of physical effects that are not always well-modelled (NLTE effects, 3D geometry, errors in loggf values...). By focusing on stars with similar stellar parameters, in a well defined logg/Teff region, and adopting a specific analysis method (Smiljanic et al. 2014), differential analysis can be performed and allows to reach very high precision in the separation of populations. It imply that the same type of target selection, observations and data analysis should be performed for high-resolution observations of the Local Group to enable detailed comparison, in particular with dwarf galaxies as potential building blocks of the Milky Way.

DRAFT

C.8 Any other issues

None

Appendix D DSC – SRO – 04 Stream kinematics as probes of the dark matter mass function around the Milky Way

Authors: Rodrigo Ibata, Jo Bovy

A.1 Abstract

As part of an extensive Galactic archaeology mission, MSE will measure the accurate velocities of many thousands of stars in stellar streams distributed throughout the Galactic halo. Stellar streams are dynamically cold features that have been stripped from globular clusters and dwarf galaxies. According to ΛCDM, the Milky Way halo should host many thousands of low-mass dark sub-halos. As these orbit in the Galactic potential, they twist the path of cold stellar structures such as stellar streams and lead to a characteristic pattern of density and velocity perturbations. By mapping the kinematics of a large number of streams, extending over large areas of sky and at a range of radii from the center of the Galaxy, MSE will be able to measure the perturbations caused by dark sub-halos and constrain their mass distribution.

A.2 Science Justification

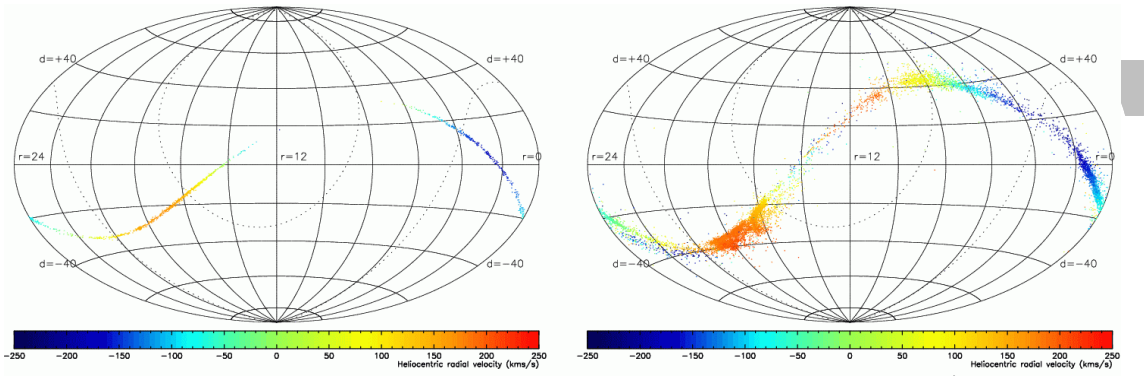

Figure 9: The effect of dark matter halo sub-structures on low-mass star streams (Ibata et al. 2002, MNRAS 332, 915). In a smooth halo (left panel), low-mass stellar streams follow narrow paths on the sky, confined to a narrow range in distance and velocity (shown in colour). In the presence of dark matter substructure (right panel), the potential becomes uneven and the stream path and velocity structure become complex. With Gaia, such studies will now finally be within reach.

Cold dark matter cosmology predicts that galaxies contain hundreds of dark matter sub-structures (Klypin et al., 1999) with masses similar to dwarf satellite galaxies. Only a small fraction of these dark satellites can be identified with the observed population of satellites, however, which raises the question of where the missing satellites are. A large body of theoretical work has demonstrated that it is possible to hide the vast majority of dark matter satellites by having their baryons expelled during the era of reionization (see, e.g., Kravtsov 2010, AdAst 2010, 8, and references therein). However, it remains a fundamental prediction of ΛCDM theory that the dark matter clumps exist in large numbers. Possibly the best means to test this prediction is to examine the dynamical influence of such structures directly in nearby galaxies where we possess the richest datasets. Indeed, Ibata et al. (2002, MNRAS 332, 915) and

Johnston et al. (2002, ApJ 570, 656) demonstrated that massive dark satellites can strongly perturb fragile structures such as stellar streams. The halo substructures change the host galaxy from a smooth force-field in the absence of CMD lumps (left hand panel of Figure 9) into a "choppy sea" where the stream and its progenitor are tossed hither and thither (right hand panel of Figure 9). The effect of this is that the stream path becomes twisted, which leads to density variations along the stream (Siegal-Gaskins & Valluri 2008, ApJ 681, 40; Yoon et al. 2011, ApJ 731, 58; Carlberg 2012, ApJ 748, 20), kinks in the stream track (Erkal & Belokurov 2015, MNRAS 450, 1136), and accompanying dynamical heating (Ibata et al. 2002, Carlberg 2009, ApJL 705, L223). Measurements of this effect allow the mass spectrum of the population of M <~ 10^8 Msun subhalos to be determined.

The globular cluster stream of highest contrast that is currently known is that of Palomar 5, which is a structure that can be seen directly in SDSS star-count maps of blue point sources (see Figure 10). Another good target is the GD-1 stream (Grillmair & Dionatos 2006, ApJ 643, L17), a long, thin stream in the northern hemisphere. However, even for these most favourable of objects, only a handful of stars in the streams are bright enough to be detectable by Gaia (their main sequence turnoffs lie at g=20.2 and g=18.5, respectively). Thus it is very unlikely that with Gaia alone we will be able to detect many distant halo streams and examine their kinematics in enough detail to detect the presence of dark-matter subhalos. Clearly this is also beyond the capabilities of surveys undertaken on 4m-class telescopes.

DRAFT

However, MSE will allow us to solve this problem. New stellar streams may be found directly in large MSE spectroscopic surveys, or indeed by following up candidate structures found for instance with Euclid or LSST photometry. As with Palomar 5 and GD-1, it is likely that (post-facto) a few giant-branch members can be associated to Gaia stars with proper motion measurements, which would provide an accurate (approximate) orbit for the detected stream.

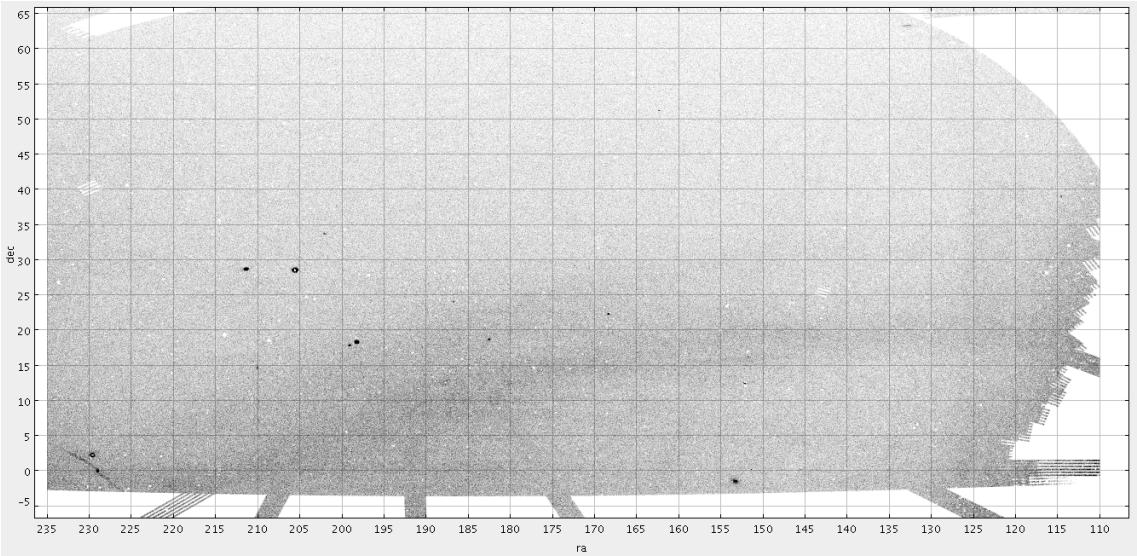

Figure 10: Main sequence turn-off stars with 0.1<g-r<0.4 in the North Galactic Cap, observed by the SDSS. The highest contrast stream here is that of Palomar 5, seen in the bottom left-hand corner.

Simulations in the presence of a large population of expected CDM mini-halos show that there will be localised heating of the globular cluster stream stars by typically a factor of two over and above the intrinsic velocity dispersion of the stream (which in the case of Palomar 5 is about 2 km/s, Kuzma et al. 2015, MNRAS 446, 3297) and changes in the mean velocity along the stream of up to 10 km/s (Carlberg et al. 2015, ApJ 808, 15) due to encounters with the larger dark structures. The spatial scale over which the increased dispersion will be present depends on the physical size of the biggest structure that has heated the stream, but are typically larger than about 1 kpc.

In addition, if ΛCDM is correct, there will also be effects from the hundreds of smaller dark matter structures that will make the Galactic potential locally quite irregular. With the mini-halo mass function adopted in Ibata et al. 2002, these cause a heating of the stream of ~5 km/s/Gyr, so that the velocity dispersion will increase approximately uniformly with distance along the tidal tail.

Finding long streams without small-scale velocity structure would provide incontrovertible proof that dark matter is smooth on small (sub-galactic scales), while discovering evidence for heating by dark clumps would be a vindication of the existence of the dark structures and a triumph for dark matter theory. Either result would be a legacy for MSE.

A.3 Key astrophysical observables

DRAFT

The key observables are stellar radial velocities capable of resolving the internal dynamics of a stream (accuracy of $< \sim 1$ km/s is required). Additionally spectroscopic metallicity and other abundances would be extremely useful for population discrimination, to separate the stream stars from other Galactic components along our sightline.

Sample size is critical. Good sampling of the spatial and velocity structure of each stellar stream will be required in order to detect kinematic “hot spots”. Carlberg (2015) estimates that around one hundred velocity measurements per kpc of stream (or a few thousand for the longest streams) are required. Further, good coverage of a large number of streams will provide sampling of the spatial distribution of dark substructures at a range of locations and radii within the stellar halo. It is envisioned that a total dataset spanning hundreds to thousands of square degrees, mapping known stellar streams, will be required (not necessarily contiguous). Completeness is important and all stars that are accessible on a stellar substructure should be observed.

This observing program can make use of all stellar velocities measured by MSE on known stellar substructures (and even substructures found via kinematics only), particularly at high and moderate resolutions where the velocity accuracy will be of ~ 1 km/s (or better) and where good stellar metallicities can be derived. It could make use of the same observations required for SRO-03, and work should proceed to combine the science goals of these 2 programs into a single survey strategy. However, it is probable that the targets for this program are generally fainter than the bulk of the targets considered in SRO-03 (i.e., g > 20 mag) due to our requirement of tracing the kinematics of the streams with good spatial resolution (hence targeting faint stars in streams if required).

A.4 Target selection

This project requires the measurement of the line-of-sight velocity of the largest possible number of stars, in order to provide good kinematic maps of known streams and to detect low contrast structures. The most interesting streams will be those that inhabit the halo (say R> 25 kpc) beyond the perturbing influence of the Galactic disk, which is expected to destroy a large fraction of the subhalos (D'Onghia et al. 2010, ApJ 709, 1138).

As mentioned above, some streams will undoubtedly be discovered by LSST, Euclid and Gaia, and their kinematic follow-up can be undertaken with a massively multiplexed spectrograph like MSE. Further, PS1 provides good quality data over the entire northern hemisphere from which many targets can be selected. Low contrast stellar streams will be detectable purely from kinematics.

A.5 Cadence and temporal characteristics

Good sampling of the halo binary population would be valuable in order to statistically correct observed velocity dispersions in a stream. However, we expect that repeat observations would only be necessary for a small number of fields per stellar substructure.

A.6 Calibration requirements

No special requirements; accurate wavelength (velocity) calibration is the primary deliverable

DRAFT

A.7 Data processing requirements

Standard processing should be sufficient.

A.8 Any other issues

This SRO requires development through detailed simulations in order to devise the optimal observing strategy (e.g., velocity accuracy per pointing versus number of pointings, value of studying a few streams in detail versus many streams, etc.).

The science goals and observing strategy of this SRO and those of SRO-03 could potentially be combined into a single survey, although the typical magnitude ranges of the sources may differ.

.

Appendix E DSC – SRO – 05, Dynamics and chemistry of Local Group galaxies

Authors: Nicolas Martin

E.1 Abstract

With MSE, we will be able to conduct a systematic survey of the kinematics and chemistry of Local Group galaxies within 1 Mpc with a level of detail that has never been achieved before and cannot be achieved anywhere else. Gaia is gathering unprecedented astrometric measurements that provide the ability to map the six-dimensional phase-space structure of a galaxy will likely usher in a "Golden Age" of Milky Way research. However, without essential complementary information from the nearest galaxies, conclusions we may draw about the process of galaxy formation from a single galaxy may be premature. It is in this context that we propose to conduct the ultimate chemodynamical decomposition of Local Group galaxies across the galactic luminosity function, including a large population of faint dwarfs as well as the sub-L_* galaxy M33, and the L_* galaxy M31. These galaxies represent the obvious stepping stones between our highly detailed description of the Milky Way, and the low-resolution studies of more distant galaxies, in the realm of a few Mpc and beyond, where we can obtain significant samples of galaxies (as a function of galaxy type, environment, mass, etc).

E.2 Science Justification

E.2.1 M31

With the MSE, we will be able to conduct a systematic survey of the kinematics and chemistry of Local Group galaxies within 1 Mpc with a level of detail that has never been achieved before and cannot be achieved anywhere else. On the scale of (large) spiral galaxies, Gaia is gathering unprecedented astrometric measurements with the accuracies needed to produce a stereoscopic and kinematic census of about one billion stars in our Galaxy. Radial velocity measurements and chemical information will also be provided by onboard instruments. This dramatic advance in our ability to map the six-dimensional phase-space structure of a galaxy will likely usher in a "Golden Age" of Milky Way research. However, although Gaia will provide a very detailed view of the structure and dynamics of our Galaxy, this information will have to be put into context by comparing the results with observations of other galaxies. Without this essential complementary information, any conclusions that we may draw about the process of galaxy formation from observations of the Milky Way would be premature. It is in this context that we propose to conduct the ultimate chemodynamical decomposition the other two Local Group spirals (M31 and M33) with the MSE. These galaxies represent the obvious stepping stones between our highly detailed description of the Milky Way, and the low resolution studies of more distant galaxies, in the realm of a few Mpc and beyond, where we can obtain significant samples of galaxies (as a function of galaxy type, environment, mass, etc.).

DRAFT

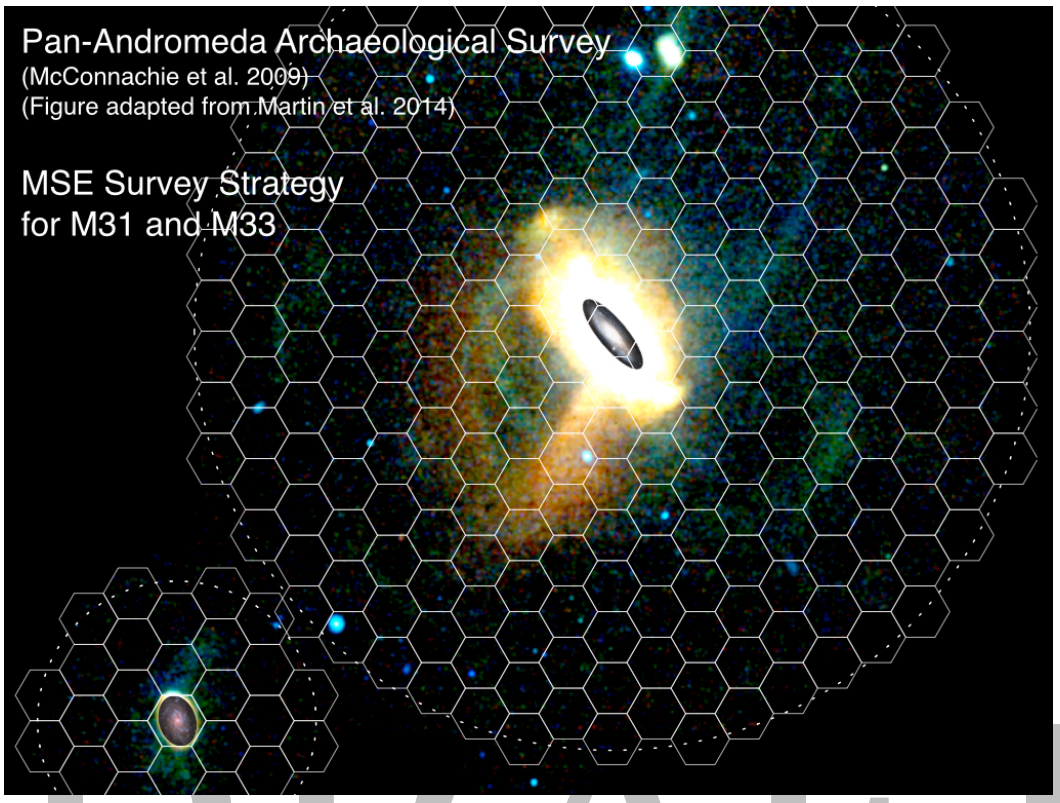

Figure 11: Spatial distribution of candidate red giant branch stars in the environs of M31 and M33, as identified from colour-magnitude cuts from the Pan-Andromeda Archaeological Survey. Dashed circles highlight maximum projected radii of 150 kpc and 50kpc from M31 and M33 respectively. The tiling strategy for an MSE survey of this region is overlaid.

DRAFT

MSE will provide a unique opportunity in this time-frame to make a pivotal contribution to the subject by undertaking a large spectroscopic and systematic survey of these two Local Group galaxies. The goal would be to obtain a statistically significant sample of stars belonging to their constituent structural components. The scientific aim of this "Galactic archaeology" theme is to understand the galactic formation process, which is clearly an open-ended endeavour. Our power to address the key issues (e.g., thick disk formation, halo formation, streams, chemical enrichment history), depend on the spectral resolution that the survey affords. In the Milky Way, current state-of-the-art spectroscopic surveys (e.g., RAVE, Gaia-ESO, HERMES) aim to sample of order one million stars. This is feasible with a reasonable allocation (i.e., a few months with MSE). In contrast to the very local (few kpc) view provided by RAVE and others, this proposed M31/M33 study would provide a uniquely powerful, global panorama of these galaxies, out to the farthest reaches of their stellar halos.

Current photometric surveys, complemented with small spectroscopic samples have revealed the very structured nature of the M31 inner halo (Ibata et al. 2005), all the way out to its furthest reaches (Chapman et al. 2006, Gilbert et al. 2013, Ibata et al. 2014), where the left overs of past dwarf galaxy accretions can be seen as stellar streams of varying width, metallicity, and distances. M33 itself appears to have its stars pulled out of its disk through tidal forces of its host (McConnachie et al. 2009). However, a qualitative comparison with expectations from

galaxy formation in a LCDM universe is currently made very difficult because of the mainly two-dimensional view we have of the M31 and M33 surroundings (e.g. Font et al. 2008). It is therefore essential that the community gathers a systematic census of additional properties (radial velocities, metallicities, alpha-abundances) on a large sample of member stars so the true picture of these two galaxies and their hierarchical history can be put together.

Error! Reference source not found. above shows the spatial distribution of candidate red giant ranch (RGB) stars in the environs of M31 and M33, as identified by colour-magnitude selection from 400 square degrees of contiguous *gi* imaging with CFHT/MegaCam as part of PAndAS. Color-coding corresponds to the color of the RGB stars, such that redder RGB stars (likely higher metallicity) appear red, and bluer RGB stars (likely metal-poor) appear blue. Dashed circles correspond to maximum projected radii of 50, 100 and 150 kpc from M31, and 50 kpc from M33. PAndAS resolves point sources at the distance of M31 (D = 783 kpc; McConnachie et al. 2005) to $g \sim 25.5$ and $i \sim 24.5$ at S/N ~ 10. PAndAS therefore reaches to (nearly) the horizontal branch level, providing photometry of sufficient depth that potential spectroscopic targets for a 10m facility could be selected. In the figure, the effective surface brightness of the faintest visible features is of order 32–33 mag arcsec^{-2}. This corresponds literally to a few RGB stars per square degree. Note that the disk of the Milky Way is located to the North so there is increasing contamination in the colour-magnitude of the RGB locus by foreground dwarfs; the reddest RGB stars are particularly affected by this source of contamination. Young, blue stellar populations — and even intermediate-age populations such as asymptotic giant branch (AGB) stars — are not present in the outer regions of M31 in any significant numbers. Thus, any spectroscopic study of the outer regions of the M31 halo will necessarily concentrate on the older, evolved, RGB population. For this reason, we consider separately surveys of the *outer halo* (characterized by a low surface density of evolved, giant star candidates) and the *inner galaxy* (with a high surface density of targets from a mixture of stellar populations).

DRAFT

- **An outer halo survey of M31/M33:** This survey aims at obtaining a complete, magnitude-limited, spectroscopic census of every star in the outer regions (40–150 kpc) of an L* galaxy halo to provide complete kinematics for every star, supplemented by metallicity estimates for most stars and alpha-abundances for the brightest ones. Ultimately, such a survey will allow us to deconstruct a nearby galactic halo into its accreted "building blocks". Such a survey will provide the ultimate testbed of the hierarchical formation of L_* galaxies and further yield the optimal data set to constrain the dark matter content of M31 and M33.
- **Faint stellar populations in the inner regions of M31/M33:** This part of the survey focusses on the study of the disk/thick-disk/halo transition region to measure the extent of the disks, characterize the relationship between these components, and to determine the role of mergers in the disk and inner halo evolution.

E.2.2 Dwarf galaxies

Intensive spectroscopic surveys are required to advance our understanding of dwarf galaxy dynamics in a meaningful way and thereby unveil the properties of the dark matter subhalos they inhabit. Recent efforts to systematically gather large, sub-km/s uncertainty radial velocity

samples for nearby dwarf galaxies have shown the power of data sets of a few thousands of spectra for a single system (Walker et al. 2009). However, as the dynamical modeling of these systems improves, these data sets are also now showing their own limitations and the necessity to gather information beyond the mere velocity of the systems and into the realm of chemical abundances (see Walker & Peñarrubia 2011 versus Strigari et al. 2014). At the moment, large uncertainties remain on the properties of their dark matter halo/ potential (cored/cusped, extent, implied dark matter density), the presence of stellar substructures in the dwarf galaxies (remnants of dwarf/dwarf mergers?), and the presence of extra-tidal stars that would hint at systems strongly affected by the presence of their host.

The MSE would bring about an entirely new era for such studies, enabling accurate kinematic measurements like this to be performed *much* more efficiently, over the full range of dwarf galaxy luminosities (10^{3-7} $L_{\odot}$), with at least an order of magnitude more stars in each system, and well beyond the peak of the rotation curve, from *all* Local Group dwarf galaxies with $\delta > -30$ degrees. Furthermore, the high multiplexing and large field of view of MSE would enable efficient spectroscopic variability surveys of the fainter half of the Local Group dwarf galaxy sample ($< 10^5$ $L_{\odot}$) so as to robustly tackle the growing concern that binaries mat significantly affect the low velocity dispersion measurements of these systems, thereby questioning the outcome of their mass modeling based on single epoch data. Crucially, the MSE would also be well-positioned to understand how the dynamics of dwarf galaxies respond to evolutionary effects, in particular tidal stripping, due to its ability to explore sparse outer fields while ensuring high completeness in the presence of strong contamination. The samples gathered with the MSE will have the power to constrain the formation and evolution of the sample of ~70 dwarf galaxies within the Local Group, the only satellite systems that can be observed in such detail. Most of these satellites will not have been studied systematically before the MSE comes online, owing either to the faintness of the target stars beyond ~100 kpc and the inability of upcoming 4m-telescope surveys to observe them, or to the lack of survey facilities on 10m-class telescopes, necessary to conduct a systematic survey.

DRAFT

Furthermore, connecting the dynamics of dwarf galaxies to their metallicities and chemical abundances is a key area of current research and will likely remain so, well into the era of the MSE. Indeed, there are at least three important open questions regarding the chemistries, metallicities, and star formation histories of dwarf galaxies that would take advantage of a highly multiplexed, wide-field instrument on a 10m telescope:

- The full metallicity distribution, including spatial gradients in metallicity and/or stellar populations. This would provide important information on whether star formation propagated inwards or outwards and whether dwarf/dwarf interactions have a significant role in heir formation/evolution. These data would also indicate if there were significant metallicity variations with time, and would make it possible to break the age-metallicity- reddening degeneracy definitively in color-magnitude diagram studies.
- The dispersion in abundance ratios at fixed metallicity: e.g., the patterns of [α/ Fe] vs. [Fe/H] and the relative proportions of other element groups in relation to the iron- peak elements (i.e., light elements, odd-Z elements, light and heavy s-process, r-process). These abundances hold important clues to the history of star formation in these galaxies

as well as their initial mass function.

- A census of rare stellar species (extremely metal-poor stars, carbon stars, etc), including their overall numbers and spatial distributions.

As an illustration of the sheer power of MSE for chemodynamical studies of nearby dwarf galaxies we consider NGC 6822, one of the nearest dwarf irregular galaxies — at an "intermediate" distance for Local Group galaxies (~500 kpc). It is one of the more intriguing targets for detailed study because of ongoing disturbances in its HI velocity field and very active star formation. There is some evidence for young stellar populations associated with infalling HI clouds, and for deviations from circular disk rotation. However, the large angular scale of the system (~ 1 degree across) and the likelihood that the substructures are represented by only a small fraction of the stars means that the system remains poorly understood, even with a small (but steadily growing) sample of stellar spectra from VLT/ FLAMES and Keck/DEIMOS.

It is, however, worth noting that it has already been demonstrated that the largest practical samples from Keck/DEIMOS and VLT have not been enough to identify the population substructures or true dynamical state of galaxies like NGC 6822 (Kirby et al. 2013, 2014). Even smaller/apparently simpler galaxies like WLM still have large uncertainties (e.g. Leaman et al. 2013). A very interesting analogue could be to the Small Magellanic Cloud, where the structure is only now becoming apparent based on spectroscopic samples of several thousand stars (e.g., Dobbie et al. 2014a, 2014b). Obtaining thousands to tens of thousands of spectra is these dwarf galaxies is therefore a necessity to understand dwarf galaxy structure and evolution.

DRAFT

With MSE, tens of thousands of member stars spanning all ages could easily be observed with multiple fiber set ups of a single pointing. It would therefore be possible, for example, *to measure radial velocities accurate to better than 5 kms^{-1} for every AGB and red supergiant star, and nearly all RGB stars within 1.5 mag of the TRGB, in just a handful of MSE nights at medium resolution and with S/N ~10 – 20*. For bright member stars, repeated observations over a period of several years would allow unprecedented studies of variability and evolutionary changes for stars in the late phases of evolution.

Closer to us, all observable stars of the recently found and most dark-matter- dominated, faint Milky Way dwarf galaxies could be targeted with a single fiber configuration but with a monthly to yearly cadence to consistently study spectroscopic variability (e.g. Koposov et al. 2010, Martinez et al. 2011). For more extended/brighter systems, the possibility to probe down to the oldest main sequence turn off will allow for an exquisite modeling of their potential with thousands of potential targets, but also enable a systematic search for the stellar extent of the dwarf galaxies, combined with a search for extra-tidal stars, similarly to what has currently only been achieved for a single dwarf galaxy (Carina; Muñoz et al. 2005), but on a much larger sample and scale.

E.3 Key astrophysical observables

Radial velocity measurements to study the dynamics of Local Group stars beyond the Milky Way usually rely on a small set of strong lines in the spectrum, typically the Calcium triplet lines at

~8500 Å. Velocity uncertainty requirements vary with targets but the typical goal is < 1 – 2 km/s, which is achievable within 1 – 4 hours down to i ~ 22.5, or S/N ~ 5 – 10 with the medium resolution grating. The 1 – 2 km/s goal is particularly important for dwarf galaxies, where multiple epochs are desired to identify binary stars that otherwise artificially boost the velocity dispersion (see discussion in McConnachie & Cote 2010).

The Calcium triplet has the added advantage of also being a well-understood [Fe/H] indicator, inasmuch as spectra are observed with S/N ~ 20 (Starkenburg et al. 2010).

Gravity sensitive indices are important to distinguish target giants from foreground dwarfs, particularly in the outer region of M31 and the dwarf galaxies where contamination is high (>>90%). In the region of the CaT, it has been shown that MgI8806 is a reasonable dwarf-giant discriminator, although there are a range of possible features across the spectrum.

In order to properly sample the very low density regions of the M31 halo, one needs to selects targets as far down as possible along the RGB. A good compromise between exposure time and depth is achieved by reaching 2–3 magnitude below the TRGB (g~24.5). With the medium resolution grating, 6h-long integrations will yield S/N ~ 4 spectra for the faintest stars, from which velocities can be measured with ~15 km/s uncertainties. This is an upper limit to the desired velocity uncertainty since it is of order the velocity dispersion of dwarf galaxies (that are either the targets, or which contribute some of the stellar streams that will be targeted in the survey of M31). The brightest stars in the sample, with much higher S/N will be use used to derive reliable [Fe/H] and [α/Fe] measurements and, when the density of a stellar structure is high enough, its velocity dispersion. Tagging stellar structures via these properties will ensure it is possible to disentangle the properties and time of infall of the accreted satellites.

DRAFT

In the central regions of M31, thousands to tens of thousands of targets can be selected at the bright end of the RGB so the inner region survey can focus on bright targets within 1 mag of the TRGB for which 1-hour long observations will yield accurate kinematics (i.e., better than 5kms^{-1}). The large density of sources however means that multiple configurations (up to ~10) for a given pointing are mandatory to maximize science.

For abundances analysis, the requirements are similar to those of the chemical tagging project of DSC-SRO-03.

E.4 Target selection

The depth reached by current panoptic surveys (SDSS, Pan-STARSS1; i~22.5) are well tailored to the needs of dwarf galaxy kinematic and chemical abundance surveys of Milky Way dwarf galaxies, but could be supplemented by wide field but deeper, targeted photometric surveys. Such observations are already available from public archives in most cases and reach 2 – 4 magnitudes deeper, more than enough for the requirements. In order to target M31 dwarf galaxies and halo stars, the PAndAS survey presented in the figure above is the ideal survey: it is deep enough to provide any stellar target we could wish to observe with a 10m telescope and its spatial extent (out to 150/50 kpc from M31/M33) is well tailored to study the stellar halo of M31 to large distances.

The source density of potential targets ranges from a few tens for the further/faintest dwarf galaxies, to tens of thousand per MSE pointing for a handful of close-by and bright Milky Way satellites. Most targets will have target densities in the hundreds to a few thousands range, perfectly tailored to the MSE set up. This is also the case for the M31 halo survey, for which the source density of potential targets ranges from a few hundred candidate stars in the outskirts of M31 (most of them MW foreground contaminant) to tens of thousand per MSE pointing for a handful of central fields.

The possibility to observe some targets with the medium-resolution grating for velocities and [Fe/H] measurements *and,* for a smaller sub-sample, the high-resolution grating for chemical abundance measurements of the brightest targets (à la FLAMES with GIRAFFE and UVES) would be strongly beneficial to this program. Given the density and faintness of targeted stars, this science requires a wide-field, multi-object spectrograph on a 10m-class telescope and, as such, is a particularly good match to the MSE specifications.

Given the wide variety but reasonably limited sample of Local Group dwarf galaxies, this program should strive to observe all known Local Group dwarf galaxies (~70 targets). Observing strategies should be tailored to the a specific regime of dwarf galaxies but should range from a few hours to a few nights per target over a period of ~5 to 10 years (estimate around 50 nights for a very comprehensive sample). Some fields would also be reobserved to provide the cadence necessary to minimize the influence of binary stars. In parallel, the M31 part of the survey would cover ~350 deg^2 if based on the PAndAS survey, which, with ~6h-long integrations per field and a 1.5 deg^2 field of view, requires ~150 nights of MSE time. In high density central regions (~40 deg^2), an average of 5 pointings with 1h integrations will require 15 nights. Thus, the M31 project would require of order 165 nights to be complete. These can also be spread over a period of 5 – 10 years and the target selection can be set up such that M31 dwarf galaxies are seamlessly included in the survey of the M31 halo.

DRAFT

E.5 Cadence and temporal characteristics

A temporal survey of dwarf-galaxy-member stars will be essential to constrain their binary population and how it impacts on the modeling of their dark matter potential. This is particularly important for the fainter half of the Local Group satellites. Little is known about their binary population of dwarf galaxies but observations have shown that variation can be presence on time-scales of months (Koposov et al. 2011) but binaries with periods below ~10 yr can likely bias velocity-dispersion measurements (McConnachie & Côté, 2010). Therefore, at least some configurations should be observed anew on both monthly and yearly timescales. An appropriate statistical modeling of the repeated observations could reduce the required repeat exposures to only a handful per galaxy.

E.6 Calibration requirements

- Wavelength calibration should be able to yield sub-km/s velocity accuracy over different configurations and repeated observations over yearly timescale for the closest targets (Milky Way satellites).
- Good sky subtraction is necessary to work reliable in the low-S/N regime of the faintest

targets. Efficient and accurate sky subtraction is also needed for the chemical abundance part of the program (cf. Milky Way abundances SRO). There are significant sky lines in the region of the CaT that could reduce the number of useable lines for velocity determination

- Flux calibration is not a significant issue for this program

E.7 Data processing requirements

Straightforward and now common procedures to go from observations to velocities, [Fe/H], and their uncertainties, further tested for systematics from repeat measurements of bright stars.

Measurement of abundances from the spectra are only now entering the large-sample era but pipelines will be in place to also straightforwardly yield abundances by the time the survey starts (see, e.g., on-going efforts with the HERMES survey, Keck/DEIMOS analyses by E. Kirby et al., etc.).

E.8 Any other issues

None

DRAFT

Appendix F DSC – SRO – 06 Nearby Galaxies and their Environments

Authors: Michael Balogh, Alessandro Boselli, Pat Cote, Simon Driver, Pierre-Alain Duc, Sara Ellison, Richard de Grijs, Laura Ferrarese, Ken Freeman, Raja Guhathakurta, Andrew Hopkins, Mike Hudson, Iraklis Konstantopoulos, George Koshy, Eric Peng, Bianca Poggianti, Aaron Robotham, Prajval Shastri

F.1 Abstract

To understand the physical drivers of galaxy evolution it is necessary to map the distribution of stellar populations and supermassive black holes to the dark matter haloes and filamentary structure that dominate the mass density of the Universe. This requires deep, spatially complete spectroscopic surveys over wide areas, ideally suited to the capabilities of MSE. We propose a wide-area survey S1-W, that obtains redshift-quality spectra for every z<0.2 galaxy over a 3200 deg^2 area. This is efficiently achieved if target selection is based on deep imaging catalogues spanning the NUV to NIR, so that precise photometric redshifts are available. This survey will, among other things, allow every halo in the area with mass $M_{halo}>10^{12}M_{star}$ to be identified with a group of four or more galaxies. We propose to follow up select regions within this survey with longer exposures, resulting in a sample covering 100 deg^2 to a depth of at least i<24.5, and spanning four decades in halo mass. This will allow us to measure the shape of the stellar mass function to the scale of the Local Group dwarf galaxies, over a large volume and a range of environments. A subset of fibers will be used to obtain long integrations on bright galaxies, yielding a final sample of >50 000 high signal-to-noise ratio spectra, for which detailed stellar population synthesis analysis is possible. This will be the definitive spectroscopic survey of the local Universe for decades to come.

DRAFT

F.2 Science Justification

F.2.1 Introduction

The evolution of structure in the Universe is dominated by dark matter, which gives rise to the cosmic web of filaments and clusters we see in the galaxy distribution. The clustering, spatial structure, and redshift evolution of these galaxies is sensitive to the underlying cosmological model, the very nature of dark matter, and the highly complex mechanism of galaxy formation. Large spectroscopic surveys, covering cosmologically relevant volumes with homogeneous selection and good calibration, have demonstrated that the distribution and growth rate of galaxies is largely decoupled from that of dark matter haloes (Behroozi, Wechsler & Conroy 2013). This is likely due to the highly nonlinear nature of cooling, star formation and heating processes such as photoionization, supernovae feedback, stellar winds and energy output from supermassive black holes. These phenomena and others operate with different strengths, over different spatial scales, and their relative effectiveness evolves with time. Thus while the broad picture is coming into focus, we are still far from understanding how galaxies ended up with the masses, structures, dynamics and stellar populations that they have today.

Within the ΛCDM paradigm, it is therefore fundamental to understand how galaxies evolve and grow relative to the dark matter structure in which they are embedded. To build a consistent

and accurate picture of galaxy growth requires carefully designed observations to measure various quantities, including:

- Spatial clustering and radial velocity information over scales ranging from tens of kpc to hundreds of Mpc, to link galaxies to the underlying dark matter distribution. Specifically, the goal is to identify galaxy locations and dynamics within bound haloes, and filamentary structures, and the distribution of those haloes relative to one another.
- Properties of stellar populations, including ages, star formation rates, chemical abundance and initial mass function parameters.
- The occurrence and strength of AGN activity, expected to play a significant role in galaxy formation by providing an important source of energy that inhibits star formation.

Such measurements require spectroscopy of at least moderate resolution (R~2000). Furthermore, the wide range of relevant spatial scales and the fact that galaxies span more than five orders of magnitude in mass, and show remarkable diversity in their morphologies and stellar populations, means large samples are required. Specifically, in order to ensure that statistical uncertainties are subdominant, when binned by parameters of interest (primarily stellar and halo mass, but also morphology, star formation rate, and others), samples should include on order 10,000 galaxies or more per bin. Volumes on the order of several $(100\ \mathrm{Mpc})^3$ are required to overcome cosmic variance limitations and to include rare structures of interest, like massive galaxy clusters.

DRAFT

It is necessary to make these observations as a function of redshift, to reconstruct directly the statistical assembly of galaxy populations. However, the local Universe plays a special role, as it will always be here that the lowest-mass galaxies can be observed, at the highest physical spatial resolution. While challenging because of the large sky areas that must be surveyed, high-quality observations of nearby galaxies serve as the anchor for all higher redshift surveys that aim to study galaxy evolution.

F.2.2 The role of spectroscopic surveys

The advent of large surveys like the 2dFGRS and SDSS resulted in a breakthrough in our understanding of galaxies in the local Universe. In particular, the SDSS Legacy survey provided well-calibrated spectroscopy for almost 1 million galaxies with r<17.77 over more than 8000 square degrees of the sky, at a spectral resolution of ~2000. This enabled an unprecedented measurement of the galaxy stellar mass function as a function of environment (Baldry et al. 2006), mass-metallicity-star formation rate relations (e.g. Kewley & Ellison 2008; Ellison et al. 2008), the galaxy formation efficiency (e.g. Marinoni & Hudson 2002; Behroozi, Wechsler and Conroy 2013) and a host of unexpected correlations with surrounding large scale structure at z<0.2 (e.g. Gomez et al. 2003; Balogh et al. 2004a).

The GAMA survey, with spectroscopy completed in 2014, improved upon the SDSS in two main respects. First, the increased depth of the survey extends the limits of the measured stellar mass function by more than an order of magnitude, from ~$5\times10^8 M_{Sun}$ to less than ~$10^7 M_{Sun}$ (see

Figure 13). The other important achievement of GAMA was to obtain spectra for nearly 100% of the magnitude-selected target sample, independent of small-scale clustering. This sampling is critical to robustly link galaxies with their dark matter haloes, and to distinguish satellite galaxies from the dominant galaxy in each halo. Though covering only 300 square degrees, this survey has been very successful at extending what we learned from SDSS to lower-mass galaxies, and to greatly improving our understanding of the role of environment. For example:

- Lara-Lopez et al. 2013a were able to explore correlations between stellar mass, metallicity and star formation rate to unprecedented depths, and showed that there is a fundamentally different behavior between low-mass and high-mass galaxies, which they are able to attribute to differences in the amount of neutral gas (Lara-Lopez et al. 2013b).
- Bauer et al. (2013) discovered a population of low-mass galaxies with surprisingly high star formation rates, implying that star formation has a substantial stochastic component that is not apparent in more massive galaxies.
- Prescott et al. (2011) used the depth and completeness of GAMA to study the radial distribution and colours of satellite galaxies, for a large sample of almost 3000 satellites. They were able to identify clear trends in colour distribution with radial distance, finding that quenching of star formation is most efficient in massive systems, and acts within ~500kpc of the host. This points to relatively slow mechanisms of gas removal, like strangulation (Larson et al. 1980; Balogh et al. 2000) as the main driver of this differential evolution.
- Robotham et al (2014) took advantage of the close pair completeness to fully characterise a wide dynamic range of mergers in the local Universe, including mass ratios larger than 1/100 for all galaxies brighter than ~$10^{10}M_{Sun}$. This was a big step beyond the capability of SDSS, enabled by the additional depth and spatial completeness of GAMA, and demonstrates that low redshift galaxy growth is dominated by mergers for stellar masses $M_{star}>5x10^{10}M_{Sun}$.

DRAFT

Surveys on larger aperture telescopes have focused on measuring galaxies out to z ~ 1; through the work of surveys like VVDS (Le Fèvre et al. 2005), DEEP2 (Newman et al. 2013), zCOSMOS (Lilly et al. 2007), VIPERS (Garilli et al. 2014) and others we now have a good picture of how *massive* galaxies evolve relative to the dark matter over the redshift range 0 < z < 1. This work has shown definitively that the growth rate of galaxies is decoupled from that of the dark matter, and that both merging and in-situ star formation play important roles, as shown in Figure 12.

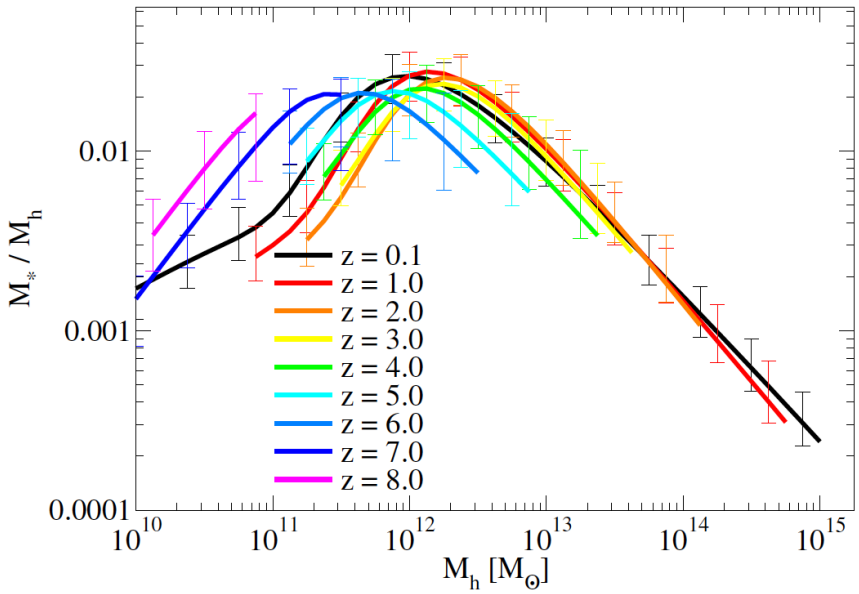

Figure 12: from Behroozi et al. (2013), this shows the evolution of stellar mass fractions (stellar-to-halo mass ratio) as a function of halo mass. The complex, non-linear nature of this plot shows the growth of stellar mass is largely decoupled from that of the dark matter.

F.2.3 Progress and the role of MSE

While we now have a good description of massive galaxies and the haloes they inhabit, this is not true of the dwarf galaxy population with masses $M_{star} < 10^9 M_{Sun}$. This population is important because these are the most numerous galaxies in the Universe, and are the building blocks of larger galaxies. Moreover, though our empirical picture of galaxy evolution is developing we are still largely ignorant of the physical drivers of that evolution, and it is in the low mass galaxies that many of the most perplexing discrepancies with current models persist (e.g. Boylan-Kolchin et al. 2011; Oman et al. 2015). The complexity can only be untangled through observations spanning a wide range of parameter space; comparing how low-mass galaxies respond to their haloes and large-scale structure to what is observed at higher masses. The GAMA survey, for example, has begun to show how changes in fundamental scaling relations as a function of mass can illuminate the physical drivers of these relations (e.g. Lara-Lopez et al. 2013b).

In order to make significant progress, a new generation of spectroscopic survey is required that will:

- Reach fainter magnitudes, and thus stellar masses $M_{star} < 10^9 M_{Sun}$.
- Cover a representative volume of the Universe, to overcome cosmic variance and sample the full range of large-scale structures.
- Be spatially complete, so galaxies can be robustly identified with dark matter haloes.
- Have a sufficiently large sample size to bin galaxies at least by halo mass, stellar mass and star formation rate, while keeping statistical uncertainties subdominant.
- Obtain higher resolution and higher signal-to-noise ratio spectroscopy, to enable chemical abundance measurements and more precise stellar ages to be measured.

With MSE we will have an opportunity to carry out such a survey. The combination of high sensitivity, wide field of view, and survey capability is perfectly suited to build upon the GAMA survey by going several magnitudes deeper and covering an order of magnitude larger sky area. Moreover, the availability of a medium resolution mode R ~ 6500 enables important stellar population work on the brighter galaxies as well as stacks of fainter objects, and higher precision velocities needed for dynamical analysis of low-mass haloes.

The survey described in Section 0 will allow transformative discoveries in many areas. A few of the most compelling measurements are outlined here.

DRAFT

i. The most fundamental measurement will be to extend the stellar mass function to masses below $10^8 M_{sun}$, for a cosmologically representative, unbiased, spatially complete spectroscopic sample, as shown in Figure 13. Through halo modelling techniques it is possible to associate the galaxies in this stellar mass function to dark matter haloes, and thus measure the efficiency of galaxy formation as a function of halo mass and environment. Extending existing work to observations of galaxies more than an order of magnitude lower in mass provides leverage on decoupling the effects of many heating mechanisms (e.g. photoionization, supernovae feedback, supermassive black hole accretion, and stellar winds) from one another. Specifically, in the Local Group, the abundance of such low mass galaxies is orders of magnitude less than expected by simply extrapolating the dark matter halo occupation of more massive galaxies (e.g. Moore et al. 1999; Boylan-Kolchin et al. 2012). This is at least partly due to the important but poorly understood heating, feedback and disruption processes; it may also be telling us about the nature of dark matter itself. However, characterization of this "missing satellites" problem is currently limited to galaxies in the Local Group, which is the only volume over which such low-mass galaxies are observable. MSE will allow the crucial step of measuring the universality, or environmental dependence, of this remarkably low efficiency of star formation.

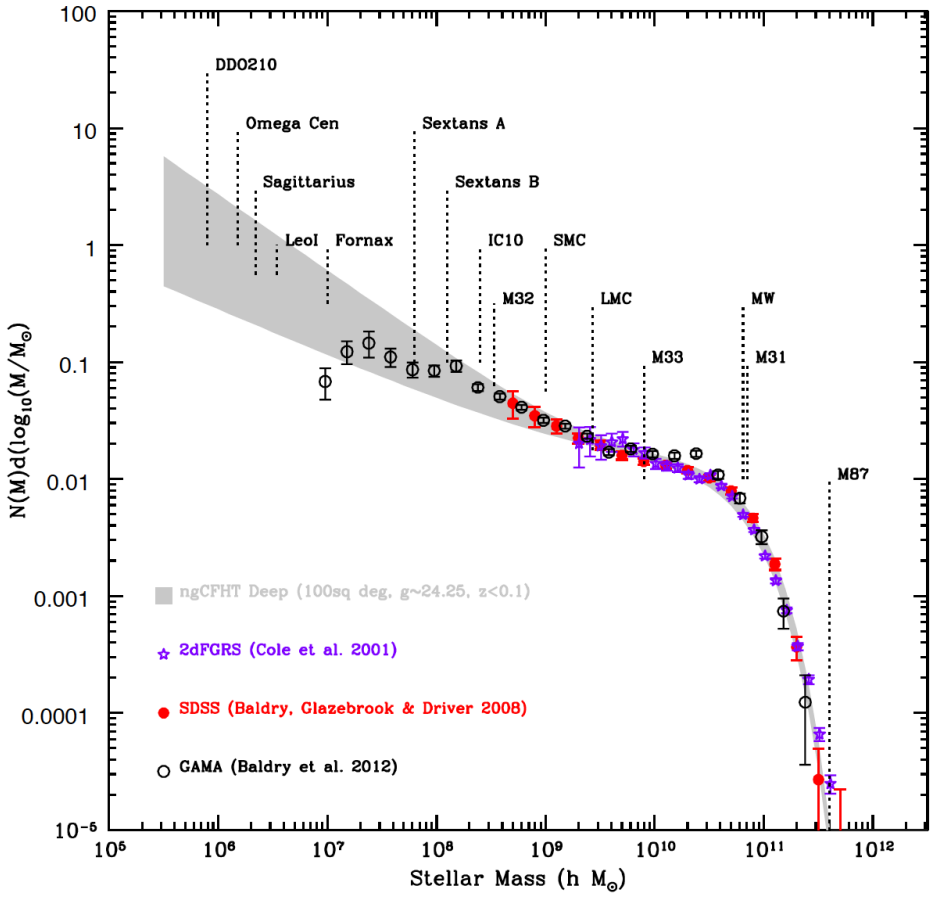

Figure 13: From the ngCFHT feasibility study, this figure shows the local stellar mass function as measured by SDSS, 2dFGRS and GAMA. GAMA is the deepest of these surveys, and probes robustly down to the scale of M32; lower mass measurements are actually lower-limits due to surface brightness limitations. The grey, shaded region shows a proposed MSE survey in the feasibility study, comparable to the S1-D survey describe in Section 0.

ii. A primary goal of the proposed surveys is to establish how the evolution of the lowest-mass satellite galaxies is influenced by their environments. Analysis of satellites in the Local Group has demonstrated that quenching of star formation has a complex dependence on stellar mass that is not understood. **Error! Reference source not found.** elow from Fillingham et al. (2015; see also Geha et al. 2012) shows that while the effectiveness with which star formation is quenched in satellite galaxies steadily declines with decreasing stellar mass in the mass regime probed by all large spectroscopic surveys, at lower masses the trend appears to reverse. While the effect is subtle, this differential measurement (comparing satellite galaxies with central galaxies) is a potentially very powerful way to constrain feedback parameters (e.g. McGee, Bower & Balogh 2014). It is important to make this measurement over a cosmologically relevant volume, and with a homogeneous selection of galaxies over the full mass range. Only

MSE has this capabi

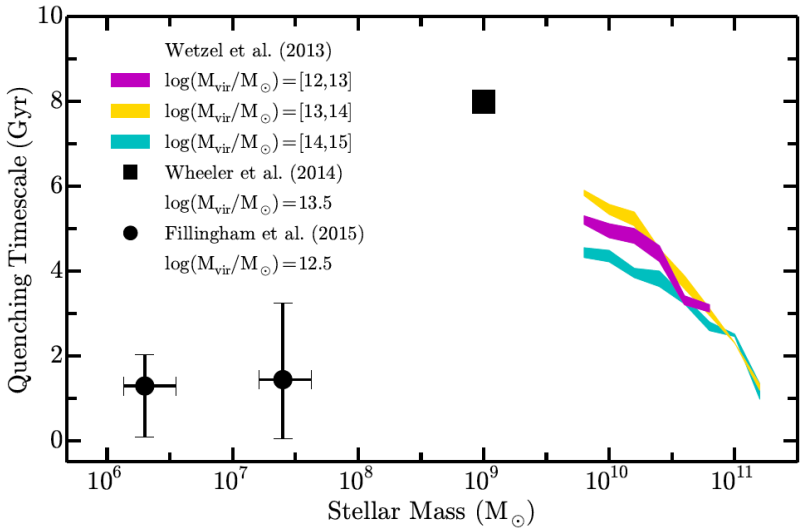

Figure 14: From Fillingham et al. (2015), this shows the inferred star formation quenching timescale of satellite galaxies as a function of their stellar mass. Short quenching timescales lead to high fractions of galaxies with little or no star formation at the epoch of observation. Large spectroscopic surveys like SDSS and GAMA have been instrumental in uncovering the trend in decreasing timescale with increasing stellar mass shown as the coloured lines at the high-mass end. However, this and other analyses of the Local Group show that the lowest-mass satellites may respond very differently to environment.

DRAFT

iii. In the past decade, imaging and spectroscopic surveys of large, unbiased samples of local galaxies, both in clusters and in the field, have revealed the existence of important scaling relations, such as those between stellar mass, SFR and metallicity, and how these depend on other parameters, such as morphology, AGN activity and environment (Brinchmann et al. 2000; Kauffmann et al. 2003; Tremonti et al. 2004; Balogh et al. 2004b), These, in turn, inform and constrain theoretical models (e.g. Lilly et al. 2013; Peng et al. 2015). However, the extension of large statistical studies into the dwarf galaxy regime is largely uncharted, due to the flux-limited nature of most surveys. At low masses, we expect chemical enrichment to become increasingly stochastic and sensitive to factors such as winds, infall and environment (Kirby et al. 2013), potentially with a metallicity floor where self-enrichment is driven by a few generations of stars (Sweet et al. 2014). Here, again, the environmental dependence of these scaling relations is mass-dependent (Ellison et al. 2009; Cole et al. 2014) and provides key evidence for the physical drivers of both satellite and central galaxies.

iv. The role of the initial mass function (IMF) for studies of galaxy formation and evolution can hardly be overstated, as the assumptions regarding its slope and mass range are the basis for the interpretation of most galaxy integrated observable properties at any redshift. Evidence has accumulated that the IMF is indeed non-universal, and may vary with galaxy mass, as shown in **Error! Reference source not found.**. But this evidence emains controversial, and because of the small samples for which such measurements are available today it is unknown to what extent the IMF depends on spatial scale,

galaxy type, mass, redshift or environment. It is possible to put useful constraints on the high-mass end of the initial mass function using combinations of Hα emission lines and galaxy colour (Kennicutt 1983; Baldry & Glazebrook 2003; Gunawardhana et al. 2011). And if spectroscopy with S/N>100 is available, a measurement of the IMF shape at the low-mass end also becomes possible (van Dokkum & Conroy 2010; Cappellari et al. 2012; Smith et al. 2014).

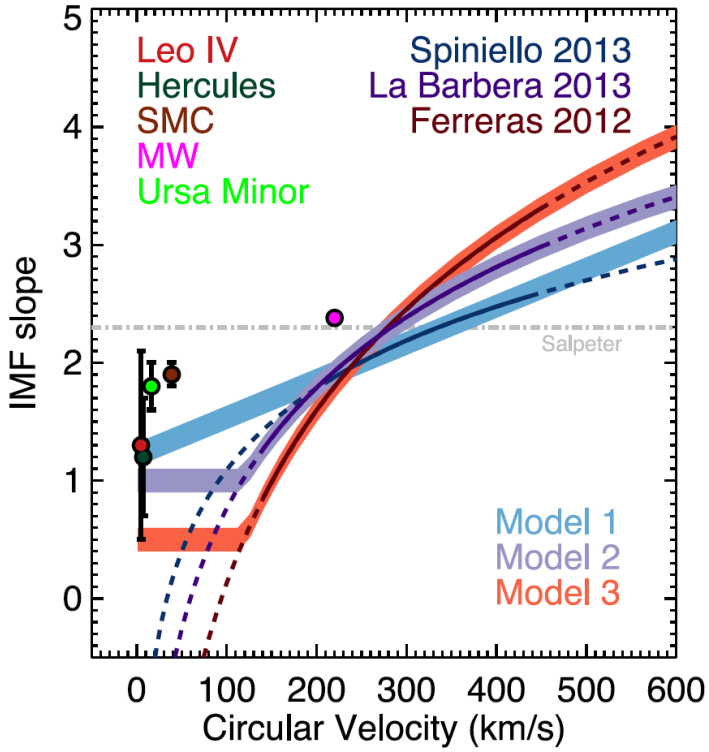

FT

Figure 15: A compilation of observed relations (black solid lines) for how the slope of the IMF varies with galaxy circular velocity, and their extrapolations (black dashed lines). Also shown are individual measurements for some Local Group galaxies, based on resolved star counts. This remains a tremendously important and controversial topic, with data limited to small samples of inhomogeneously selected galaxies. *(Figure from McGee, Goto & Balogh 2014).*

v. Galaxies today have assembled their mass today through a combination of in-situ star formation and mergers with other galaxies. For massive galaxies we have developed a good picture of how the star formation rate depends on stellar mass, halo mass and epoch (e.g. Behroozi et al. 2013). At low redshift it is clear, for example, that low mass galaxies are moderately more efficient at forming stars (e.g. Gilbank et al. 2010; Bauer et al. 2013). There is evidence that the relationship becomes much steeper for dwarf galaxies, in a way that is not predicted by current state-of-the-art simulations (**Error! eference source not found.**). MSE will extend the analysis shown in **Error! Reference source not found.** by at least an order of magnitude in stellar mass, over a much larger area. Furthermore it will be possible to measure any dependence on halo mass, which is a prediction of most satellite quenching models but remains controversial

observationally (e.g. McGee et al. 2009; Wetzel et al. 2013; Vulcani et al. 2010; Rasmussen et al. 2012; Lu et al. 2012)

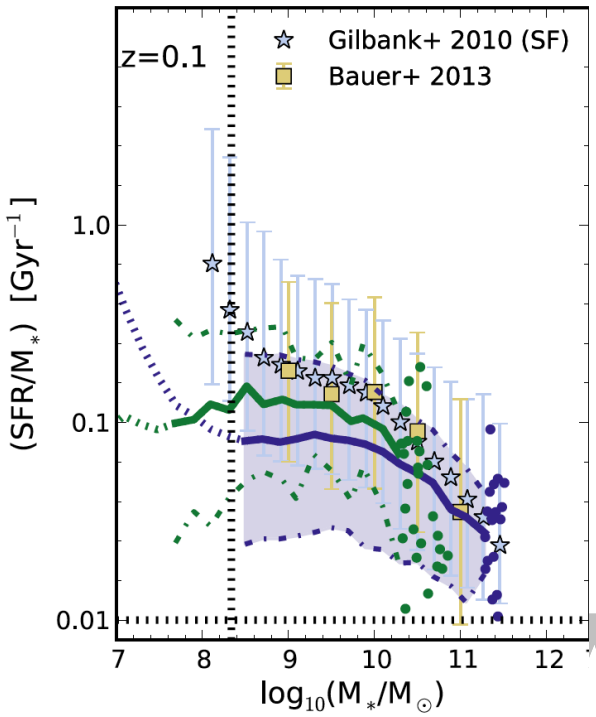

DRAFT

Figure 16: Predictions of the sSFR-mass relationship from the EAGLE hydrodynamic simulations, compared with observations at low redshift. The purple and green solid lines are low and high-resolution simulation results, respectively; the dashed lines indicate where resolution effects may be important. There is indication of a discrepancy with the SDSS Stripe 82 analysis of Gilbank et al. (2010) at the lowest stellar masses probed. *(Figure from Furlong et al. 2015).*

vi. The other mechanism by which galaxies grow is from merging with other galaxies. This hierarchical assembly is a fundamental prediction of cold dark matter models, and plays a particularly important role in the evolution of galaxy sizes and densities (e.g. Trujillo et al. 2006). Merger rates can be estimated from the frequency of close pairs, potentially including morphological information (Robotham et al. 2014; Casteels et al. 2014). Highly complete spectroscopy is essential for such measurements, in order to identify close pairs in velocity as well as space. Such a measurement provides not only a test of the underlying dark matter model prediction, but also, together with the in-situ star formation rate, provides a complete empirical description of galaxy growth rates at a given epoch.

vii. From analysis of emission line ratios is will be possible to determine the occupation fraction of active galactic nuclei (AGN) in low mass galaxies, and determine whether supermassive black holes relate more closely to the spheroidal (bulge) component or other properties of the host (e.g. total gravitational mass). The canonical view of AGN is that they are hosted by massive galaxies, and that the black hole mass scales with the

mass of the bulge component. However, populations of low mass and/or bulgeless galaxies have recently been discovered to host AGN, which challenges this picture (e.g. Greene & Ho 2004; Reines et al. 2013; Satyapal et al. 2014).

viii. The overall abundance of dark matter halos as a function of mass is among the most important outstanding issues in modern astrophysics. This quantity is sensitive to both the form of the inflationary perturbations and to the nature of the dark matter particle itself: i.e., whether it is collisional or collisionless, decaying, self-interacting, warm (light), or cold (massive). Establishing its functional form at low redshift, with high precision, is critical for measuring its evolution and in turn constraining fundamental cosmological parameters. This survey will enable a direct measurement of the dark matter halo mass function, through dynamical analysis of galaxies in haloes with masses $M_{halo}>10^{12}M_{star}$. From the relatively shallow data of the SDSS, this has been possible only for massive clusters, $M>10^{14}M_{Sun}$ or so (Rines et al. 2007; Tempel et al. 2014). The deeper GAMA survey allows this measurement to be extended by about a decade in mass (Robotham et al. 2011), though the small area limits its utility for the purpose of cosmological constraints.

F.2.4 Competition and synergies

Before MSE is operational, further progress in the field will be made. The most comparable instrument is the Prime Focus Spectrograph (PFS, Takada et al. 2013) on Subaru. It will have similar capabilities to MSE, with a spectral range 380 – 1300 nm and a R = 5000 resolution mode. It will nominally be conducting $z < 1$, $i < 21.5$ and $1 < z < 2$, $i < 23.9$ photo-z pre-selection surveys (based on HSC data), but over only 16 square degrees. Low redshift galaxies will not be a priority, and the surveys planned now will not produce a competitive sample of $z < 0.2$ galaxies.

DRAFT

Large surveys planned with 4-m class telescopes will make significant progress on at least two fronts. On the one hand, surveys like SAMI, MaNGA, WEAVE and MUSE will revolutionize our understanding of the nearby Universe by providing spatially resolved spectroscopy for large samples of relatively bright galaxies. In many cases, the nature of single-fiber spectroscopy from surveys like SDSS and GAMA is the single most important limitation in our ability to decipher the physical drivers of galaxy evolution.

The other approach of the 4-m class telescopes is to carry out very wide-field redshift surveys, at relatively bright magnitudes. For example, the relevant low-redshift DESI survey is the Bright Galaxy Survey (BGS), spanning $0.05 < z < 0.4$ (DESI Technical Design Report, June 1, 2015). This is a bright-time survey, nominally targeting galaxies with $r < 19.5$ over 14 000 square degrees. It will be observed in three layers to achieve high spatial completeness and is therefore comparable to the GAMA survey but over a cosmologically significant area almost fifty times larger.

For fainter galaxies the proposed survey of most interest is WAVES, using the 4MOST spectrograph on VISTA (Driver et al. 2015). The survey consists of two parts, the most relevant here being WAVES-Wide. Though this survey is still in the planning stages, the current design is to target galaxies with $r < 22$ selected to have photometric redshifts $z < 0.13$, over 1500 deg^2.

The WAVES-Deep survey reaches the same depth over a much smaller area, but extends to higher redshift.

MSE will play an important and unique role among these surveys, reaching depths requiring 10-m aperture but with the sort of sky coverage only currently accessible to smaller telescopes (see Figure 17). Another feature that potentially provides MSE with an advantage over all these surveys is the use of LSST (and Euclid/WFIRST) photometric source catalogues. These catalogues will only become available post 2020, and offer a paradigm shift in optical quality. The resulting homogeneity and precise calibration will improve the robustness of almost every type of analysis made. Given the fast survey speed of MSE, once LSST and Euclid data become available it will dominate the next generation of spectroscopic surveys.

F.3 Key astrophysical observables

F.3.1 Survey design

The proposed strategy consists of two surveys, both targeting galaxies selected to lie at z<0.2. For both surveys we require to cover the full spectral range up to 800nm, and there is significant advantage in extending to 1500nm in order to obtain Paβ and IMF-sensitive absorption features at z<0.2.

DRAFT

We plan to use the moderate-resolution setting (R~6500), as long as it does not compromise this wavelength coverage. The choice of moderate resolution improves the radial velocity measurements of all galaxies, important for association within small groups and pairs; moreover it enables precision stellar population measurements, including of IMF-sensitive features, for high signal-to-noise spectra. It is expected that the faintest-galaxies in our sample will only be read-noise limited at the bluest wavelengths, <4300A; it is only there that there will be a small but significant cost to rebinning the low S/N spectra. This is likely an acceptable compromise, but a final choice of resolution will await a more detailed study. An alternative solution would be to use low resolution fibers on the faintest targets, and higher resolution fibers on the others. This will in fact be necessary if the simultaneous wavelength range accessible in R=6500 mode is less than the required 370—1500nm. In that case, two configurations would be needed, and this could be accommodated for a subset of galaxies since the strategy will always include at least two fiber configurations per pointing.

Targets will be selected based on i-band magnitude and photometric redshift. The choice of i-band is made to obtain a sample that is close to a stellar mass-limited sample. Near infrared selection would be even better in this respect, though the gain is not large. Note, however that in order to obtain good redshifts and stellar population constraints for this low redshift sample it will be important to obtain sufficiently high signal-to-noise at *blue* wavelengths, ~400nm. Given the lower instrument throughput at these wavelengths, and the intrinsically red colours of galaxies, the attainable depth of a complete i-selected sample is shallower than would be the case for a higher redshift sample where the features of interest lie at >600nm.

To achieve our science goals of studying the lowest mass galaxies, within a well-defined, cosmological large scale structure, we consider two surveys *S1-W* and *S1-D*. These surveys will

serve as the anchor for the higher redshift surveys *S2-S8* described elsewhere. *S1-W* aims to cover a cosmologically representative, contiguous volume, while still reaching substantially deeper than previous surveys. *S1-D* targets specific environments over a smaller area, to exceptionally deep limits. Table 1 and Figure 17 summarize the depth, area and sample size proposed for each survey, described in more detail below, compared with other existing and proposed low redshift galaxy surveys.

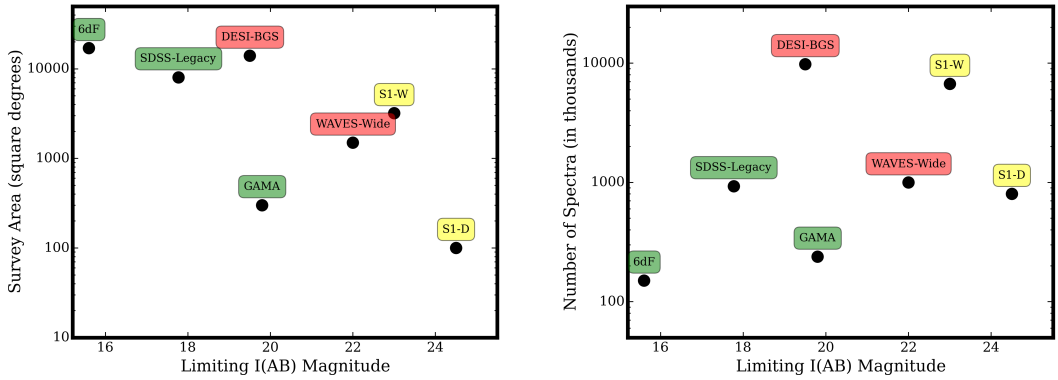

Figure 17: Left: Survey area as a function of equivalent limiting i-band magnitude, for spectroscopic surveys of the z<0.2 Universe. Completed surveys are shown with green labels; proposed surveys with red labels; and the two proposed MSE surveys described here are shown with yellow labels. Right: Same, but now comparing the number of spectra in the final z<0.2 samples as a function of limiting magnitude.

DRAFT

Table 1: The two proposed surveys, S1-Wand S1-D, are compared with other relevant spectroscopic surveys in terms of their area, depth and sample size. To compare r-selected surveys with the proposed i-selection, we assume a colour of (r-i)=0, typically of the bluest galaxies at 0<z<0.2. This is appropriate to determine the faintest i-band magnitude for which a r-selected sample would be complete.

Survey	Area (sq. deg)	Depth	Depth (equivalent i)	Sample size
S1-W	3200	i<23	i<23	6.7M
S1-D	100	i<24.5	i<24.5	800,000
SDSS-Legacy	8032	r<17.77	i<17.77	928,567
6dF	17046	K<12.75	i<15.6	150,000
GAMA	300	r<19.8	i<19.8	238,000
MS-DESI	14000	r<19.5	i<19.5	9.8M
WAVES-Wide	1500	r<22	i<22	1.0M

F.3.1.1 S1 – W

The volume of this wide-area survey is set by the desire to minimally contain a 300x300x300 Mpc/h co-moving cube, so that the volume is large enough to ensure Universal homogeneity in all three dimensions (Scrimgeour et al 2012, Driver & Robotham 2010). With an upper redshift limit of z=0.2 this drives a requirement of >3200 square degrees, in a contiguous region with comparable angular extents in RA and Dec. The total volume is about 0.18 Gpc^3, and the cosmologically representative box lies at z>0.1. In a blind 3000 sq degree survey, we expect to cover ~10 massive galaxy clusters ($M_{halo}>10^{15}M_{Sun}$), and >200 low-mass clusters ($M_{halo}>5x10^{14}M_{Sun}$). For these systems we will be able to study the properties of galaxies out to arbitrarily large distances from the cluster centre. This is critical for many of the remaining questions about galaxy transformations in dense environments (e.g. Bahé et al. 2013).

Since galaxies are highly clustered on the sky, and fibers cannot be placed arbitrarily close together, a minimum of two fiber configurations are required, whatever the source density of targets. The minimum integration time should be 1 hour; anything less than that can be expected to be firmly in the domain of 4-m class telescopes. With the 1.5 deg^2 MSE field of view, and assuming 20% overheads, it will therefore take at least 5100 hours to complete the survey.

DRAFT

To estimate the depth we first use the preliminary exposure time calculator, for a point source elliptical galaxy at z=0 in dark skies. For an i=23 galaxy, the predicted signal-to-noise ratio at 400nm is ~1.4 per resolution element using the low-resolution grating[1]. From past experience and published results (e.g. Newman et al. 2013), this S/N is likely an aggressive minimum for which one can expect to get redshifts with high completeness. A limit of i < 23 in 1h is also comparable to that of the VIPERS survey (I < 22.5 in 2700s at R=230, Garilli et al. 2014), DEEP2 (R < 24.1 in 1h at R=6000, Newman et al. 2013), and the planned PFS low-redshift galaxy survey (J < 21 in 20 minutes, Takada et al. 2014). The larger aperture and possibly higher throughput of MSE may lead to improved performance relative to these surveys; for now we consider it prudent to be conservative in our estimates.

[1] This drops to 0.9 per resolution element at R=6000; for galaxies at the limit, though, we would expect to effectively rebin to lower resolution, and we see that there is little loss in S/N in doing so.

We therefore aim to select galaxies with i < 23, and photometric redshifts z < 0.2. The expected source density of i < 23 galaxies with z < 0.2 is 2100/square degree, based on analysis of galaxies in the COSMOS field with photometric redshifts (Figure 18), and with a cosmic variance over a 1.5 square degree field of +/- 30% (Scrimgeour et al 2013, Driver & Robotham 2010). This is well matched to the usable fiber density of 1900/square degree, and two configurations is likely sufficient to attain high completeness in most areas.

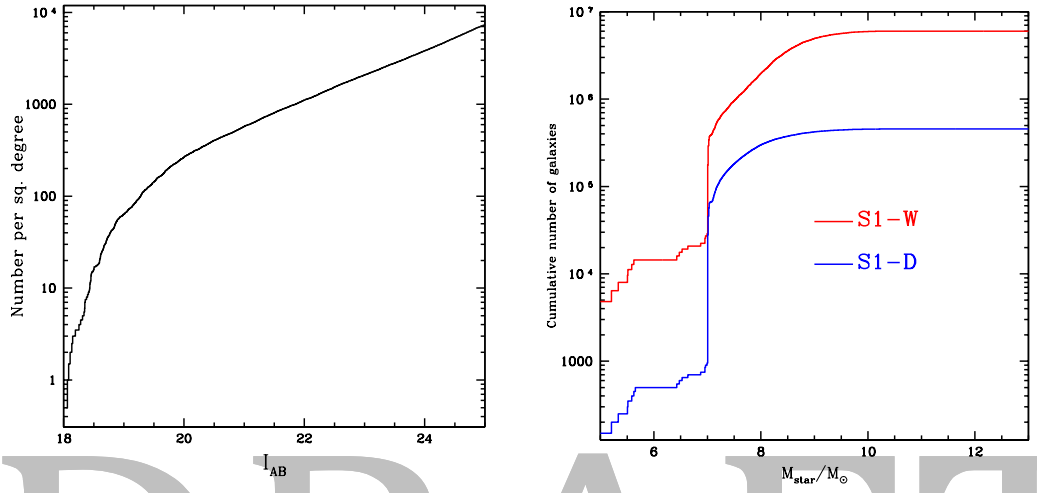

Figure 18: Left: Cumulative magnitude distribution of galaxies with z<0.2 per square degree, as determined from the COSMOS photometric redshift catalogue (Ilbert et al. 2009). Right: The same, but for stellar mass. The COSMOS field is small, only 2 square degrees, and thus not ideal for estimating the abundance of low mass galaxies at low redshift; but it should be indicative.

DRAFT

This survey will be volume-limited for galaxies with $M > 10^{8.5}$ and, as shown in Figure 18 will include about 1.5 million haloes with total masses $M \sim 10^{12}$. Most importantly it will also include more than 1 million galaxies with stellar masses $M < 10^{8}$, probing well into the dwarf regime where we currently have little understanding of how galaxies relate to their haloes.

In Figure 19 we show the theoretical halo mass function, with coloured lines indicating how many of those haloes in the S1-W survey are hosted by multiple galaxies with I < 23. With a high sampling completeness, the proposed survey will identify the haloes of all galaxies at the peak of the star formation efficiency function (Figure 12) within the z < 0.2 survey volume. In the right panel we show how the S1-W survey will compare with other surveys, existing and proposed, in terms of the number of haloes populated by at least four detected galaxies.

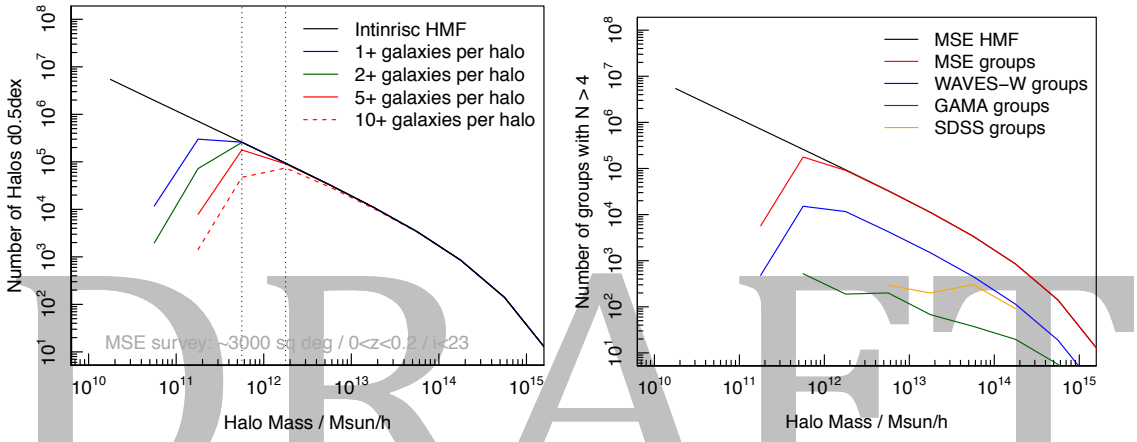

DRAFT

Figure 19: Left: The expected number of dark matter haloes in the S1-W survey that are populated by 1 or more galaxies with i<23 are shown by the coloured lines. If the survey is 100% efficient in obtaining redshifts for all galaxies to this limit, this is the expected performance. Galaxies at the peak of the galaxy formation efficiency curve, with halo masses $M_h=10^{12}M_{Sun}$, are all identified with at least one galaxy throughout the survey volume, with most populated by 5 or more galaxies. Right: The number of haloes populated by at least four observable galaxies, is shown for different surveys including the S1-W (MSE) proposed here. All haloes with $M>2x10^{12}M_{Sun}/h$ in the survey volume will be robustly detected.

F.3.1.2 S1 – D

To include the lowest-mass dwarf galaxies in our sample, and to robustly probe the structure of more massive haloes using plenty of tracers, we require a survey that takes full advantage of MSE's large aperture relative to most other survey-capable spectroscopic facilities. From a simple scaling assuming Poisson distributed sky-limited spectra, an integration time of 15h will enable observations of galaxies with i<24.5 to be observed with comparable S/N as for the S1-W sample. In practice, the depth achieved will depend on how well the sky subtraction can be done; these depths will be challenging with fiber spectroscopy. There is great advantage to pushing as deep as possible, and reaching i=25 would allow a complete sampling of all $M_h>10^{12}M_{Sun}$ haloes in the survey volume with at least 5 tracers. This depth is reached for example by the VUDS survey (Le Fèvre et al. 2014) in 14h for higher redshift galaxies; but this is slit spectroscopy and relies on the signal-to-noise ratio at ~840nm. As noted earlier, reaching

sufficient S/N at blue wavelengths for z<0.2 galaxies is more challenging at a given i-magnitude. For the present purposes we will adopt i<24.5 as an appropriately conservative limit.

As shown in Figure 18, extending the S1-W survey to i = 24.5 would add anther 3000 z < 0.2 galaxies per square degree on average. To sample this population well requires another two configurations per pointing, so a minimum of 36h per pointing with overheads can be expected in addition to the time required to observe the brighter population, presumably as part of the S1-W survey. A survey on the order of 100 square degrees is feasible in a few years to this depth.

The survey area need not be contiguous, but rather should be chosen to sample a wide and cosmologically relevant range of environments and halo masses. A recommended strategy would be to select haloes from the S1-W survey, and follow them up more deeply. A possible selection is described in the Table below.

Mass (10^{13} M_{Sun})	**Number of pointings**	**Number of fiber configurations per field**	**Survey time (h) including 20% overhead**
>50 (rich clusters)	10	5	900
10-50 (poor clusters)	10	3	900
1-10 (groups)	15	3	810
0.1-1 (massive galaxies)	30	2	1080
0.01-0.1 (M* galaxies)	50	2	1800
Total:	**105**	**285 fiber configurations**	**5490**

DRAFT

In total S1-D will yield over 800 000 redshifts, primarily for galaxies with z < 0.2 and 23 < i < 24.5. However, in addition to pushing the limit to fainter magnitudes, this survey has a role in obtaining high signal-to-noise (and possibly higher resolution) spectroscopy for brighter galaxies. In 15h we will reach SNR > 20 for galaxies with I < 22, and SNR > 100 for galaxies with i < 20.5. We propose to allocate ~200 fibers in each configuration to such galaxies (50 with i < 20.5 and the remainder at i < 22). By the end of the survey we will have a sample of ~15 000 spectra with SNR > 100 and ~44 000 with SNR > 20. These will enable detailed population analyses, including study of the initial mass function, in low-mass galaxies. In the clusters we can do even better, since the survey anticipates five deep fiber configurations per field. A subsample of fainter galaxies might be reobserved in each configuration, to build up a total integration time of

75h. This would achieve final spectra with SNR > 20 for galaxies with i < 23, and SNR > 100 for galaxies with i < 21.3, extending the stellar mass range with such exquisite data into the interesting dwarf regime.

For a subset of large galaxies, we might also consider placing the fiber at different locations within, say $2R_e$, during repeat observations to better sample the full, integrated stellar population and test for systematic effects.

F.3.2 Observables and diagnostics

Redshift measurements require spectra with low SNR, about 3 integrated over a typical absorption line, and can be obtained through cross-correlation template fitting using auto-z (Baldry et al 2014) or similar software. We will easily be able to obtain emission line equivalent widths necessary for measuring star formation rates and identifying AGN/LINER activity with data of this quality. To obtain robust redshifts for non-emission galaxies the presence of Ca-H&K lines, the 400 nm break feature and the G-band at 430nm is a minimum requirement. At low redshift this is an important constraint. For a passive galaxy at z = 0, the SNR at 4000A is about a factor 4 lower than it will be at 7000A. In this sense it is harder to get redshifts for z = 0 galaxies than those at z = 0.7.

Velocities need to be measured with a precision of ~30 km/s or better, in order to identify substructures and obtain a robust dynamical description of the lowest-mass haloes in the sample. This is achievable with resolution R~3000, but analysis of close galaxy pairs and dynamics of low mass haloes would benefit from R~6500.

DRAFT

In principle, such low SNR spectra can also be useful for studying the star formation rate and gas-phase metallicity using nebular emission lines. In order to determine gas-phase metallicities and AGN contributions, the minimum wavelength range must cover from Hβ (4863 A) to [NII] 6583 A, which encompasses the minimum number of lines required to make a dust correction (Hα and Hβ) and use strong line metallicity diagnostics (e.g. [OIII] 4959, 5007, Kewley & Ellison 2008). Our survey will also have access to "direct" chemical abundances at lower masses and metallicities, from the weak [OIII] 4363 auroral line. Furthermore, coverage of [OII] 3727 provides a direct oxygen abundance, and is particularly valuable in galaxies where there may be non-standard N/O ratios, as has previously been shown by Berg et al. (2011). These same emission lines can be used for standard AGN classification (e.g. Kauffmann et al. 2003). The [SII] doublet at 6717, 6731A, visible throughout our redshift range with MSE, is additionally useful for metallicity measurements. Finally, Paβ (1.282 μm) enables an accurate determination of the dust attenuation in the gaseous component, and thus a more accurate measurement of the star formation rate, since it is much less attenuated than the Balmer lines.

To measure the stellar metallicity and older stellar populations of galaxies generally requires spectra of higher signal-to-noise ratio and resolution than redshifts alone. The required exposure time is determined by requirements to measure continuum features (absorption lines and spectral breaks). To break the age-metallicity degeneracy and so obtain more precise ages of the dominant red population, one needs absorption line indices from high continuum SNR (> 25) spectra, with resolution ~5000 or greater. For red galaxies, mean stellar ages and

metallicities can be determined to 20% and 0.1 dex respectively, at this depth. This will be possible in 1h exposures for galaxies with r < 21, and in ten hours to r < 22.2. The most challenging observations would be the measurement of tracers of the initial mass function shape in a large sample of galaxies. This requires very high SNR (>200) spectroscopy of dwarf-sensitive lines such as TiO4770, CaH6380, Na I8183, 8195, FeH 9916 (Wing-Ford) and CaI10345 lines (Spiniello et al. 2014; van Dokkum & Conroy 2010; Smith 2012). A moderate resolution of R ~ 5000 is required to deblend these weak lines from their neighbours.

An important consideration is how the fiber diameter compares with the physical size of the galaxy targets. Physical interpretation beyond redshifts is compromised when only the central regions are probed. For galaxies fainter than i = 19.5, though, the average effective radius of galaxies is comparable to or smaller than the fiber diameter (e.g. Griffith et al. 2012). Brighter galaxies will be effectively studied with DESI and IFU surveys like SAMI and MaNGA anyway, so MSE provides the perfect complement by targeting the fainter population.

F.4 Target selection

F.4.1 General consideration

Targets need to be selected from uniform, well-calibrated, multicolour imaging with a 5σ point source depth that is at least a magnitude deeper than the spectroscopic limit (so I = 24 for the Wide survey and i < 25.5 for the Deep). In order to obtain a mass-complete sample, surface brightness selection effects must also be considered (e.g. Phillipps & Disney 1986; Cross & Driver 2002; Baldry et al. 2012). GAMA target selection is based on SDSS imaging, and with a surface brightness limit of $\mu_r < 23.5$ mag/arcsec^2 incompleteness becomes important at stellar masses $M_{star}<10^{8.5}M_{Sun}$ (Baldry et al. 2012). LSST, for example, will push much fainter, with a ten year depth of about 27 mag/arcsec^2 in the i-band.

DRAFT

Good photometric redshifts are essential for efficiently assigning fibers to targets of interest; otherwise it becomes extremely inefficient to sample faint galaxies at low redshift, with fainter apparent magnitudes naturally pushing the peak in the n(z) distribution to higher redshifts. To make the survey efficient we require photometric redshifts, and these must be accurate to $\sigma_z/(1+z) \sim 0.01$ in order to select galaxies at z < 0.2 without significant contamination from higher redshifts. Because of the low redshift, deep coverage in the u-band and preferably bluer is required to ensure sufficiently good photometric redshifts. We note that with u-band data CFHTLS, for example, achieves $\sigma_z/(1+z) \sim 0.04$ at z > 0.13, but breaks down at lower redshifts because the u-band is not blue enough.

Good spatial resolution is needed to distinguish low-mass galaxies from stars, though stars are not dominant at the magnitudes of interest. High spatial resolution imaging will also provide morphological information, crucial for identifying possible triggers for changes in stellar populations, such as tidal interactions and stripping events. Such imaging is also required to identify the bulge component, closely linked to supermassive black hole activity. In particular for dwarf galaxies it will provide the opportunity to identify bulgeless AGN.

As galaxy formation and evolution is a complex, multiscale process, it is desirable to have as much multi-wavelength data as possible. Of particular value are measurements of the gas content from ALMA, SKA and its precursors ASKAP and MeerKat, to couple with all the metrics we will obtain from the spectra and imaging (SFRs, O/H, M_* etc.).

Targets need to be selected from uniform, well-calibrated, multicolour imaging with a 5σ point source depth that is at least a magnitude deeper than the spectroscopic limit (so i=24 for the Wide survey and i<25.5 for the Deep). In order to obtain a mass-complete sample, surface brightness selection effects must also be considered (e.g. Phillipps & Disney 1986; Cross & Driver 2002; Baldry et al. 2012). GAMA target selection is based on SDSS imaging, and with a surface brightness limit of μ_r<23.5 mag/arcsec^2 incompleteness becomes important at stellar masses $M_{star}<10^{8.5}M_{Sun}$ (Baldry et al. 2012). LSST, for example, will push much fainter, with a ten year depth of about 27 mag/arcsec^2 in the i-band.

Good photometric redshifts are essential for efficiently assigning fibers to targets of interest; otherwise it becomes extremely inefficient to sample faint galaxies at low redshift, with fainter apparent magnitudes naturally pushing the peak in the n(z) distribution to higher redshifts. To make the survey efficient we require photometric redshifts, and these must be accurate to $\sigma_z/(1+z)\sim0.01$ in order to select galaxies at z<0.2 without significant contamination from higher redshifts. Because of the low redshift, deep coverage in the u-band and preferably bluer is required to ensure sufficiently good photometric redshifts. We note that with u-band data CFHTLS, for example, achieves $\sigma_z/(1+z)\sim0.04$ at z>0.13, but breaks down at lower redshifts because the u-band is not blue enough.

DRAFT

Good spatial resolution is needed to distinguish low-mass galaxies from stars, though stars are not dominant at the magnitudes of interest. High spatial resolution imaging will also provide morphological information, crucial for identifying possible triggers for changes in stellar populations, such as tidal interactions and stripping events. Such imaging is also required to identify the bulge component, closely linked to supermassive black hole activity. In particular for dwarf galaxies it will provide the opportunity to identify bulgeless AGN.

As galaxy formation and evolution is a complex, multiscale process, it is desirable to have as much multi-wavelength data as possible. Of particular value are measurements of the gas content from ALMA, SKA and its precursors ASKAP and MeerKat, to couple with all the metrics we will obtain from the spectra and imaging (SFRs, O/H, M* etc.).

F.4.2 S1 – W

Given the northern location of MSE, a good option for imaging would be a Large Survey with CFHT, covering the northern Euclid footprint. The Canada-France Imaging Survey (CFIS) idea, currently under development, would potentially meet our needs. One proposed plan is to cover 6500 square degrees in four filters, to i = 24.5.

Alternatively, the LSST survey single-visit depth of i = 24 is also sufficient for target identification, and a survey area of 3200 square degrees is likely to be easily accessible by MSE.

The WFIRST High Latitude Survey will cover about 2000 square degrees, but be located in the South. It is unclear how much of that area will be accessible to MSE. It is expected that WFIRST will ask LSST to prioritize observations in such a way as to reach the full 10-year depth within this region as soon as possible. It would be advantageous to target as much of this area as possible, spectroscopically.

F.4.3 S1 – D

The S1-D survey requires 100 square degrees of deep (i > 25) multicolour imaging; not necessarily contiguous but in fact including rare, massive clusters. Here the LSST survey would be ideal, as it will reach the required depth in about one year. Alternatively, some of the HSC survey fields might be appropriate, at least for the lower-density environments. The ~20 galaxy cluster fields should be selected based on their X-ray emission and bright-galaxy spectroscopy. Suitable X-ray catalogues already exist, and will be further improved by eROSITA, though access to the latter remains uncertain. In order to cover the virialized region in a single MSE pointing, clusters should be at z > 0.1; lower-redshift clusters, for which the lowest-mass galaxies can be studies, should be the focus of a separate survey.

F.5 Cadence and temporal characteristics

None

DRAFT

F.6 Calibration requirements

The wavelength calibration needs to be accurate to better than the desired velocity accuracy throughout (~30 km/s), to remove any systematic biases from the redshift distributions. The expectation would be to have pixel level or better calibration accuracy.

The main sky features will need to be either well subtracted or potentially (for stronger line) masked entirely. Experience from GAMA suggests that 1% sky subtraction accuracy is probably adequate for obtaining good redshifts. This will be a challenge for the S1-D survey, where galaxies are much fainter than the dark sky. Sky residuals should therefore be no more than a few percent of the Poisson noise. In order to achieve this, nod & shuffle (Glazebrook & Bland-Hawthorn 2001) or similar techniques must be considered.

For the core redshift science the spectrophotometric calibration does not need to be especially good. Getting Hα SFR from EW also does not require particularly good flux calibration. However, for stellar population work, accurate relative spectrophotometry is required. This should be at least as good as for the SDSS, at the level of 1 – 2% over the wavelength range covered.

In the absence of an IFU, we may rely on repositioning fibers, and/or allocating multiple fibers to a single galaxy, to extract some spatial information as a secondary goal. This requires good repeatability and fiber-to-fiber calibration of spectrophotometry and wavelength calibration. These systematic uncertainties should be subdominant to those of a single fiber observation; i.e. 1 – 2% spectrophotometry and wavelength calibration accurate to ~10km/s. For the same

reasons, the position of each fiber must be known to within a fraction of a galaxy scale radius, <0.1". This precision is also needed to accurately place fibers on faint galaxies.

F.7 Data processing requirements

At a minimum we would expect to return sky subtracted, wavelength calibrated, but not flux calibrated, 1D spectra for each targeted object. We would also produce redshift measurements with quality estimates for each object. We expect to do this using a tool similar to auto-z (Baldry et al 2014). Instrumental signatures (the major ones) will need to be removed prior to redshift measurements. Auto-z is fairly robust to poor flux calibration and even imperfect sky subtraction issues, but the wavelength calibration would need to be very good throughout. Potentially the exact wavelength calibration could be left as a variable within auto-z, but this is probably non-ideal, and likely to create degenerate solutions.

Higher order products, depending on the data quality (since these products will not drive the survey design), are potentially equivalent width for various features. The expectation would be to do this via direct line summation or Gaussian fitting technique (e.g. Hopkins et al 2013).

A mechanism for rapidly assessing whether any given target has a reliable redshift and can therefore be removed from the target list would be hugely beneficial to the survey. Such dynamic feedback would prevent time wasted increasing S/N beyond what is required for the core case. This would require a pipeline that can dynamically reduce, stack and redshift the individual short integrations (e.g. 20 mins) for each galaxy. Scheduling software that can cope with such dynamism (currently not an option at ESO survey facilities) would give MSE an appreciable advantage in the domain of extra-galactic surveys.

DRAFT

F.8 Any other issues

F.8.1 Survey locations

A lot of thought needs to go into the careful design of the survey regions, with consideration given the historic datasets in certain regions. This is particularly true for the UV and FIR, since this data will not be substantially improved for low redshift studies for a generation (the wide field GALEX and Herschel telescopes are now decommissioned). Thought must also be given to upcoming facilities. In the radio the SKA (based in South Africa and Australia) will be a game-changer for extra-galactic HI and continuum studies out to $z = 1$ (current facilities observe to only $z \sim 0.1$). Clearly the SKA will be optimal for Southern hemisphere fields, and MSE will be located in the Northern hemisphere. To combat this any proposed fields should be close to the equator, making them reasonably observable by facilities in either hemisphere. It is also vital that MSE has some influence and involvement in the location of the future Euclid and WFIRST deep fields. If these are placed at declination below -40 deg then they become unviable for MSE because the airmass at Mauna Kea is always poor. There is currently pressure within the WFIRST team to locate the high-latitude survey at southern declinations in order to avoid the ecliptic plane. In general it is advisable that the MSE survey volumes avoid the ecliptic and Milky-Way plane since this at least ensures shallow Euclid coverage with improved resolution compared to LSST.

F.8.2 Development options

The surveys described here will be a significant advance on anything that has come before them (e.g., Figure 17). No other planned facility has the same combined strengths of telescope aperture, field of view, and survey capability. Only Subaru/PFS would even be capable of competing, should that community decide to dedicate the telescope to spectroscopic surveys with that instrument.

Nonetheless, between now and first light, progress will continue to be made, as described above, with 4m class telescopes covering large areas and 10m class telescopes probing the faint galaxy population. And the surveys described here are enormous undertakings, taking ~11 000 hours to complete. Given RA constraints, weather considerations and the requirement for dark skies, this would take more than ten years, and is just one of many compelling science cases that MSE could carry out. Compromising on depth or area is not likely to yield a competitive survey; thus we should consider ways to improve either the observing strategy, or the technical capabilities of the facility.

Strategically, a better coordination with the proposed 4m surveys could be advantageous. For large areas of > 1000 square degrees, 4m telescopes with wider fields of view (e.g., 4MOST) are very effective. It is worth exploring in more detail what might be done with a survey like WAVES-Wide, to a shallower magnitude (~21.5) but over an area of ~3000 square degrees, complemented by a survey like lowz-Deep proposed here.

DRAFT

Technically, barring a way to significantly increase the sensitivity (aperture or throughput) or field of view of MSE, the biggest advantage would be to increase the fiber density. Even though the baseline fiber density is well-matched to the target density in this science case, increasing the density would improve the ability to observe targets pertaining to multiple science cases simultaneously. This would make a ten year survey much more palatable.

References

Bahé, Y., McCarthy, I., Balogh, M. & Font, A. 2013 MNRAS, 430, 3017
Baldry, I.K. et al. 2014 MNRAS 441, 2440
Baldry, I.K. et al. 2012, MNRAS 421, 621
Baldry, I.K., et al. 2006, MNRAS 373, 469
Baldry, I. & Glazebrook 2003 ApJ 593, 258
Baldry, I., Glazebrook, K. & Driver, S. 2008 MNRAS 388, 945
Balogh, M., Navarro, J., Morris, S. 2000 ApJ 540, 113
Balogh, M.L., et al. 2004a, MNRAS 348, 1355
Balogh, M.L. et al. 2004b, ApJ 615, 101
Bauer, A.E. et al. 2013, MNRAS 434, 209
Behroozi, Peter S., R.H. Wechsler, & C. Conroy, 2013, ApJ 770, 57
Berg, D., Skillman, E. & Marble, A. 2011 ApJ 738, 2
Boylan-Kolchin, M., Bullock, J., Kaplinghat, M. 2011, MNRAS 415, 40
Brinchmann, J. et al. 2004 MNRAS 351, 1151
Cappellari, M. et al. 2012, Nature 484, 485
Casteels, K. et al. 2014, MNRAS 445, 1157
Cole, S. et al. 2001, MNRAS 326, 255
Cole, A. et al. 2014 ApJ 795, 54

Cross, N. & Driver, S. 2002 MNRAS, 329, 579
Driver, S., et al. 2015, arXiv:1507.00676
Driver, S. & Robotham, A. 2010 MNRAS 407, 2131
Ellison, S.L., D.R. et al. 2008, ApJ 672, 107
Ellison, S., Simard, L., Cowan, N., Baldry, I., Patton, D., McConnachie, A. 2009 MNRAS, 396, 1257
Ferreras, I. et al. 2013 MNRAS 2013
Fillingham, S., et al. 2015, MNRAS, submitted, arXiv:1503.06803
Furlong, M. et al. 2015 MNRAS 450, 4486
Garilli, B. et al. 2014 A&A 562, 23
Geha, M., Blanton, M., Yan, R. & Tinker, J. 2012 ApJ 757, 85
Gilbank, D.G., Baldry, I., Balogh, M.L., Glazebrook, K. & Bower, R. 2010 MNRAS 405, 2594
Glazebrook, K. & Bland-Hawthorn, J. 2001, PASP 113, 197
Gomez, P.L., et al. 2003, ApJ 584, 210
Greene, J. & Ho, L. 2004 ApJ 610, 722
Griffith, R. et al. 2012 ApJS 200, 9
Gunawardhana et al. 2011, MNRAS 415, 1647
Hopkins, A. et al. 2013 MNRAS 430, 2047
Ilbert, O. et al. 2009 ApJ 690, 1236
Kauffmann, G. et al. 2003 MNRAS 346, 1055
Kennicutt, R. 1983 ApJ 272, 54
Kewley, L.J., and S.L. Ellison. 2008, ApJ 681, 1183
Kirby, E., Cohen, J., Guhathakurta, P., Cheng, L., Bullock, J. & Gallazzi, A. 2013 ApJ 779, 102
La Barbera, F., Ferreras, I. & Vazdekis, A. 2015 MNRAS 449, 137
Lara-Lopez, M. et al. 2013a, MNRAS 433, 35
Lara-Lopez, M. et al. 2013b, MNRAS 434, 451
Larson, R., Tinsley, B. & Caldwell, C. 1980, ApJ 237, 692
Le Fèvre et al. 2005, A&A 439, 845
Lilly, S. et al. 2007 ApJS 172, 70
Lilly, S., Carollo, C.M., Pipino, A., Renzini, A. & Peng, Y. 2013 ApJ 772, 119
Lu, T., Gilbank, D., McGee, S., Balogh, M. & Gallagher, S. 2012 MNRAS 420, 126
Marinoni, C., and M.J. Hudson 2002, ApJ 568, 101
McGee, S., Bower, R. & Balogh, M. 2014 MNRAS 442, 105
McGee, S., Goto, R. & Balogh, M. 2014 MNRAS 438, 3188
McGee, S., Balogh, M., Bower, R., Font, A. & McCarthy, I. 2009 MNRAS 400, 937
Moore, B. et al. 1999, ApJ 524, 19
Newman, J. et al. 2013 ApJS 208, 5
Oman, K. et al. 2015, MNRAS, in press, arXiv:1504.01437
Peng, Y., Maiolino, R. & Cochrane, R. 2015, Nature 521, 192
Phillipps, S. & Disney, M. 1986 221, 1039
Prescott, M. et al. 2011 MNRAS, 417, 1374
Rasmussen, J., Mulchaey, J., Bai, L, Ponman, T., Raychaudhury, S., Dariush, A. 2012 ApJ 757, 122
Reines, A., Greene, J. & Geha, M. 2013 ApJ 775, 116
Rines, K., Diaferio, A. & Natarajan, P. 2007 ApJ 657, 183
Robotham, A. et al. 2011 MNRAS 416, 2640
Robotham, A. et al. 2014 MNRAS 444, 3986
Satyapal, S., Secrest, N., McAlpine, W., Ellison, S., Fischer, J. & Rosenberg, J. 2014 ApJ 784, 113
Scrimgeour, M. et al. 2012 MNRAS 425, 116
Smith, R., Lucey, J. & Carter, D. 2012, MNRAS 426, 2994
Smith, R. 2014 MNRAS 443, 69
Spiniello, C., Trager, S., Koopmans, L. & Conroy, C. 2014 MNRAS 438, 1483
Sweet, S. et al. 2014 ApJ 782, 35
Takada, M. et al. 2014 PASJ 66, 1
Tempel, E. et al. 2014 A&A 566, 1
Tremonti, C. et al. 2004 ApJ 613, 898
Trujillo, I. et al. 2006, ApJ 650, 18

DRAFT

van Dokkum, P. & Conroy, C. 2010, Nature 468, 940
Vulcani, B., Poggianti, B., Finn, R., Rudnick, G., Desai, V. & Bamford, S. 2010 ApJ 710, 1
Wetzel, A., Tinker, J., Conroy, C. & van den Bosch, F. 2013, MNRAS 432, 336

DRAFT

Appendix G DSC – SRO – 07 Baryonic structures and the dark matter distribution in Virgo and Coma

(Final draft in progress)

G.1 Abstract

Galaxy clusters act as (nearly) closed boxes, retaining the entire thermal and gravitational history of their assembly and growth. Here we propose an ambitious survey targeting all baryonic structures (mostly galaxies and globular clusters) brighter than $g \sim 24.5$ within the virial radii of the two nearest large clusters, Virgo and Coma. The brightest subset of sources ($g < 22$; some 50 000 sources in Virgo) will also be observed at high resolution. With this unprecedented complete dataset, we will map the dark matter distribution of halos on the largest scales by examining the line of sight velocities of all baryonic tracer particles in these clusters. This will provide a precise measurement of the dark matter mass distribution in the clusters, and reveal coherent structure in phase space that can be used to infer the accretion history within the cluster potential. The MSE Virgo+Coma survey will be unrivalled for exploring all aspects of galaxy evolution, especially with respect to stellar populations and low mass galaxies. This is because the Virgo and Coma clusters afford us the best opportunity to study the galaxy population in its totality, from quiescent to star forming galaxies, from the high density cores to the low-surface brightness haloes, across a wide mass range, on all spatial scales, in a controlled environment in which all other baryonic substructures are also well characterized.

DRAFT

G.2 Science Justification

G.3 Key astrophysical observables

G.4 Target selection

G.5 Cadence and temporal characteristics

G.6 Calibration requirements

G.7 Data processing requirements

G.8 Any other issues

Appendix H DSC – SRO – 08 Evolution of galaxies, halos, and structure over 12 Gyrs

Authors: Aaron Robotham, Michael Balogh, Luke Davies, Simon Driver, Carlo Schmid, Yue Shen

H.1 Abstract

Here we propose an ambitious design of nine photo-z selected survey cubes that will allow MSE to measure the build up of large scale structure, stellar mass, halo occupation and star formation out to z = 5.5. By targeting (300 Mpc/h)^3 boxes, each volume will measure "Universal" values for an array of potential experiments.

At low redshift we will directly observe halo abundances below 10^{12} $M_{\odot}$, which means we can measure the occupation of halos and their abundance over a four decade range in halo mass, accounting for the majority of stellar mass in the low-redshift Universe. At higher redshifts our survey volumes will trace the transition from merger-dominated spheroid formation to the growth of disks, covering the peak in star-formation and merger activity.

This combination of depth, area and photo-z selection is not possible without a combination of LSST and MSE. As such, MSE will be able to produce the definitive survey of structure, halos and galaxy evolution over 12 billion years. With the nominal design of MSE these proposed surveys will take ~7 years to observe.

DRAFT

H.2 Science Justification

Current surveys that span the low (z < 0.3, e.g. GAMA/SDSS), moderate (z ~ 1, e.g. zCOSMOS, Lilly et al 2007) and high redshift (z > 3, e.g. VVDS, Le Fevre 2013) Universe come from hugely different telescopes. At low redshift the extra-galactic field is dominated by the Sloan Telescope and the Anglo-Australian Telescope (2.5/4m, FoV ~ 3/2 deg) and at higher redshifts a mixture of large facilities dominate (8+m, FoV << 1 deg). Low and high redshift surveys also tend to target photometric data from different facilities. Historically, co-moving volumes for high redshift surveys are tiny (comfortably dominating the error term for any 'Universal measurement') and tend to be high incomplete. In particular, surveys that use Ly-α to obtain redshifts have very poor velocity accuracy (due to the complex nebula component) and only probe a minority of available galaxies within a survey volume (~20%, VVDS, Le Fevre 2013). By designing a suite of surveys with equal co-moving volumes from low redshift (z ~ 0) to high redshift (z ~ 5.5) MSE will definitively answer a host of science questions over 12 Gyrs in look-back time.

The critical dark matter halo mass range in terms of stellar mass content is the decade around $10^{12}M_{\odot}$ (see left panel of Figure 20). This halo mass range contains our own Milky-Way halo and that of our nearest large spiral galaxy M31. To investigate galaxies in their most common environment requires an ambitious experiment. To robustly detect groups with a low false-positive rate we require at least 5 galaxies to be observable within a group/halo, and to measure dynamical halo mass within a factor ~3 accuracy requires 10 or more galaxies to be observed within a group/halo (Robotham et al 2011). Also, to obtain reasonable number statistics for rare massive clusters/halos a large volume of the Universe must be surveyed. If these science cases are combined to coexist within the same volume (both sky coordinates and redshift window

aligned) then we require a large sky area and a robust photo-z selection in order to improve the efficiency of the volume overlap. Without a photo-z selection (i.e. only an apparent magnitude selection) we would naturally find more massive clusters at higher redshifts only, and we would have a comparatively small volume that contains the full range of $10^{12}M_{\odot}$ - $10^{15}M_{\odot}$ halos (see Figure 16 in Robotham et al 2011). Also, without a photo-z selection it becomes extremely inefficient to sample faint galaxies at low redshift, with fainter apparent magnitudes naturally pushing the peak in the n(z) distribution to higher redshifts.

With this aim in mind, and with the knowledge that such a study opens up a large suite of complementary science such as ultra-large dynamic range close-pair and halo occupation distribution (HOD) studies (see Robotham et al 2014), we have designed an ambitious survey that only MSE is reasonably able to conduct on a sensible timescale (~7 years). The basic goal is to observe 3200 square degrees of the Northern extra-galactic sky (overlapping fully with the proposed LSST survey region and substantially with the current SDSS footprint) between redshift 0 and 0.2 and down to a limiting magnitude of i_{AB}=23 selected from LSST standard depth multi-year survey (see SRO 7 survey S1-W). To efficiently probe down to low mass halos it is advantageous to observe as large an area as possible, and 3200 sq deg over the suggested redshift extent minimally contains a 300 x 300 x 300 Mpc/h co-moving cube. This means our volume is large enough that we reach Universal homogeneity in all three dimensions (Srimgeour et al 2013, Driver & Robotham 2010). By observing to i = 23 within z = 0.2 we expect to be deep enough that essentially all $10^{12}M_{\odot}$ mass halos are both detected and have a reasonable mass estimate, with 10 or more galaxies identified (see RHS of Figure 20).

DRAFT

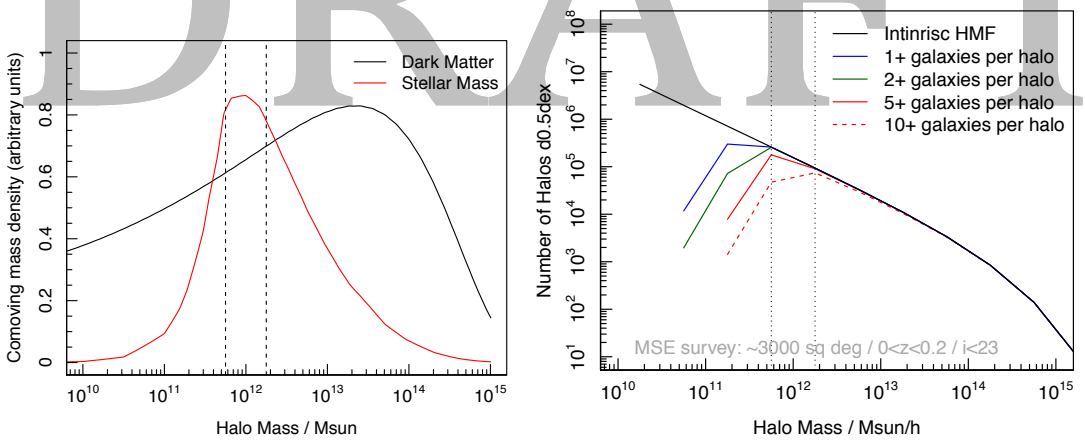

Figure 20: Left panel presents the distribution of dark matter and stellar mass as a function of halo mass. It is clear that we expect it to be highly dominated by $10^{12}M_{\odot}$ halos. Right panel presents the expected galaxy occupation frequency as a function of halo mass. Our proposed survey will sample the $10^{12}M_{\odot}$ halo mass regime with better than 5 galaxies per halo, allowing for per-halo dynamical mass measurements.

By repeating the basic survey design (in particular the target volume) for this low redshift HOD and halo abundance focused science case, we can open up a new suite of science. Figure 21 shows a basic possible observing strategy, where a co-moving 300 Mpc/h cube is targeted in nine separate redshift windows using a mixture of LSST photo-z selection (S1-W to S7) and Euclid photo-z selection (S8 and S9). Each survey region proposed would be targeted down to a

different i/Y-band limit but with ~100% completeness within each volume (certainly better than 95%, i.e. ~SDSS). Such a suite of surveys allows detailed halo occupation modelling out to z = 5, spanning the rapid increase and slow decline in universal star-formation (top panel of Figure 21), the era of merger dominated mass build-up (z > 2), the transition into galaxy disk formation and in-situ star-formation dominating build-up (z < 2) and the epoch of rapid large-scale structure formation (z > 2). For obtaining robust "Universal values" for merger rates and star formation history the co-moving volume analysed and the stellar mass depth observed is key. By selecting common 300 Mpc/h cubes we will have sub per-cent sample variance independent of look-back time. By aiming to be complete to stellar masses at least 1 dex below M_* for S1 to S4 we can definitely explore the interplay between mass build up through merger and star formation (see Robotham et al 2014 for a z=0.2 version of this experiment). Beyond this range we are limited by the high quality photo-z i < 25.3 sample provided by LSST. Despite this, we can still probe the dominant component of stellar mass (M_*) and its halo occupation distribution out to z = 2 with S5 and S6. This takes our galaxy evolution analysis out to 10 Gyrs in consistent co-moving volumes that have high statistical quality.

New survey possibilities are opened up if MSE has a spectral range covering 380-1800 nm. Importantly OII becomes visible out to z > 3, i.e., it becomes a common emission feature that S1 to S8 can all observe, offering a consistent star-formation tracer over nearly 12 Gyrs from a single facility. If we have access to Ly-α and OII then direct measurements of the feedback of gas into the inter-stellar medium is possible. With the extended range this direct fuelling can be measured for S7 and S8. We will also be able to observe Hα, and construct a full BPT diagram out to z = 2 (i.e. S1 to S6) with an extended spectrograph range (1800nm).

DRAFT

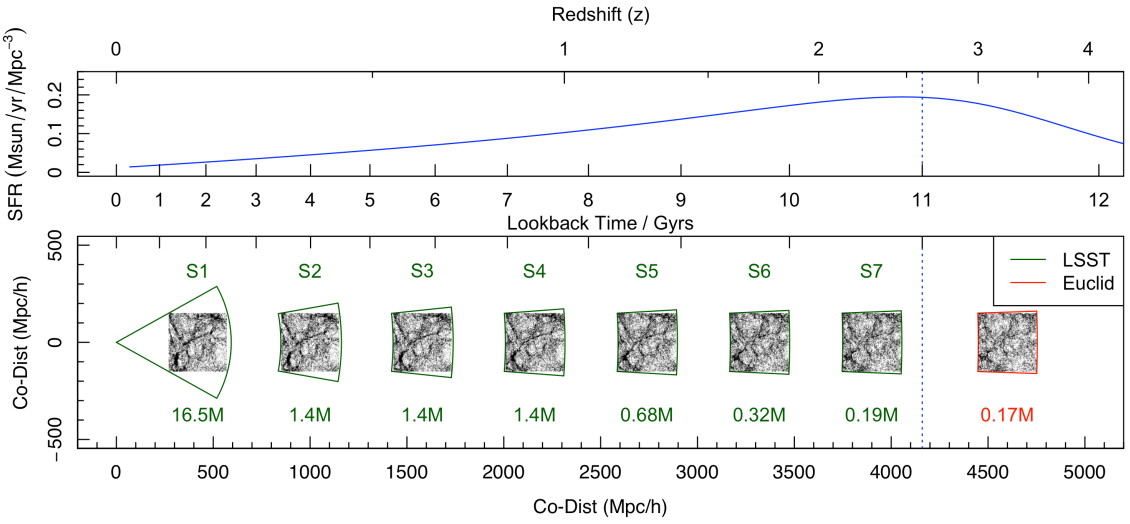

Figure 21: A proposed range of equi-comoving MSE survey cubes (S1 to S8). The top panel shows the cosmic SFH from Hopkins & Beacom 2006. The lower panel shows the proposed surveys, showing the growth in large-scale structure in TAO simulated (50 Mpc/h)^3 survey cubes.

It is clear that such a survey suite opens up a vast amount of science that is not accessible to any other facility. A non-exhaustive summary is given below, where we will:

- Measure halo occupation (through group finding) below $10^{12}M_{\odot}$. This combined with an HOD analysis will definitively uncover the interplay between stellar mass and halos, and will put any detailed study of individual halos (e.g. future Milky-Way and M31 "archeology" studies) into a proper cosmological context.

- Directly observe the evolution of the massive end of the halo mass function out to redshift 1 (half the age of the Universe). This is step beyond cluster count cosmology, and will be conducted with a homogenous selection with LSST (the selection function is one of the major limitations of current cluster cosmology work).

- Study the evolution of the large-scale structure and cosmic web out to z = 5 with a consistent galaxy tracer with homogenous bias.

- Study the merger rate and star-formation history for all galaxies down to $M_{*}/10$ (covering the converged majority of stellar mass) out to z = 1.

- Study the close clustering and merger rate of massive galaxies ($10^{11}M_{\odot}$) out to z = 5.

- With photometry from LSST we will be able the majority of the stellar component of the cosmic spectral energy distribution (CSED) out to z = 2.

DRAFT

- Together with other next generation telescopes (most significantly LSST, Euclid, WFIRST, SKA, 30+m telescopes) we these surveys will have a vital role in:
    - Measuring morphological evolution to z = 1
    - Studying the interplay between gas, dust, stars and environment
    - Providing IFU targets for 30+m telescopes for well understood samples at multiple epochs
    - Offering the sample superset for high SNR observations of individual galaxies in order to ascertain the evolution of metals through cosmic time.

- Especially at higher redshifts, exciting work looking at the clustering of AGN is viable. This would naturally be a subset of the proposed surveys, but extended AGN focused science cases could be constructed and incorporated into the nominal design.

The main competition to MSE in doing such a combined survey is Subaru/PFS (Takada et al 2013) and VLT-MOONS (Cirasulo et al 2012). PFS will have a spectral range 380 – 1300nm. It will nominally be conducting $z < 1$, $i < 21.5$ and $1 < z < 2$, $i < 23.9$ photo-z pre-selection surveys (based on shallower HSC data). In both regimes the surveys discussed here are at least a magnitude deeper (a factor ~3 in stellar mass) and over much larger areas (fixed 16 square degrees for PFS, 400 to 30 square degrees over the same range for MSE. The huge advantage of MSE compared to all of the proposed PFS surveys is that we will be extending to the scale of homogeneity in all three dimensions. For many of the science cases laid out here (and

foreshadowed on a smaller scale by PFS) the definitive measurement will be made by MSE, with no further appreciable improvements to be made by moving to larger survey volumes (since many extra-galactic measurements are dominated by sample variance not Poisson statistics of the sample itself).

Regarding potential competition, VLT/MOONS will have a spectral range 680 – 1800nm and is focusing on surveys at z > 1. Where MSE has a potentially huge advantage is the LSST and Euclid/WFIRST photometric source catalogues. These telescopes will only become available post 2020, and offer a paradigm shift in optical quality. In particular, using LSST allows us to conduct surveys S1 (3200 square degrees) to S7 (22 square degrees) with identical photometry and photo-z technique. Such homogeneity will improve the robustness of almost every type of analysis made. Given the fast survey speed of MSE, once LSST and Euclid data become available no other facility will be able to keep up with the observing speed of MSE, i.e. it will dominate the next generation of spectroscopic surveys from 0 < z < 6.

Cirasulo, 2012, arXiv, 1208.5780
Driver, 2010, MNRAS, 407
Hopkins, 2006 ApJ, 651
Le Fevre, 2013, A&A, 559
Lilly, 2007, ApJS, 172
Robotham, 2011, MNRAS, 424
Robotham, 2014, MNRAS, 444
Srimgeour, 2012, MNRAS, 425
Takada, 2013, arXiv, 1206.0737

DRAFT

H.3 Key astrophysical observables

For all clustering related experiments the core observation will be a redshift. This can be obtained through cross-correlation template fitting using auto-z (Baldry et al 2014) or similar. Value added products would be to get better signal-to-noise for star-formation features (Hα and OII) and for absorption features (Mg and Na). Broadly speaking our required spectral range is $372.7(1+z_{lo})$ to $372.7(1+z_{hi})$ [for tracing OII, our main driver]. Similarly we have $517.5(1+z_{hi})$ [for tracing Mg-b] $589.4(1+z_{hi})$ [for tracing Na] ($656.4(1+z_{hi})$ [for tracing Hα].

The nominal range of 380 – 1300nm for MSE is adequate for a large amount of HOD related science (see Figure 3), allowing Hα measurements out to z=1 (S4) and Mg-b absorption out to z=1.5 (S5). For robust redshifts for non-emission galaxies the presence of C-K and g-band (i.e. the 400 nm break feature) is probably a sensible minimum requirement, meaning we can do reasonably unbiased HOD target selection and analysis all the way to an upper limit of z = 2 with the nominal design. This is within the regime of interest, and allows for a possible analysis of the interplay between merging and star-formation at z = 2 (S6). If the spectrograph is extended out to 1800 nm (i.e. H-band limit) then OII (and H-K and g-band) is visible out to S8 (z = 3.5), allowing high fidelity velocity measurements (and therefore HOD analysis, at least for massive halos) for S1 to S8. High quality OII redshifts are only possible in S9 if the spectrograph range is increased to 2400 nm (i.e. K-band limit). It should be noted that the regular spacing of S1 to S7 could not be continued for S8 and S9 because the important OII line becomes highly attenuated by the sky, even at an excellent site such as MSE on Mauna-Kea. The S8 and S9 volumes were therefore

adjusted to optimally sit within the H and K bands respectively. By some cosmic conspiracy a 300Mpc/h LoS baseline almost exactly fits within these two bands.

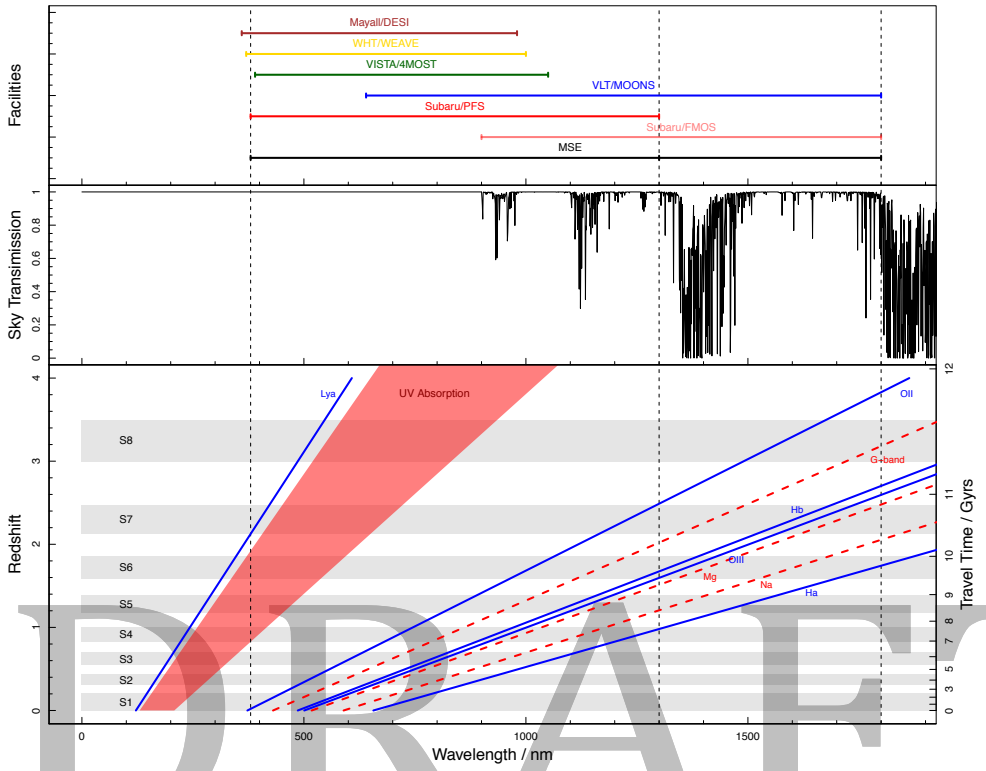

DRAFT

Figure 22: Accessibility of different spectral features for the different proposed volumes. The nominal 380-1300 nm MSE limit is shown as vertical dashed lines, with proposed extensions at 1800 nm (H band) also displayed. S1 – S7 via the OII line are still viable with a 380 – 1300 nm facility, but S8 is not viable).

For redshift measurements the key requirement is velocity accuracy. Pragmatically, a velocity accuracy that is within the typical velocity width of individual galaxies is appropriate. With moderate (R ~ few thousand) resolution we can expect to obtain a velocity accuracy of a few tens of km/s, where no more than 30 km/s is ideal. $10^{11/12}M_{\odot}$ halos have typical velocity dispersions of 100/200 km/s, and with 10 galaxies in a group we would expect relative velocity dispersion errors of 10% / 5% respectively, which is perfectly adequate for the more stringent group finding and halo occupation analysis requirements. It is not worth attempting to get much higher velocity accuracy because the internal dispersion of even a $10^{9}M_{\odot}$ galaxy is ~100 km/s, so velocity accuracy rapidly becomes limited by the complex internal kinematics of galaxies, not the spectral resolution. OII will provide a good estimate of the systemic galaxy velocity for all nine surveys, and Hα will also be an excellent velocity measure where available (to S4/S6 if the spectrograph limit is 1300/1800 respectively). Ly-α is a complex feature that contains high velocity nebula components and severe self-attenuation, so group finding (and associated halo science) based on Ly-α alone is likely to be highly compromised.

To extract the useful information for the data (i.e. redshifts) we would expect to require a basic reduction and then we would run auto-z (Baldry et al 2014) or similar. This is a proven technique

for extracting redshifts via absorption or emission lines, and does not rely on good flux calibration or continuum templates. This is a proven process from the GAMA survey, and should work equally well on MSE data given we will be operating in a similar SNR regime.

A successful redshift measurement requires good continuum SNR in the rest-frame optical regime (i.e. SNR of a few). From experience with GAMA, this is typically adequate to extract robust redshifts with a feature cross-correlation fitting code (auto-z, Baldry et al 2014). We expect to be able to obtain emission line equivalent widths and associated star formation rates with data of this quality. We would expect to be able to measure reasonable Hα derived star formation rates (which have higher SNR and are usually more robust than OII derived rates) from S1 to S4/S6 if we have a 380 to 1300/1800nm spectrograph range. These are also the survey limits in which we can plausibly construct a full BPT diagram to separate AGN/LINERS/star-forming galaxies. Such a division increases the scientific quality of the survey because AGNs and LINERS can otherwise be a strongly contaminating population for any star-formation measurement.

H.4 Target selection

Table 2 specifies the major characteristics of the required surveys. S1 – S7 will use a LSST defined survey selection. LSST is being designed to produce robust photometric redshifts for i < 25.3 out to z = 2.5 and over the entire visible sky, so this comfortably covers the proposed area of S1 (3000+ sq deg) and the redshift limit of S7. For S8, a Euclid or W-FIRST photo-z selection would be required, using the proposed deep surveys. These are nominally of the required depth, although it is uncertain where on the sky they will be placed. Clearly it is vital they are visible to MSE, since this is the only plausible source of photo-z optimized targeting for S8. For S2 – S7 it is possible that a similar selection could be made using photo-z from the Subaru/HSC surveys, but S1 is substantially larger than the proposed HSC fields. Having uniform photometry throughout is optimal, so LSST-based input catalogues for all of S1 – S7 is preferable.

DRAFT

Table 2: Main characteristics of the 9 proposed equi-comoving MSE survey volumes

Survey	z low	z high	Area / deg^2	Vol / Gpc^3	Photo	Selection	SM lim / $M_\odot$	Gal N (M)	Fibre H (M)	Passes
S1	0	0.214	3233.8	0.0674	LSST	i<25.3	$5x10^7$	16.5	5.7	2.8
S2	0.305	0.435	398.6	0.0399	LSST	i<22.5	$5x10^9$	1.4	0.1	2
S3	0.547	0.695	143.17	0.0345	LSST	i<24.0	$5x10^9$	1.4	0.8	5.4
S4	0.83	1.004	72.792	0.0322	LSST	i<25.3	$5x10^9$	1.4	6.1	10.7
S5	1.171	1.383	43.921	0.031	LSST	i<25.3	$3x10^{10}$	0.68	4	8.6
S6	1.591	1.858	29.347	0.0303	LSST	i<25.3	$1x10^{11}$	0.35	2.5	6.1
S7	2.126	2.472	20.982	0.0298	LSST	i<25.3	$2x10^{11}$	0.2	1.7	5
S8	3.001	3.496	14.906	0.0293	Euclid	Y<25.7	$2x10^{11}$	0.17	2.8	6
S9	4.607	5.43	10.877	0.029	Euclid	Y<26	$2x10^{11}$	0.09	2.7	3.6

For S1 to S7 the limiting magnitude is never fainter than i = 25.3 (see Table 2 above, and left panel of Figure 4) for S8 and S9 the input comes from Euclid and/or W-FIRST. In these cases the limiting magnitudes are Y = 25.7 and Y = 26 respectively. It is plausible that LSST and Euclid/WFIRST could be encouraged to survey a region appropriate for S7, S8 and S9 even deeper, allowing an improved stellar mass limit of $10^{11}M_\odot$ throughout all nine survey volumes

(approximate limits with current depths are shown in the right panel of Figure 20).

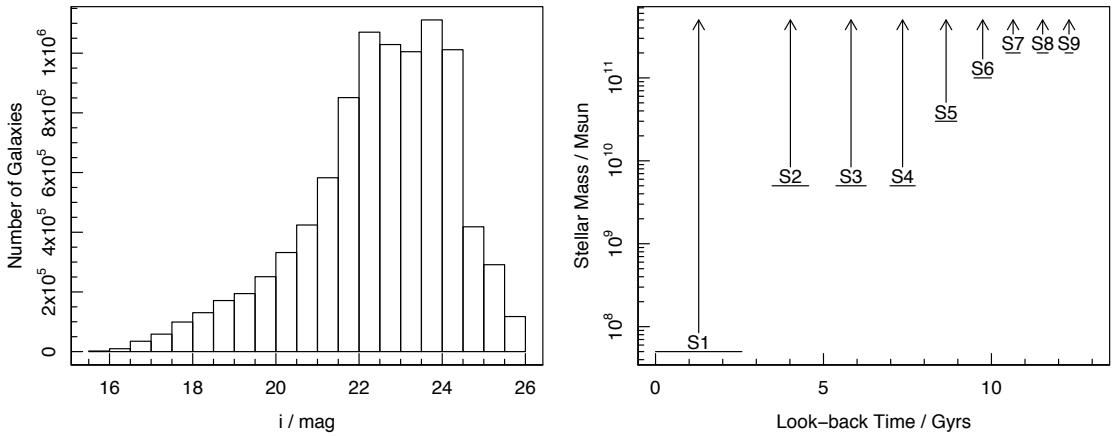

Figure 23: Left panel: Distribution of apparent i-band magnitudes for surveys (S1 to S9). Right panel: approximate stellar mass limits for all surveys as a function of look-back time.

The expected sources density is presented in Table 2. All surveys are effectively 2+ pass (assuming an MSE design of 3200 fibres over 1.8 square degrees). In practice, S1 will have significant inhomogeneous structure meaning that where galaxies are targeted the true MSE tiling density is probably a factor of a couple greater. The main mechanism to speed the surveys up is therefore to increase the proposed number of fibres. Even if the number of fibres were doubled (and FoV kept static) the proposed suite of surveys would still make excellent and efficient use of the facility.

Being able to target close-pairs efficiently is a key requirement. With GAMA we found that even with ~1000 targets per square degree we required on average ~10 passes, with some regions obtaining 14 passes, to ensure we were not biased against close-pairs (part of the most important science case for the proposed surveys here). Being able to pack fibres closer than 10" would be hugely beneficial for the proposed surveys, since the number of passes will not actual approach the ~10 of GAMA (i.e. we know that a 2.8 pass average will not be sufficient for S1 if the fibre collision limits are similar to the AAT). The physical size of the MSE focal plane might alleviate some of the difficulty in close fibre positioning, but the design used (e.g., echidna) might introduce further constraints (there might be a hard limit on how many fibres can be close-packed due to patrol area limitations). Related to this, it may be the case that using a small number of dedicated IFUs to target highly clustered regions could be the most efficient approach to obtaining redshifts. A detailed cost-benefit analysis would need to be made to answer this question using realistic sky simulations.

In total we are proposing to observe 22M galaxies over the nine survey cubes. There is, of course, scope to scale the surveys down, but there are clear scientific compromises to this. The survey volumes have been selected to guarantee the smallest contiguous volume that has obtained homogeneity in all dimensions (Srimgeour et al 2013, Driver & Robotham 2010). This means all measures of large-scale structure (fractal nature, halo abundance) and galaxy evolution (particularly cosmic star formation rate and merger accretion rate) can be directly

DRAFT

interpreted as a Universal average. Similar studies over substantially smaller volumes by competing facilities (e.g., Subaru/PFS and VLT/MOONS) will be primarily limited by sample variance, which has been historically a huge source of uncertainty at high redshift. The photo-z pre-selection minimises wasted observations that are not within the windows of high interest, and hence LSST (and at higher redshift Euclid or WFIRST selection) is vital. The photometric limits are such that beyond S2 we do not attempt to be complete below a stellar mass value of $5x10^9$ $M_\odot$ (see right panel of Figure 23). This takes us 1 dex below M_* in the range of surveys where the limit is applied, which appears to be enough to ascertain the full Universal fraction of mass accretion through mergers (see Robotham et al 2014) since the integrated mass should be convergent in this regime. This sliding limit is applied for S2 to S4. For S5 and above it is not feasible to get down to such a depth given a hard photo-z pre-selection limit from LSST of i = 25.3, unless there is future deep-field coordination between MSE and LSST. In summary, the current design is the minimum in depth and volume required for the range of potential science outlined.

There is scope to drop entire survey cubes with the loss of potential science. For exploring entirely new parameter domains S1 and S8 are objectively the most compelling for their proposed depth and volume respectively. S7 is the next most compelling due to the paucity of contiguous volume surveys in these regimes. S5 to S8 collectively span the increase, peak and decline in star-formation, mergers, large-scale structure formation and quasar activity. They also cover the transition between turbulent clumpy star-formation to smoother disk growth mechanisms. For this reason doing all four of S5 – S8 is highly compelling. S1 to S4 are the surveys that will have a consistent HOD analysis given their equivalent stellar mass limits (deeper in the case of S1). A case could be made for only doing a subset of S2/S3/S4, perhaps merging S2 and S3 into an intermediate volume. S4 in particular is expensive in terms of fibre-hours required (6.1m, the most of all surveys), but it does offer an 8 Gyr look-back timescale for the HOD science case (over half the age of the Universe), so from a galaxy evolution and halo evolution standpoint it is a more interesting survey regime than S2 or S3. Pragmatically, a merger between S2 and S3 would be the first option to consider, should the survey scale outlined be considered too ambitious for MSE.

DRAFT

We can make an approximate estimate to the total time to conduct all nine surveys using a few assumptions. If we assume MSE will have double the integration efficiency compared to VVDS (conducted using VIMOS an 8.1m VLT since 2003) then we approximately expect to obtain a redshift in T = 0.5 x 4.5^(i – 23), i.e. ~0.5/2/10 hours for i = 23/24/25 respectively. Using this rough estimate we can calculate the number of fibre hours required for each of the nine survey volumes (these numbers are given in Table 2). The distribution of i-band magnitudes is shown in the left panel of Figure 23, where it is clear that only a minority of sources are fainter than i = 24, i.e., extreme integration times should be quite rare. In total our 22M objects will require 26M fibre hours (assuming efficient survey tiling, and that we do not integrate longer than required on sources). Assuming we observe for 100 dark/grey nights per year, for 10 hours a night and using a nominal 3200 multiplex we have 3.2M fibre hours per year for the surveys (this assumes no survey inefficiency, simulations are required to determine the true fibre placement efficiency). This means all nine surveys will take approximately seven years to complete. The main telescope-side speed-up that is possible is to increase the multiplex of MSE. If MSE has the

same multiplex as DESI (5000 fibres) then the combined surveys will take 4.4 years to complete. A survey-side option is to reduce the number of surveys (as outlined above). A strong case can be made for not reducing the volumes or depths of the proposed survey volumes, so the first option to consider is whether a subset of the proposed S1 to S8 surveys could be merged. Another survey-side is to spread the RA baseline such that the surveys are observable across all available ~200 dark/dark-grey nights. This could speed up the survey campaign by a factor ~2 (i.e. all nine surveys will take 3.5 years) but at a serious cost to any other dark sky (particularly extra-galactic) science case.

A note on the higher redshift (S8 and S9) volumes: pure drop-out selected z ~ 5+ samples are highly contaminated from M-T dwarf stars and lower-z galaxies (z ~ 1 for z ~ 5 selections), where either saw-tooth-like dwarf stellar spectra or the 400nm break are identified consistently with the target Lyα break. Ambiguity arises in these selections as they traditionally only observe in three bands (one short-ward and two long-ward of Lyα at the target redshift, e.g. r/i/z for z ~ 5), and simply aim to select sources with a strong continuum break and relatively flat-continuum - as expected for high-z sources where we are probing the UV-continuum region. With only a single colour in this continuum region it is difficult to differentiate true high-z sources from their low-z counterparts (see Stanway 2008 for a detailed discussion on contamination in high-redshift photometric selections).

DRAFT

However, with additional bands (specifically NIR from Euclid or WFIRST) selections can be improved to rule out such contaminating sources. For example, multiple NIR bands allow for a much more detailed analysis of the spectral slope long-ward of the break, allowing the removal of sources with non-flat spectral shapes. In addition, with high quality data out to K-band, we should be able to identify the 400nm break in high-z sources out to z = 5.5 (between H and K). This will significantly improve the fidelity of our photo-z measurements and aid in the removal of contaminating sources.

H.5 Cadence and temporal characteristics

Repeat observations are not required for the proposed surveys.

H.6 Calibration requirements

The wavelength calibration needs to be accurate to better than the desired velocity accuracy throughout (~30 km/s, for reasons outlined above). This is to ensure we do not have any systematic biases in our redshift distributions. The expectation would be to have pixel level or better calibration accuracy.

The main sky features will need to be either well subtracted or potentially (for stronger line) masked entirely. Experience from GAMA suggests that 1% sky subtraction accuracy is probably adequate for obtaining good redshifts.

For the core redshift science the spectrophotometric calibration does not need to be especially good. Getting Hα SFR from EW also does not require particularly good flux calibration (only relevant for the low-z HOD science case).

H.7 Data processing

Instrumental signatures (the major ones) will need to be removed prior to redshift measurements. Auto-z is fairly robust to poor flux calibration and even imperfect sky subtraction issues, but the wavelength calibration would need to be very good throughout. Potentially the exact wavelength calibration could be left as a variable within auto-z, but this is probably non-ideal, and likely to create degenerate solutions.

The zeroeth-order quantity we need from the data is the redshift. We expect to do this using a tool similar to auto-z (Baldry et al 2014). Higher order products, depending on the data quality (since these products will not drive the survey design), are potentially EW for various features. The expectation would be to do this via direct line summation or Gaussian fitting technique (e.g. Hopkins et al 2013). The primary requirement for all nine surveys is redshifts, with additional science made possible if spectral analysis is possible (potentially only for the brighter targets observed).

For the core HOD related science we require robust multi-band photometry (optical and NIR restframe ideally), and stellar mass estimates, for all targeted objects. Since we will be requiring photo-z to enable optimal pre-selection we should expect to have this information in place prior to redshifts being obtained. For various science applications it is possible to imagine further data being obtained (e.g. restframe UV, MIR, FIR and radio), but this is not a specific requirement for the core science cases. The most obvious source for such data over ~3200 sq deg is LSST and Euclid/WFIRST. Other teams are responsible for producing the photometric data products for these surveys, but there may be an advantage (or even requirement) for MSE to be collaboratively involved with these teams at an early stage.

DRAFT

At a minimum we would expect to return sky subtracted, wavelength calibrated, but not flux calibrated, 1D spectra for each targeted object. We would also produce redshift measurements with quality estimates for each object.

H.8 Any other issues

How the surveys are distributed across the sky and how they are scheduled is a very serious issue that requires careful consideration. As shown in Figure 24, S1 is likely to be appropriately centred close to RA=180 and Dec=0. There is no strong science led reason to require S2 to S6 to overlap on the sky, so serious survey-speed gains might be possible if they are spread out over a large RA baseline. The big difference between traditional extra-galactic surveys (e.g. SDSS, GAMA, z-COSMOS) and the proposed MSE surveys is that they will be photo-z selected, so there is no particular observing gain through stacking them (wedding cake style) in overlapping parts of the sky. They are separated along the co-moving line-of-site such that even large-scale structure is barely associated between adjacently numbered survey volumes. At a minimum the fields should be spread over ~ 7 – 8 hours in RA (105 – 120 degrees) to ensure the proposed surveys can be observed efficiently by MSE throughout a night (i.e. if all surveys shared the same central RA then the observing efficiency drops by a factor of a few, meaning the combined survey would take 20+ years).

A number of science cases could be made for placing S7 – S8 within the extent of a foreground field since they will contain extremely bright AGNs. A number of science cases can potentially make use of bright background AGN, e.g., as probes of the inter-galactic medium (IGM) at lower redshifts via the study of absorption features in the spectra of the distant AGN. S7 and S8 in particular are close to specifying the same survey requirements as the DSC-SRO-11, concerning the 3D mapping of the IGM.

A lot of thought needs to go into the careful design of the survey regions, with consideration given the historic datasets in certain regions. This is particularly true for the UV and FIR, since this data will not be substantially improved for low redshift studies for a generation (the wide field GALEX and Herschel telescopes are now decommissioned). Thought must also be given to upcoming facilities. In the radio the SKA (based in South Africa and Australia) will be a game-changer for extra-galactic HI and continuum studies out to z = 1+ (current facilities observe to only z ~ 0.1). Clearly the SKA will be optimal for Southern hemisphere fields, and MSE will be located in the Northern hemisphere. To combat this any proposed fields should be close to the equator, making them reasonably observable by facilities in either hemisphere. It is also vital that MSE has some influence and involvement in the location of the future Euclid and WFIRST deep fields. If these are placed at declination below -40 deg then they become unviable for the MSE S8 volume because the airmass at Maunakea is always poor. In general it is advisable that the MSE survey volumes avoid the ecliptic and Milky Way plane (possible for S2 – S8, see Figure 24) since this at least ensures shallow Euclid coverage with improved resolution compared to LSST.

DRAFT

In summary, a huge amount of coordinated effort is required if maximum science is to be extracted from the proposed MSE surveys.

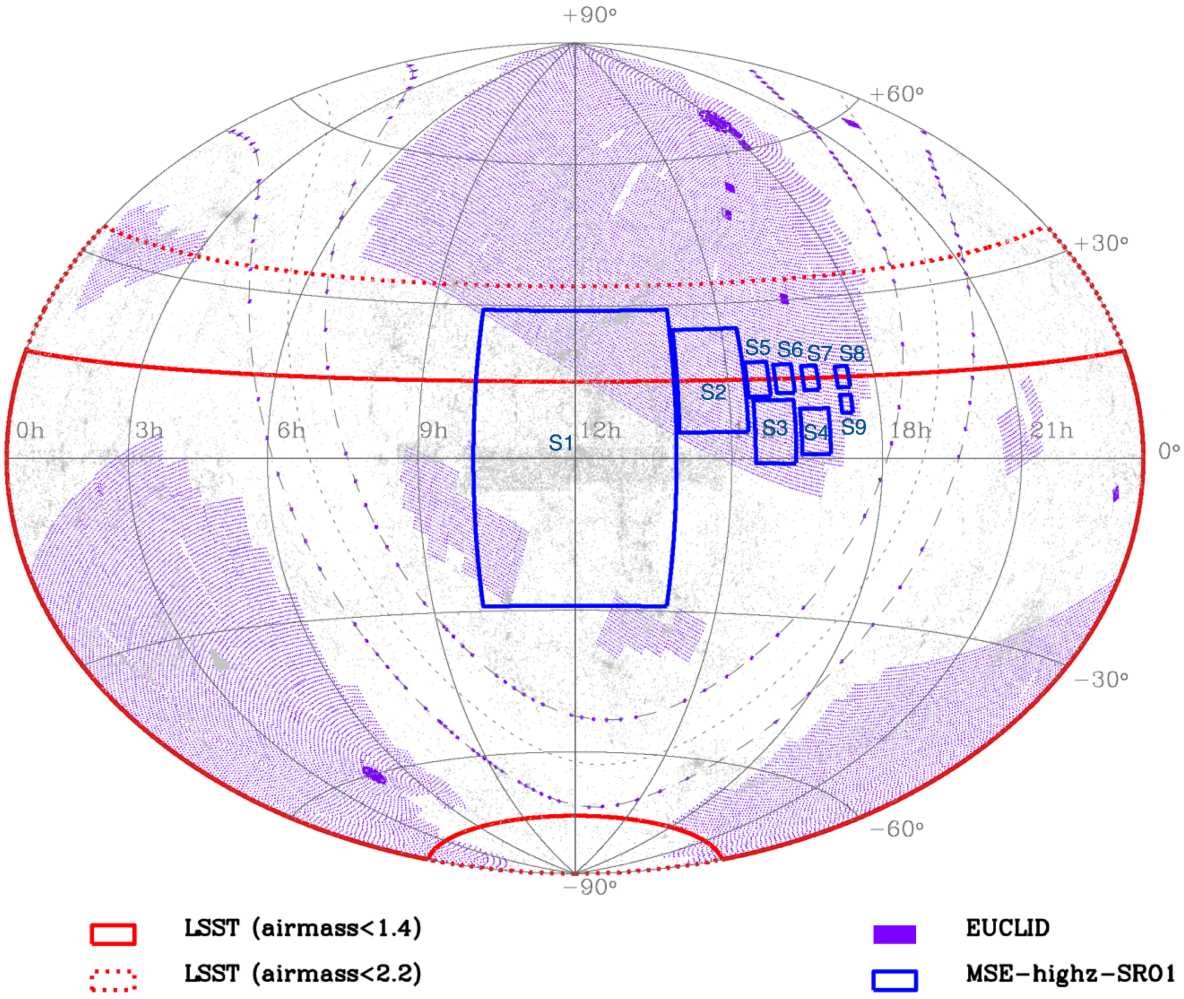

Figure 24: Straw-man locations for proposed S1 – S8 regions, that are visible from both Maunakea (+20 deg latitude, MSE) and Cerro Pachón (-30 deg latitude, LSST). The Milky Way and Ecliptic can be seen as great circles of avoidance for the proposed Euclid shallow survey (purple). The distribution shown here is such that the proposed MSE survey volumes are only observable in one semester, but with a broad RA baseline allowing them to use full nights efficiently. A number of permutations for the survey design and sky distribution are possible, so effort must be invested into the optimal design of the MSE survey suite.

The size of fibres on sky is a potential issue. The nominal 1" fibre size is clearly optimised for expected point-spread-function at a good seeing site such as Maunakea. For extra-galactic work a fibre size of 2" (e.g. AAT) to 3" (e.g. SDSS and the VLT/KMOS IFU unit size) is considered optimal. Galaxy sizes become almost constant for $z > 1$ at ~2 – 3", so all of S1 – S8 would likely achieve better throughput with larger fibres (especially S1). Having a range of available fibre sizes would also be advantageous. Detailed study of the optimal fibre size distribution is required to fully assess this issue, since uniformly larger fibre size would have a certain negative impact on stellar focussed science.

There are still a significant number of unknowns that could seriously impact any future multi-epoch HOD focussed survey. The core requirement for the highest priority elements of the

science case is for high completeness at all angular scales regardless of clustering on sky. How efficiently MSE can do this will clearly be a function of the intrinsic source clustering and the fibre placement technology. Any time estimates could be out by a factor of ~2 if the Universe and technology conspire to make high completeness on small spatial scales difficult. This is a complex issue to overcome, and will require detailed simulations to understand fully.

A mechanism for rapidly assessing whether any given target has a reliable redshift and can therefore be removed from the target list would be hugely beneficial to the survey. Such dynamic feedback would prevent time wasted increasing SNR beyond what is required for the core case. This would require a pipeline that can dynamically reduce, stack and redshift the individual short integrations (e.g., 20 minutes) for each galaxy. Scheduling software that can cope with such dynamism (currently not an option at ESO survey facilities) would give MSE an appreciable advantage in the domain of extra-galactic surveys.

DRAFT

Appendix I DSC – SRO – 09 The chemical evolution of galaxies and AGN over the past 10 billion years (z < 2)

Authors: Simon Driver, Luke Davies, Bianca Poggianti

I.1 Abstract

We propose a high-SNR (SNR>30) spectroscopic study of carefully selected volume-limited samples from the present epoch to the peak of star-formation 10 billion years earlier. Each volume-limited sample should contain 10k galaxies uniformly spanning the broadest possible stellar-mass range, and in regular 1Gyr intervals (i.e., 10 volume-limited samples of 10k galaxies resulting in a total survey of 100k galaxies). The volume-limited samples could be selected either from photo-z catalogues identified by LSST, EUCLID or WFIRST, or from a redshift pre-survey of the selected regions (i.e, such as that proposed by MSE-highz-SRO1). Key requirements for this survey are high throughout (i.e., maximum aperture, 12+m), near-IR spectral coverage (extending as red-ward as physical possible, e.g., 2micron), but relatively low to modest resolving power (R∼1000). Integration times are likely to extend up to ∼50hrs for the faintest highest redshift systems. Hence, the full study will require 50 – 100 nights of observations (assuming a multiplex factor i.e., ∼1000 targets per field-of-view), resulting in a legacy sample for multiple and diverse studies of the chemical evolution of galaxies and AGN.

DRAFT

I.2 Science Justification

The chemical evolution of galaxies and AGN over cosmic time, and in particular the gas- and stellar-phase metallicities, is a topic of significant current attention (e.g. Zahid et al. 2014, and references therein). Relatively strong evolution has been reported in the stellar-mass metallicity relation (Tremonti et al. 2004) from nearby samples to those close to the peak of cosmic star-formation history. See, for example, samples assembled by Zahid et al. (2013) and Figure 25. However, the sample sizes are relatively modest and arguably biased towards the highest star-forming systems at each epoch. This is because the selection is typically made short-wards of the 400nm break for the very high-redshift intervals, and as such probes only the most UV-bright galaxies. Locally we know that the specific star-formation rate, stellar mass, and metallicity form a fairly complex surface (e.g., Lara-Lopez et al. 2013a). Moreover gas-phase metallicity (usually the only measurement accessible in high-z surveys) is harder to interpret that the stellar-phase metallicity, as the former are very sensitive to recent infall and outflows. Ideally one would wish to study the sSFR-stellar mass-metallicity trifecta using both gas and stellar-phase metallicities, for representative populations at regular time steps. By assuming the earlier population evolves into the later population one can build up a complete picture of the global evolution of both the gas and stellar-phase metallicites over time, and the impact of both sSFR and stellar mass on metallicities (and vice-versa) at a range of epochs. The required infall and outflow models can then be determined through comparisons to simple analytic models, with potentially some additional constraints coming from the comparison of the emission line-widths (sensitive to dynamics and outflows) to the absorption line-widths (sensitive to just the dynamics) using multi-Guassian line-fitting (e.g., McElroy et al. 2015). However, the measurement of stellar-phase metallicities, essential for such an analysis, require significantly higher-S/N spectra than are typically attained in surveys such as zCOSMOS, VVDS and Deep2 –

being reliant on absorption rather than emission line measurements. Modelling of line-broadening through dynamics and outflows also requires significant signal-to-noise levels in the spectral features and for the features to be clean (i.e., away from night sky lines). As one pushes towards higher-redshift this later aspect becomes harder because of the preponderance of telluric features, etc. This can potentially be overcome by using UV metal-lines (e.g. Sommariva et al., 2012., and see Figure 26 which shows the drift of key spectral features with look-back time). By constructing a high-S/N sample of a series of well selected and sufficiently extensive samples we can address a number of compelling questions by:

(1) Providing a fully empirical description of the sSFR-stellar mass metallicity relation for systems with masses greater than $10^9 M_{sol}$ to the peak of the cosmic star-formation history at $z \sim 2$ (Figure 25). This empirical relation would include measurements of both the gas and stellar-phase metallicities, removing any biases due to recent gas infall/outfall. Such an empirical result would provide an ideal benchmark for the further calibration and development of numerical (hydro-dynamical) and semi-analytic models, which as yet have very few high-z metallicity constraints.

(2) Quantifying the decline in the abundance and frequency of AGN activity within the normal galaxy population at all redshifts to $z \sim 2$ (the epoch of peak AGN activity) using high S/N emission line diagnostics, such as BPT and WHAN. This would enable the exploration of the co-evolution of galaxies and AGNs by measuring both the star-formation history of the galaxy population, the decline in the luminosity density of AGN and any coupling between these two.

DRAFT

(3) Measuring and comparing the gas-phase and stellar-phase metallicities to constrain the degree of pristine gas infall/outflow as a function of look-back time. Some models suggest galaxies initially evolve according to a closed-box model afterwhich fresh pristine gas arrives significantly reducing the gas-phase metallicity. The clear signature of a closed-box model is a stellar-phase metallicity approximately half that of the gas-phase. Detailed comparisons of the stellar and gas phases will provide constraints on the degree of infall and outflow which can then be monitored over the range of time sampled.

(4) Performing detailed stellar population measurements to determine the progression of stellar-evolution. Earlier epochs of star-formation are typically hidden within later waves of star-formation, however detailed analysis of the complete spectrum on a pixel-by-pixel rather than line basis can reveal the full star-formation histories. These histories of later volume-limited samples need to mesh with what is seen in the earlier volume-limited samples enabling detailed test of our star-formation models. It is also worth nothing that such an analysis as outlined in 3) and 4), combined with ASKAP/SKA HI measurements (at the lower-z end), will provide a comprehensive test of the star-formation history and baryonic composition of individual galaxies, placing strong constraints on likely galaxy evolution scenarios.

(5) Using multiple star-formation tracers (e.g., Hα v UV v mid or far-IR) to study the onset of star-formation with dynamical separation and/or environment.

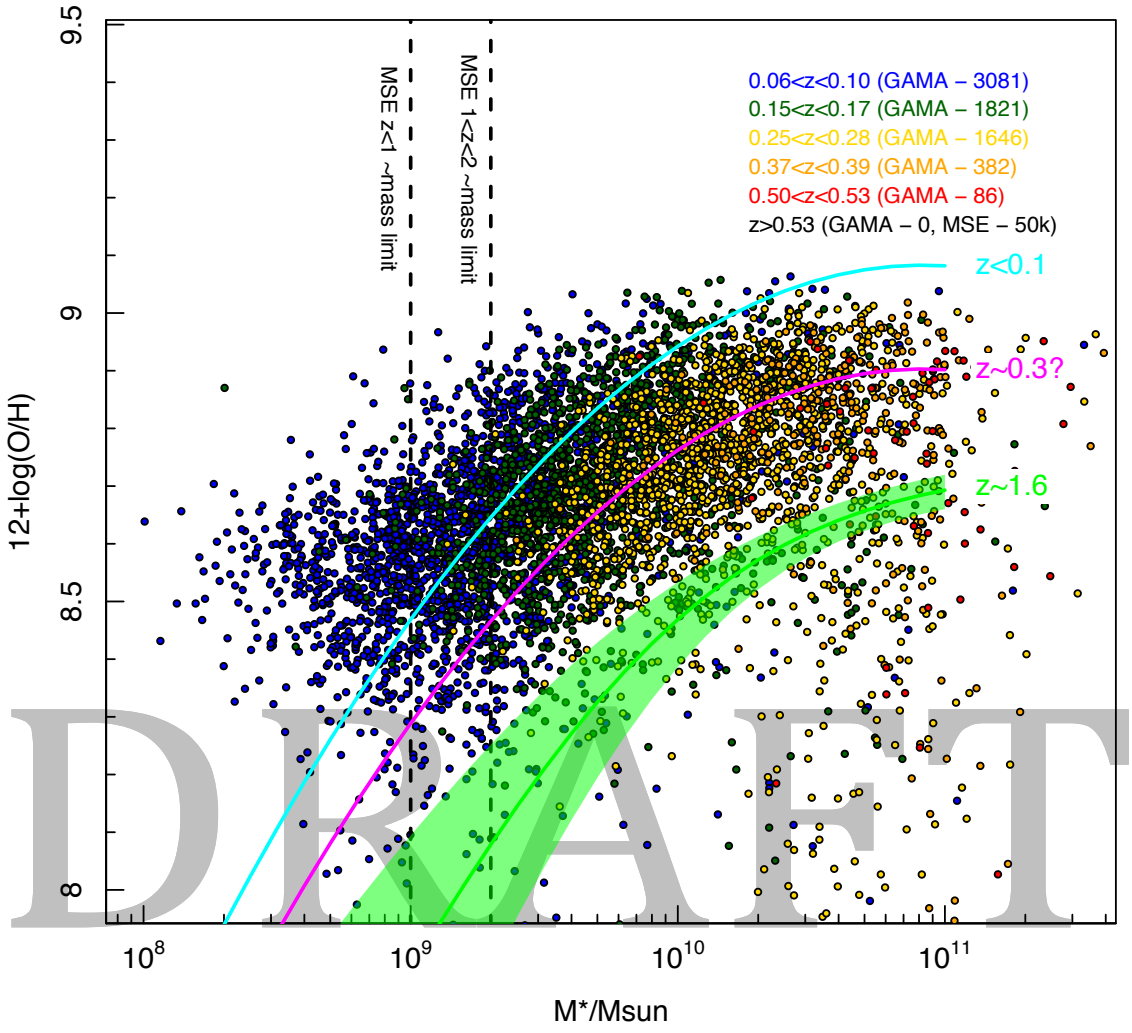

DRAFT

Figure 25: The mass-metallicity relation currently seen by GAMA and with the redshift ranges proposed by the SRO shown ($0.1Z_{sol}$ lies at the lower limit of the plot). The proposed SRO will probe mass limits similar to GAMA at z < 0.1 and z < 0.2 but out to z < 1 and z < 2 respectively. The z < 0.1 M-Z relation from SDSS+GAMA (Lara-Lopez, et al. 2013a) is displayed as the cyan line, the magenta line show the same relation normalized to the 0.25 < z < 0.39 sample and the green polygon shows the stacked galaxy z∼1.6 relation from Zahid et al. (2013). These observations clearly predict a strong evolution in the M – Z relation as a function of redshift. The proposed MSE observations will probe this evolution using individual galaxies, in a comparatively un-biased sample out to z∼2.

To identify AGN, star-forming, and inert galaxies, measure their chemical composition, and to achieve the objectives listed above, requires not only a robust redshift measurement, but also sufficient signal-to-noise spanning a broad range of emission and absorption features. Typically, to robustly distinguish AGN from star-forming galaxies one requires S/N > 5 in the rest-frame 370-680nm (OII → Na), to measure gas-phase metallicity ($0.1Z_{sol}$) and star-formation rates to modest levels ($1M_{sol}$/yr) one requires SNR ∼ 10 – 15 (Choi et al. 2014), and to recover stellar-phase metallicites using, for example Lick indices (400-650nm) or UV metals lines (130-200nm) to $0.1Z_{sol}$, we require SNR ∼ 20 – 30.

Massive samples are not critical here, although in order to fully map out a 3D structure in sSFR, stellar mass and metallicity does require volume-limited samples of ~10k systems. This assumes an average of 20 galaxies per bin and ~8 bins each in SF, stellar-mass and metallicity. Here we propose to obtain $S/N_{continuum}$ ~30 spectra from 0.4 to ~2.0micron for 10 samples each containing 10k galaxies, at regular Gyr time steps from the present epoch to a look-back time of 10Gyrs years. This limit of 10Gyrs samples from the peak of the star-formation activity at z~2, to the present epoch. In total, the proposed project would target 100 000 galaxies, which would be either spectroscopically pre-surveyed with MSE itself, or selected from the upcoming photo-z surveys of LSST, EUCLID and WFIRST.

The potential of MSE here is to provide significant statistics to have a transformation impact and fully map the evolution of the mass-metallicity relation to the peak of the star-formation activity at z ~ 2. Existing facilities are capable of constructing modest samples but only with the high throughput, high fibre density and extensive spectral coverage that MSE can provide, do we have the potential to move beyond detections to robust statistics (without unrealistic investments of telescope time). These observations will span, not just the most luminous systems, but those systems which contain the bulk of the stellar mass at the current epoch (and hence the bulk of metals in the Universe).

Driver S., et al., 2013, MNRAS, 430, 2622
Lara-Lopez, M et al., 2013, ApJ, 764, 178
McElroy, M et al., 2015, MNRAS, astro-ph/1410.6552
Sommeriva et al., 2012,A&A, 539, 136
Tremonti, M et al., 2004, ApJ, 613, 898
Zahid, H et al., 2013, ApJ, 771, 19
Zahid, H et al., 2014, ApJ, 791, 130

DRAFT

I.3 Key astrophysical observables

The required observables are the following spectral features observed for the full range of our target sample from z~0 to z~2: [OII](373nm), Hb(486nm), [OIII](501nm), Mg b(517nm), NaI(589nm), NII(655nm), Ha(657nm), plus the Lick indices (400-650nm), and redshifted UV metal lines (130-200nm). As such, this requires a combined UV/optical/near-IR spectrograph extending from ~360nm to 1.8micron. Figure 26 shows the progression of the key spectral lines noted above with lookback time/redshift. With the nominal MSE 1.3micron limit, the key metallicity indicators are lost at z~1. However, extending to 2micron would allow all of the the features discussed above to be traced to z~2.0, coincident with the peak of the cosmic star-formation history (although we note that at z > 1.7 robust measurments of Hα and NII lines are likely to be problematic due to reduced sky transmission at 1.8 – 2.0micron – see Figure 26).

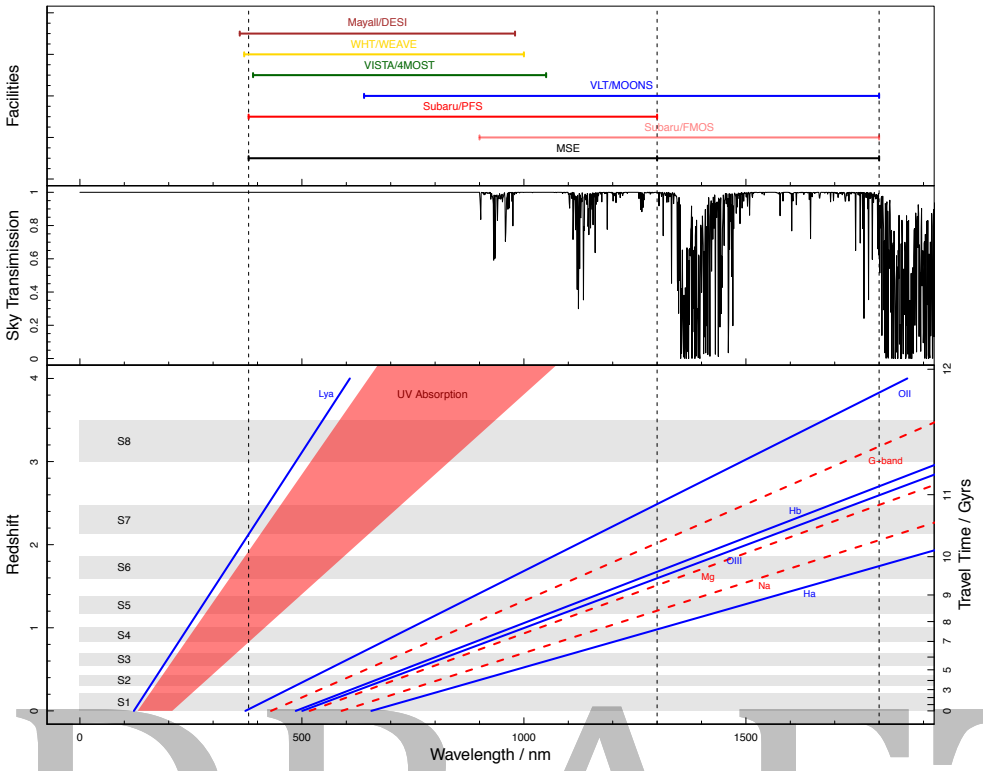

Figure 26: Accessibility of different spectral features for the different proposed volumes. The nominal 380-1300 nm MSE limit is shown as vertical dashed lines, with proposed extensions at 1800 nm (H band) also displayed. S1 – S7 via the OII line are still viable with a 380 – 1300 nm facility, but S8 is not viable).

DRAFT

I.4 Target selection

Target selection should arise from either a spectroscopic pre-survey of the region to obtain redshifts (preferable – such as in DSC-SRO-09) or photo-z selection. LSST and EUCLID will provide deep and vast samples with redshift accuracy of Dz/(1+z) ~ 0.03 to i~25 or H~24 (AB mags), and one would preferably target fields within their deep imaging regions to obtain the best complementary imaging data. Note: In reality multiple-filters may be used to select stellar mass-limited samples. From these catalogues, samples can be constructed of 10k galaxies in relatively narrow DTime intervals (approximately ±0.1Gyr) at redshifts equivalent to 1Gyr time-steps (i.e., 0.08, 0.16, 0.26, 0.38, 0.51, 0.67, 0.88, 1.13, 1.5 and if possible 2.0) over a 10Gyr time-line, to sample the peak of cosmic star-formation history. There is no requirement for the objects to be fully or partially sampled, so source selection can be matched to the final field-of-view and fibre density.

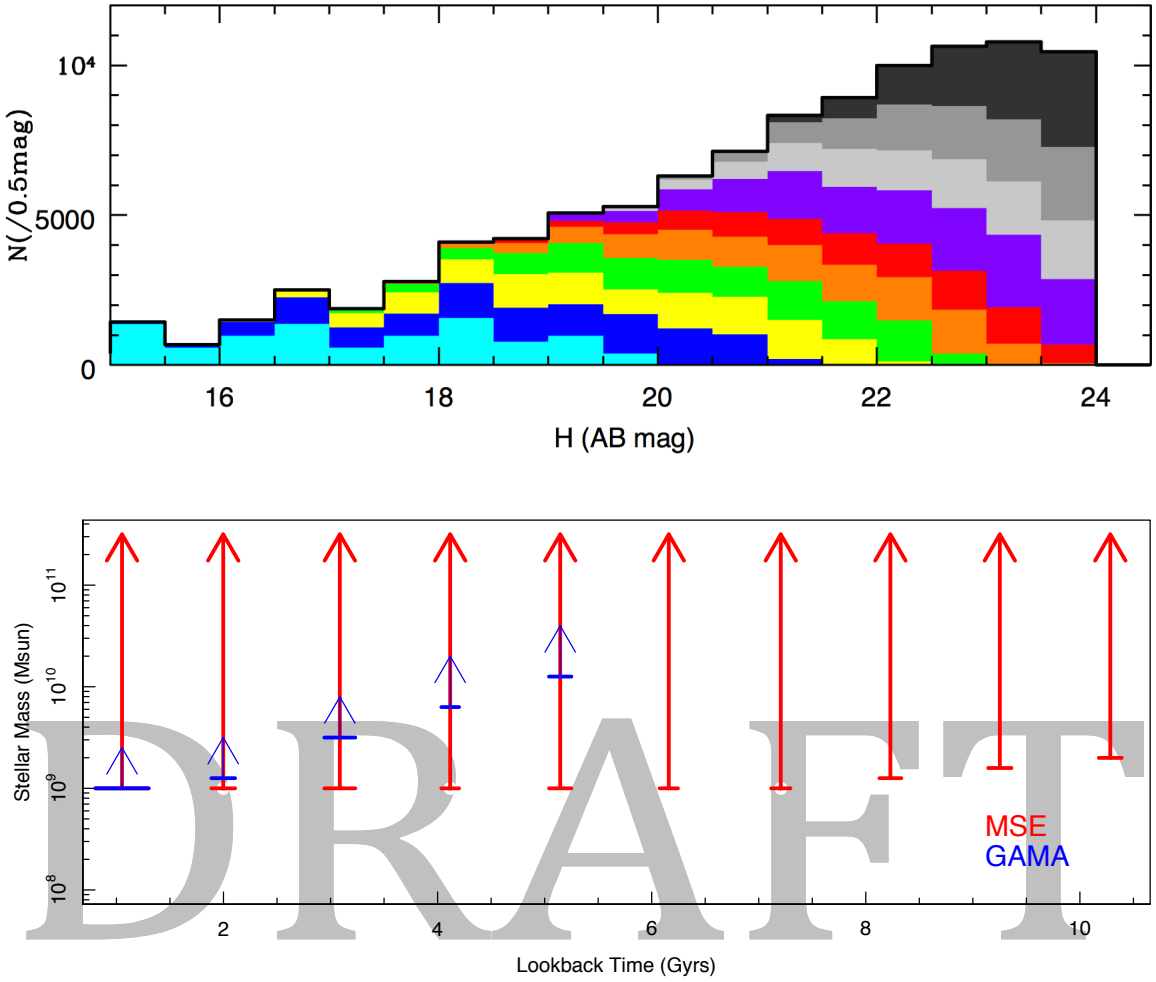

Figure 27: Top: The number-density distribution for each of the volume-limited slices (where cyan is the lowest redshift slice and black the highest). In total there are 100k targets with 10k in each interval. Bottom: the range of stellar-mass probed with lookback time.

In order to estimate the required FOV and integration times required to perform such an experiment we have used the Theoretical Astrophysics Observatory (http://tao.asvo.org.au/tao) and our own number-counts models to simulate a 1 square degree area to $H_{AB} < 24.0$ mag, and $M_* > 10^9 M_{sol}$ (see Figure 27). The resulting target fibre densities at each redshift are shown in Table 3 (note these values will be uncertain to within a factor of 2).

Exposure times to reach SNR ~ 30 for these sources are extremely uncertain given the current ambiguity in the final MSE characteristics, but are likely to be of order 5/20/100hrs for 22/23/24 K mag (scaling from DSC-SRO-09). Hence, the total survey will take of order ~400hrs (50 nights, assuming a fibre density of 5000) – however, we note that this number may easily be in error by a factor of 2.

Table 3: Survey information for DSC-SRO-09

Age	Redshift	Density (/sq deg)	Area (sq deg)
1±0.25	0.06-0.10	51	200
2±0.1	0.15-0.17	284	33
3±0.1	0.25-0.28	479	20
4±0.1	0.37-0.39	1617	5
5±0.1	0.50-0.53	3646	3
6±0.1	0.66-0.69	4500	2
7±0.1	0.86-0.90	5200	2
8±0.1	1.11-1.17	5662	2
9±0.1	1.45-1.54	9439¶	1
10±0.1	1.96-2.10	11385¶	1

¶ values highly uncertain as model dependent

I.5 Cadence and temporal characteristics

No cadence constrains are required, although numerous repeat visits will be needed. As such, this SRO could be dove-tailed with other SROs which require low-density, but a particular cadence.

DRAFT

I.6 Calibration Requirements

To measure outflows from emission line diagnostics we require a velocity accuracy of 10km/s. High SNR is the key requirement of our observations, to maximize measurement of both absorption and emission line strengths from UV to NIR wavelengths. As such, we will require high fidelity flux calibrations across the full wavelength range. As we will aim to measure faint absorption line features across a broad range of wavelengths, excellent sky subtraction is also a pre-requisite of our calibration requirements, as minor sky subtraction errors may bias any line diagnostics obtained (especially if binning to lower resolution or stacking to increase SNR).

I.7 Data processing

Data will need to be de-biased, flat-fielded, flux and wavelength calibrated to a high degree of accuracy, and stacked via signal-to-noise weighting. Line measurements (absorption or emission) will need to be made from multi-Gaussian line-fitting.

I.8 Any other issues

The main issue for consideration is that of wavelength coverage. Ultimately this sets the upper redshift limit for which meaningful chemical measurements can be made. Otherwise this SRO is massively complimented by high-resolution imaging such as that which might be available from EUCLID and/or WFIRST.

Appendix J DSC – SRO – 10 Connecting high redshift galaxies to their local environment: 3D tomography mapping of the structure and composition of the IGM, and galaxies embedded within it.

Authors: Luke Davies, Simon Driver, Khee-Gan Lee, Celine Peroux, Patrick Petitjean, Christophe Pichon, Aaron Robotham

J.1 Abstract

We propose to simultaneously use high-z (z>2.5) Quasi-Stellar Objects (QSOs) and bright galaxy sight-lines to probe the Lyman-α forest and metal content of the IGM at z ~ 2 – 2.5, and target photometrically selected faint galaxies within ~1Mpc of each sight-line to directly identify sources associated with the IGM structure. Moderate resolution (R~5000), deep spectra would be obtained for all sources to target wavelengths from Lyman-α to OIII, and intervening stellar absorption lines, at z ~ 2 – 2.5. This will push the capabilities of MSE, requiring good sensitivity and moderate spectral resolution from 3600Å to 1.8μm – with the primary instrumentation requirement of excellent sensitivity at 3600 – 4250Å. Such a study would allow a reconstruction of the dark matter distribution and associated galaxies at high-z, detailed modeling of galactic scale outflows via emission lines, investigations of the complex interplay between metals in galaxies and the IGM, and the first comprehensive, moderate resolution analysis of large samples of galaxies at this epoch.

DRAFT

J.2 Science Justification

At high redshift (z > 2), the Intergalactic Medium (IGM) contains the bulk of the baryons in the Universe. As such, it provides the reservoir of gas available for any galaxy to evolve, with IGM accretion fuelling mass growth via star-formation. While mass growth at high-z is likely to be increasingly dominated by mergers (e.g. Conselice, 2014), recent results have indicated that in the majority of cases this does little to affect star-formation (Robotham et al 2013, Davies et al, in prep). Therefore, the primary mechanism through which typical galaxies form new stars is through IGM gas accreting onto their halos. Conversely, star-formation in these galaxies emits highly ionising photons, which heat the IGM and drive superwinds, which expels metals out of the galaxy (e.g. Heckman et al. 1993, Ryan-Weber et al. 2009). Detailed understanding of the complex interplay between the IGM and the galaxies embeded within it is essential to our understanding of the factors driving galaxy evolution and the large-scale baryon distribution in general. By simultaneously probing the IGM structure and composition, and galaxy distributions, nebular gas dynamics and metallicity we can build a complete picture of the interplay between galaxies and their larger scale surroundings. The spatial distribution of the IGM at high-z is also directly related to the dark matter distribution and as such, by fully mapping the IGM will allow a complete reconstruction of the matter density field (the cosmic web) at a given epoch.

i. *3D reconstruction of the Intergalactic medium* – Deep observations of high-z quasar and bright galaxy spectra display numerous absorption lines blue-wards of Lyman-α (e.g. Petitjean & Aracil, 2004). Such features are produced via absorption from line-of-sight intervening gas in a warm photoionised IGM and thus can be used to trace the IGM

distribution and composition (Lee et al 2014a,b). The primary diagnostic line for mapping the IGM is Lyman-α absorption (the Lyman-α forest, see Cisewski et al. 2014). By targeting a sufficiently large numbers of bright, background sources it is possible to use the distribution Lyman-α absorption features to fully reconstruct the IGM distribution at a given epoch using Bayesian inversion techniques – so called, IGM tomography (see Lee et al., 2014a for such a process completed on much smaller volumes than those proposed here). The IGM distribution is directly linked to the dark matter distribution and as such, it is possible to reconstruct the full matter density field on scales of order of the mean separation of lines-of-sight (e.g. Pichon et al 2001; Caucci et al., 2008). In addition to mapping the distribution of the IGM through the Lyman-α, we can also probe its metallicity. Metal absorption lines from the line of sight IGM are also seen in the spectra of high redshift quasars and can be used to map the distribution and evolution of metals in the Universe (Petitjean & Aracil, 2004). By observing systems with sufficient resolution and sensitivity, we can distinguish these metal absorption lines from those of the Lyman-α forest at the same epoch and map the distribution of metals in the IGM.

ii. *The interplay between galaxies and the IGM* – Understanding how the galaxies embedded in this IGM structure interact with the large scale baryonic distribution is key to understanding how these systems evolve with time. By probing the dynamics of nebular material in galaxies in the vicinity of the IGM sight-lines we can build a picture of how they exchange material with the surrounding environment. Detailed analysis of nebular emission line profiles such as Lyman-α and OII (e.g. Verhamme et al. 2008, Weiner et al. 2009) in combination with stellar absorption lines, will allow the identification of galactic scale inflows/outflows and an estimate of the mass exchange between galaxies and thier immediate surroundings (e.g. Pettini et al 2001). Previously, the large samples of high signal-to-noise and moderate resolution spectra required for this analysis have been constrained to a small number of sources. As such, our understanding of both outflows from super-winds and gas accretion is limited. However, the observing strategy required for IGM tomography lends itself to directly to a combined study of the galaxies within the IGM. High signal-to-noise, moderate resolution and good sensitivity over a wide wavelength range are essential for both projects and as such they can be completed simultaneously. With addition of the measurements of galaxy metallicities (see below), it will also be possible to directly compare the chemical content of galaxies and the surrounding IGM, probing the pollution of the circumgalactic medium and the buildup in metals outside of galaxies. With comparable resolution spectra between the IGM mapping and galaxy studies, we will be able to directly associate these galaxies with absorption features in the line-of-sight galaxy/QSO spectrum to investigate the properties of individual neutral hydrogen absorbers and the regions they inhabit.

iii. *The buildup of metals at z >2* – With the high signal to noise and moderate resolution observations discussed above, we will obtain highly robust spectra of a large number of high redshift sources. These spectra will allow the first detailed analysis of both the stellar- and gas-phase metal content of individual galaxies at high-z. Stellar-phase metals

DRAFT

of the brighter sources can be obtained through rest-frame UV-continuum stellar absorption lines (using process similar to that discussed in Sommariva et al. 2012), while spectral observations out to 1.8μm will enable the identification of the emission line features required to determine gas-phase metallicities via the R_{23} diagnostic. Current state of the art observations of galaxies at this epoch consist of either tens of sources observed with low resolution spectrographs (R ~ 200, e.g. Popesso et al, 2009 & Henry et al., 2013), which rely on stacking analysis to identify stellar absorption lines and are limited to statistical analyses of the full population, or small numbers of well studied sources at moderate resolution (R~1000-3000, Belli et al., 2013, Maier et al. 2014). With the prosed IGM mapping observations we would target ~140,000 sources at $z > 2$ with the signal-to-noise required to fully investigate stellar absorption/nebular emission lines in individual galaxies. Target spectra could be further binned in resolution elements to increase signal to noise, while retaining sufficient resolution to identify key features required to determine stellar metallicities. In combination with deep photometric data, to derive stellar masses, we will probe the M-Z relation (e.g. Lara-Lopez et al., 2013) for a large sample of individual galaxies. Though such a study we would, for the first time, produce a detailed large statistical study of the buildup of metals at $z > 2$ and witness the formation of the M-Z relation in a robust sample of galaxies.

MSE is the only current or upcoming facility which can perform such a project. While current 8m+ telescopes and the next generation of ELTs will have the sensitivity to perform these observations, they are limited by their field of view and low simultaneous source targeting. The requirements of the IGM mapping case are a large number of targets simultaneously observed over a large area and as such, would be problematic with non-survey instruments. Other large spectroscopic survey instruments either lack the sensitivity (e.g. 4m class, VISTA-4MOST, WHT-WEAVE and Mayall-DESI) or resolution (e.g. R=2000 at ~4000Å, Subaru-PFS). Subaru-PFS, at its very upper limits, could attempt an IGM tomography experiment, however, this does not directly form part of the PFS extragalactic science case (Takada et al., 2014). IGM tomography could be undertaken as a bi-product of the proposed PFS galaxy evolution survey. However, such a survey will not have sufficient resolution to determine the metal content of the IGM, will not identify the faint galaxies associated with the IGM structure at $2 < z < 2.5$ (with a proposed $J < 23.4$ limit) and will not have the sensitivity and wavelength coverage to determine the stellar- or gas-phase metallicity of individual galaxies at this epoch. It is therefore unlikely that this science will be successfully undertaken until the construction of MSE and no planned instrument will be able to complete such a project to the high fidelity level of MSE.

By simultaneously probing the IGM and the galaxies embedded within it at $2 < z < 2.5$ we will build a complete picture of both the IGM and galaxy, distribution and composition at this epoch. We will probe the build-up of metals in both environments, and witness the complex interplay between galaxies and their surroundings. We will preform the first detailed high S/N and moderate resolution analysis of a extensive sample of galaxies at $z > 2$ – increasing sample sizes by orders of magnitude, and fully map the IGM distribution on scales inaccessible to any current or proposed instrument other than MSE.

Conselice, C., 2014, ARAA, 52, 291

DRAFT

Lee, KG et al., 2014a, ApJ, 795, 12
Lee, KG et al., 2014b, ApJ, 788, 49
Caucci, S., et al., 2008, MNRAS, 386,211
Sommariva, V., et al., 2012, A&A, 539, 136
Takada, M., et al., 2014, PASJ, 66, 1
Robotham, A., et al, 2013, MNRAS, 431,167
Heckman et al., 1993, ASSL, 188,455
Cisewski, J., et al., 2014, MNRAS, 440, 2599
Verhamme, A., et al., 2008, A&A, 491,89
Popesso, P., et al., 2009, A&A, 494, 443
Maier, C., et al., 2014, ApJ, 792, 3
Belli, S., et al., 2013, ApJ, 772, 141
Ryan-Weber, E., et al., 2009, MNRAS, 395, 1476
Petitjean & Aracil, 2004, A&A, 422, 52
Picon, C. et al., 2001, MNRAS, 326, 597
Pettini, M., et al., 2001, ApJ, 554, 981
Henry, A., et al., 2013, ApJ, 776, 27
Lara-Lopez, M., et al., 2013, MNRAS, 434, 451
Weiner, B., et al., 2009, ApJ, 692, 187

J.3 Key astrophysical observables

To detail the key observables required for this project, we split our observables into those required for the IGM distribution and metallicity mapping, and the study of galaxies associated with the IGM structure:

DRAFT

i) IGM mapping – For a pure mapping of the IGM distribution at $2 < z < 2.5$ a minimum spectral resolution of ~20km/s (R~2000) is required (comparable to the spatial separation of sightlines). However, in this project we also aim to identify individual Lyman-α absorption features and metal absorption lines associated with the IGM, which requires a velocity resolution of <~10km/s (R~5000).

To fully map the IGM to the degree required by our science objectives, simulations (Figure 1) predict that 500 randomly distributed targets per deg^2 are required to recover the matter distribution on 1 – 2' scales at $z \sim 2$. These line of sight sources must fall at $2.5 < z < 3.0$, in order for their Lyman-continuum region to probe the IGM at $2.0 < z < 2.5$. Using the central $1deg^2$ of the COSMOS field as a test region, and the photometric redshifts of Ilbert et al. (2008), which are complete down to $r < 25.5$, we find that $r < 24.0$ sources have the required source density at this epoch. In order to identify IGM column densities of order $\sim 10^{14}$ cm^{-2} we require continuum SN>4 per resolution element. Scaling from current ground based spectrographs, we predict ~20h exposures to obtain this S/N for r~24 sources with MSE, at a resolution of R~5000. In these observations Lyman-α absorption lines from intervening sources at $2 < z < 2.5$ will fall at ~3600 – 4250Å. Therefore, **the main technical specification of our IGM tomography observation is high sensitivity at blue wavelengths**. However, we will also target metal absorption lines in the spectra which will extend out to 9800Å (MgII[2800] at $z = 2.5$), and thus we also require good sensitivity across the whole of the optical range. Note, that we will also obtain detailed measurements of the host galaxy properties for all of these sources, as discussed below.

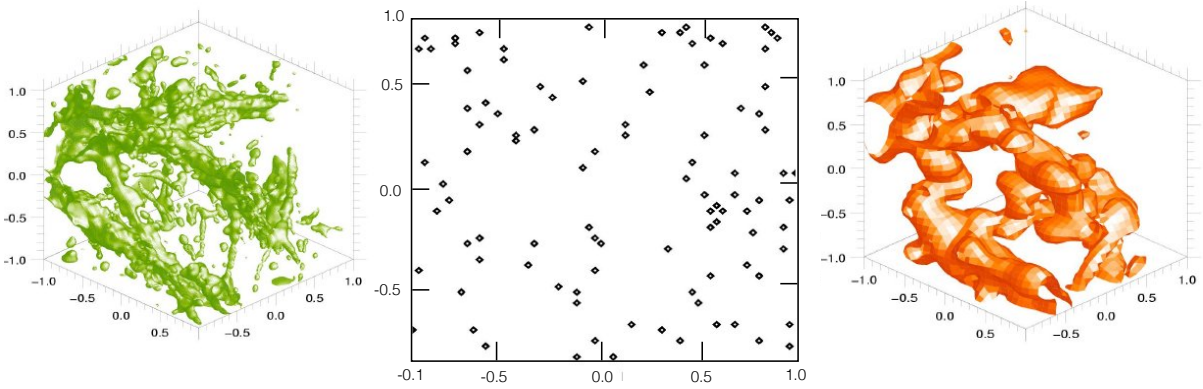

Figure 28: Left: The 3D density field in a 50Mpc^3 N-body simulation box. Middle: 100 random sight-lines to are draw through this simulation box and a spectrum is simulated for each sight-line. Right: The density field is reconstructed using Bayesian inversion. Structure on scales of the mean line-of-sight separations are recovered.

To probe a cosmologically significant volume at z ~ 2, and to avoid sample variance, the simulations also predict that observations would have to be undertaken over >20 deg^2 (also see DSC-SRO-08 for a description of the scales required to avoid issues with sample variance at these epochs). However, MSE's great strength over potential competing experiments in this field is survey speed. The prosed PFS extragalactic survey, which could be used to undertake an IGM tomography experiment (modulo the caveats discussed in the science justification), will cover 16deg^2. As such, to remain competitive in purely an IGM tomography sense, we recommend a survey covering 40deg^2. The full set of observations required to map the IGM would be 40 × 20h, 1deg^2 field observations, targeting at total of 20000, z > 2.5 sources. This yields a total observation time of ~ 1000h (including 20% overheads). We note that this project can be scaled back to a minimum area of 20deg^2 (~500h, 10000 z > 2.5 sources, 60000 2 < z < 2.5 sources) and still achieve our science goals, albeit at lower fidelity and cosmological significance.

ii) Galaxies associated with IGM – The key physical galaxy properties with we wish to determine for this experiment are: redshift positions to the accuracy of individual Lyman-α absorption features in the IGM tomography observations, nebular outflow velocities from modelling of emission lines, stellar-phase metallicites from UV-continuum stellar absorption line strengths in the brightest sources, and gas-phase metallicites from nebular emission line strengths.

We aim to target sources down to r < 25.3 in the region surrounding our IGM tomography sight-lines but embedded within the IGM structure (see below – this limit is constrained by the robust photo-z range of LSST). Assuming simultaneous observations of both the galaxies and IGM tomography sources we will obtain 20h integrations at R=5000. For these integration times, we will be able to determine the redshifts of emission line sources to within the accuracy of the IGM mapping experiment (~10km/s) and directly associate individual Lyman-α absorption features with emission line galaxies in the line of sight. Lyman-α emission is the main redshift diagnostic for galaxies at this epoch. However, Lyman-α emission is only seen ~ 20% of sources,

DRAFT

and Lyman-α derived redshifts are found to be offset from absorption line redshifts by up to several hundred kms^{-1} – and thus, do not delineate the true systematic redshift of the galaxy. As such, we aim to target both Lyman-α and OII lines simultaneously to obtain a robust measurement of the galaxy redshift. For sources where redshifts are not obtained at R=5,000, we will bin in spectral resolution to increase signal to noise (binning to R∼3000 we will still obtain redshift to a accuracy of ∼30km/s and at this resolution we will easily obtain redshifts for all sources in 20h integrations). If OII lines are not available for redshift identification, we will use absorption/emission line features at longer wavelengths (Ca H & K, G-band, Hb and OIII – which will all be covered in our observations out to 1.8μm). Once redshifts have been obtained, all other science goals do not require R = 5000 spectra. As such, will bin to various lower spectral resolutions depending on the specific science goal, as follows:

i) For stellar metallicities we will heavily bin to R∼100 for all galaxies and identify UV-continuum absorption line features in the rest-frame 1300-2000Å range (3900 – 7000Å at 2 < z < 2.5). Sommariva et al. (2012) obtain stellar-phase metallicity measurements for 23.0 < r < 24.5 sources at R∼100 in 38h integrations with VLT/FORS2. Assuming a factor of 2 decrease in MSE integration time for improved sensitivity, throughput and mirror diameter, we will obtain stellar-phase metallicities for the brightest sources in our sample. Thus, **to probe the stellar-phase metallicty of high-z sources we require the maximum possible throughput and sensitivity in the 3900 – 7000Å region**. Note that we will also obtain steller-phase metallicities for the majority of the 20,000 IGM tomography targets, as all sources will be at r<24.0 (brighter than most of the galaxies discussed in Sommariva et al). This will increase the number of z>2.5 sources with know stellar-phase metallicities by ∼ 2 - 3 orders of magnitude.

DRAFT

ii) For gas-phase metallicties we will use the R_{23} diagnostic which requires OII[3727], OIII[4959/5007] and Hβ[4861] emission lines. At 2 < z < 2.5, for detection of the OIII[5007] line we need spectral coverage out to ∼1.8μm. As such, **to fully map the gas phase metallicity of high-z sources we require a minimum spectral range of 3600Å – 1.8μm**. Should the MSE spectrograph be extended to 2.4μm (also desirable for DSC-SRO-08) we will be able to probe H-α and NII lines for our full sample of galaxies, allowing us to determine gas phase metallicites, SFRs and AGN fractions too a much higher degree of fidelity[2]. For spectral line diagnostics we do not require significant resolution, and as such, we do not require an R>1000 spectrograph past ∼1.3μm. With 20h integration and no requirement of resolution in our line diagnostics, we shall bin to lower resolution (R∼1000) and obtain high S/N, robust measurements of emission line features for our full galaxy sample.

iii) To determine nebular outflow velocities we will bin to R∼2000 to increase signal to noise and model Lyman-α emission lines in a similar manner to Verhemme et al (2008), using systematic galaxy redshifts obtained from the OII emission lines. R∼2000 is sufficient for detailed modelling of the lines and will allow us to determine the nebular dynamics within the system. Such an observation will probe the exchange rate of material between the galaxy and IGM, and allow us to investigate the rate at which metals are being expelling into the galaxy's surrounding environment.

[2] Extending beyond H band, while retaining blue-optical throughput over a very wide field, is not technically possible due to the lack of available substrates that could be used to construct a wide field corrector.

J.4 Target selection

As discussed above, we will observe 500 randomly distributed r < 24.0 sources at 2.5 < z < 3.0 per deg^2 covering a total of 40 deg^2 to perform the IGM tomography experiment. During these observations all other available fibres would be placed on photometrically pre-selected 2 < z < 2.5 within an angular distance of ~ 1.25' from the IGM mapping line-of-sight (~650kpc at z = 2.25). To identify the sources associated with absorption features we must probe to faint magnitudes (r < 25.3 – as discussed above). The number density of r < 25.3 sources using a 2 < z_{photo} < 2.5 preselection is ~ 2 arcmin^2, and therefore, ~8 within ~ 1.25' of each line-of-sight (assuming no overlapping sources). For 500 lines of sight per deg^2, and assuming a nominal 3200 MSE fibers all placed in the central deg^2, this gives on average 5.5 fibres per line-of-sight to place on surrounding galaxies. Once again using the COSMOS region as a test-bed, we take 511 sight-lines to r < 24.0 sources at 2.5 < z < 3.0, and identify all r < 25.3 galaxies at 2 < z < 2.5 within 1.25'. In total there are 2827 galaxies which meet this criteria (Figure 2.). This gives a simultaneous observation of ~3400 fibres - close to the nominal MSE fibre density. If the MSE fibre density were increased, we could either simultaneously observe a larger field of view (i.e. for 5000 fibres we could observe ~700 sightlines over 1.4deg^2 while retaining 6 fibres per sightline for the surrounding r<25.3 sources) or extend the volume around each sightline in which r<25.3 sources are targeted (i.e. to simultaneously probe all r<25.3 sources within a ~1Mpc (2') radius around each sightline with a fixed deg^2 FOV, we would also require ~5000 fibres).

DRAFT

To estimate the potential fibre collision rate in such an observation, we calculate the minimum separation between all possible r<25.3 sources in each sightline, for the simulated COSMOS observation above. We find that the median separation between the closest galaxies is ~21''. For a typical fibre separation of 10'' we would obtain fibre clashes for 18% of our sample (or in other words, allowing ~5/6, r<25.3 source per sightline to be targeted). This would limit the simultaneous observations to ~3000 sources, for the initial observational setup discussed above (500 sightlines and 5x500 lower-z galaxies). If we were able to pack fibres to within 5'' this fibre collision rate would drop to <7% (simultaneous observations of ~3300 sources - see Figure 29). Hence, **close fibre density will be highly beneficial to these observations**. However, collisions in our observational setup will not result in unused fibres, as such fibres could be placed on other r<25.3 galaxies slightly outside of the initial sightline radius (i.e. green points which lie close to lines of sight in Figure 29) or target marginally fainter galaxies within the 1.25'' radius.

Photometric source selection for the full project will be obtained from upcoming deep large area surveys such as LSST. We will require accurate photometric redshifts to r < 25.3 over a contiguous 40 deg^2 region, which will be available from LSST by the time MSE is constructed. Choice of field position is non-essential to this project, and is only limited to the deep optical data required for source selection, and would preferably contain the maximum possible bright QSO source density at 2.5 < z < 3.0. Regions with extensive multi-band coverage are ideal, to provide accurate stellar mass measurements with which to probe the M – Z relation. With these caveats, we are flexible on scheduling and can adapt to the position of deep fields which are available at the time of observations.

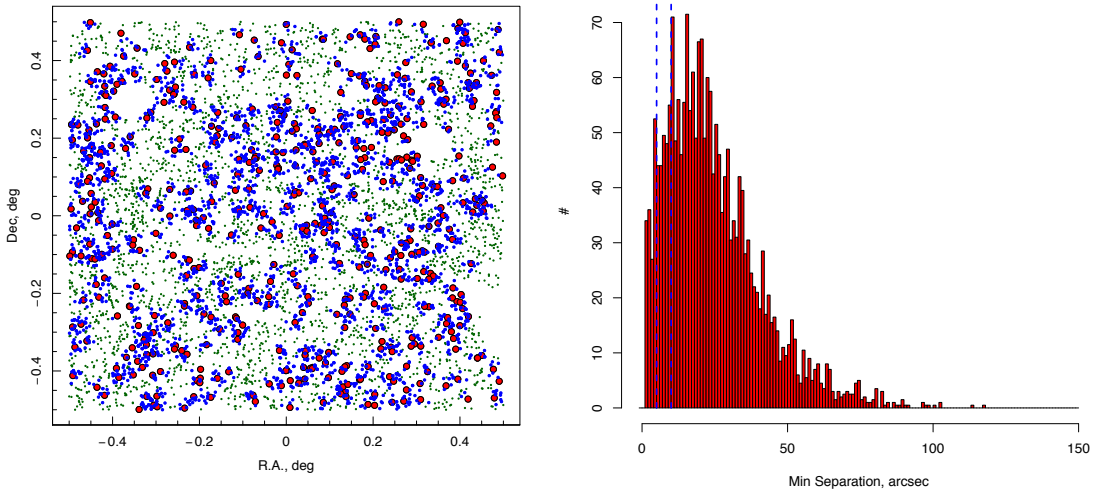

Figure 29: Left - Simulated observation of ~500 sight-lines to 2.5<z_{photo}<3.0 sources in a single 1 deg^2 region of the COSMOS field. Red points display sight-lines, blue points show all r<25.3 sources with 2.0<z_{photo}<2.5 within 1.25'of a sight line. Green points show all other r<25.5, 2.0<z_{photo}<2.5 sources. Right – The closest separation between r<25.3 galaxies within 1.25' of each sightline. Vertical lines display potential 10'' and 5'' fibre separations, containing 18% and 7% of sources respectively.

DRAFT

J.5 Cadence and temporal characteristics

No cadence constraints or repeat observations are not required.

J.6 Calibration requirements

Our observations will require a high level of spectroscopic fidelity for both the identification of Lyman-α absorbers and galaxy redshifts. We require maximal throughput to obtain good signal to noise, specifically at ~3600 – 4250Å for the IGM tomography and 3900 – 7000Å for stellar phase metallicities, and robust flux calibration from ~3600Å – 1.8µm to derive accurate faint emission line strengths. As such, we will require accurate wavelength and spectrophotometric calibrations. Excellent sky subtraction is required for stellar absorption features in 2.0 < z < 2.5 galaxy sample as we will be heavily binning in resolution elements (4500 – 7000Å). The region probed in the IGM tomography (~3600 – 4250Å) is largely free from sky emission, however, even minor over subtraction of sky emission can lead to confusion in reconstruction the IGM matter distribution. Hence, we require excellent sky subtraction over the full optical range and robust removal of instrument signatures.

J.7 Data processing

Data will be debiased, flat-fielded, sky subtracted and, flux and wavelength calibrated to a high degree of accuracy. Bayesian inversion techniques will be used to reconstruct the IGM distribution, Gaussian line fitting will be applied to all emission and absorption line features for

metallicity measurements and more complex line fitting will be undertaken to derive nebular outflow velocities.

J.8 Any other issues

None.

DRAFT

Appendix K DSC – SRO – 11 Mapping the Inner Parsec of Quasars with MSE

Authors: Sarah Gallagher, Kelly Denney, Patrick Hall, Anna Pancoast, Yue Shen, Chris Willott

K.1 Abstract

The centre of every massive galaxy in the local Universe hosts a supermassive black hole that likely grew between a redshift of 1 to 3 through active accretion as a luminous quasar. Despite decades of study, the details of the structure and kinematics of the inner parsec of quasars remain elusive. Because of its small angular size, this region is only accessible through time-domain astrophysics. The powerful technique of reverberation mapping takes advantage of the changing emission-line properties of gas near the black hole in response to variations in the luminosity of the black hole's accretion disk to measure the sizes and velocities of the line-emitting regions; with this information, we can map the quasar inner parsec and accurately measure black hole masses. This information is essential for understanding accretion physics and tracing black hole growth over cosmic time; reverberation mapping is the only distance-independent method of measuring black hole masses applicable at cosmological distances. We propose a ground-breaking MSE campaign of ~100 observations of ~5000 quasars over a period of several years (totaling ~600 hours on-sky) to map the inner parsec of these quasars from the innermost broad-line region to the dust-sublimation radius. With high quality spectrophotometry and spectral coverage from 360 nm to 1.8 μm, this unprecedented reverberation-mapping survey will map the structure and kinematics of the inner parsec around a large sample of supermassive black holes actively accreting during the peak quasar era. In addition, a well-calibrated reverberation relation for quasars offers promise for constructing a high-z Hubble diagram to constrain the expansion history of the Universe.

DRAFT

K.2 Science Justification

At the present epoch, supermassive black holes are ubiquitous in the centres of massive galaxies. The black holes grew predominantly around redshifts from 1 to 3, when the universe was approximately a fifth to a half of its current age through active accretion as luminous active galactic nuclei (AGN), also known as quasars. Remarkably, subparsec quasar accretion disks can outshine their host galaxies – thousands of times larger – by two to three orders of magnitude. Despite their small size, black holes are fundamentally linked to their host galaxies as shown through the strong scaling relations between the black hole mass and host galaxy properties. Energy injection during the quasar phase in the form of feedback may regulate these scaling relations; in any case, supermassive black hole growth clearly occurs alongside the build-up of stellar mass in galaxies. *Measuring accurate black hole masses and understanding the inner structure of distant quasars is essential to advancing our knowledge of supermassive black hole growth, AGN physics and phenomenology, the mechanisms for launching quasar outflows, and the co-evolution of supermassive black holes and their host galaxies.*

Though quasars have been studied in radio through X-ray wavelengths for decades, there remain fundamental, open questions about accretion physics. For example, the well-known Shakura & Sunyaev (1973) prescription for describing the light distribution of the UV-optical emitting region of accretion disks underestimates their sizes by factors of several (Blackburne et

al. 2011; Jimenez-Vicente et al. 2012; Edelson et al. 2015). The geometry and kinematics of the region generating the broad emission lines – the most prominent features of quasar optical-UV spectra – are still poorly constrained. These distant, cosmic powerhouses have such small angular sizes that they cannot be resolved with existing or near-term technologies; our only access to constraining their structure empirically is through time-domain astrophysics.

In particular, we can use time resolution to substitute for angular resolution by measuring the rest-frame time lag of the response of a broad emission line's flux to changes in the continuum illuminating the broad-line region (Blandford & McKee 1982).

Strong, broad, resonance lines are seen from ions with a large range of ionization states, from O VI to Mg II; the gas is photoionized with lower-ionization gas at larger radii out to the dust-sublimation radius. The recombination times in the broad-line region are short, and so the time lag between the continuum and broad-line flux variability corresponds to the light travel time between the central, ionizing UV continuum source and the broad-line region. Measuring this time lag thus provides a characteristic distance between the broad-line region gas and the supermassive black hole, R_{line}. The broad emission lines (with widths of thousands of km s^{-1}) also reveal the Doppler motions of dense gas close to the central black hole. With a characteristic distance (from the time lag) and velocity (from the line width), the black hole mass is given by $M_{BH} = f(\Delta v)^2 R_{line}/G$ where G is the gravitational constant, Δv is a measure of the width of the emission line, and f is a factor of order unity which accounts for the geometry and kinematics of the broad-line region (see, e.g., Peterson 2011, and references therein).

DRAFT

Furthermore, for an individual quasar, the time lags and the average continuum luminosities generate an R_{line} value for each line. Comparison of the characteristic time lags from different lines puts powerful constraints on the structure, kinematics, and physical conditions (e.g., gas density and ionization parameter) of the broad-line region gas (Korista & Goad 2004). In the best cases, with appropriate velocity resolution and time sampling, high-fidelity velocity-delay maps (line responsivity as a function of line-of-sight velocity and time delay; see Figure 30) can be obtained with a reverberation-mapping (RM) campaign with a duration $T_{dur} > 6\tau_{line}$, where τ_{line} is the time delay for a given line. Such data from multiple broad emission lines with varying ionization potentials have the power to image even complex structures in the central regions, for example spiral arms in a disk of accreting material.

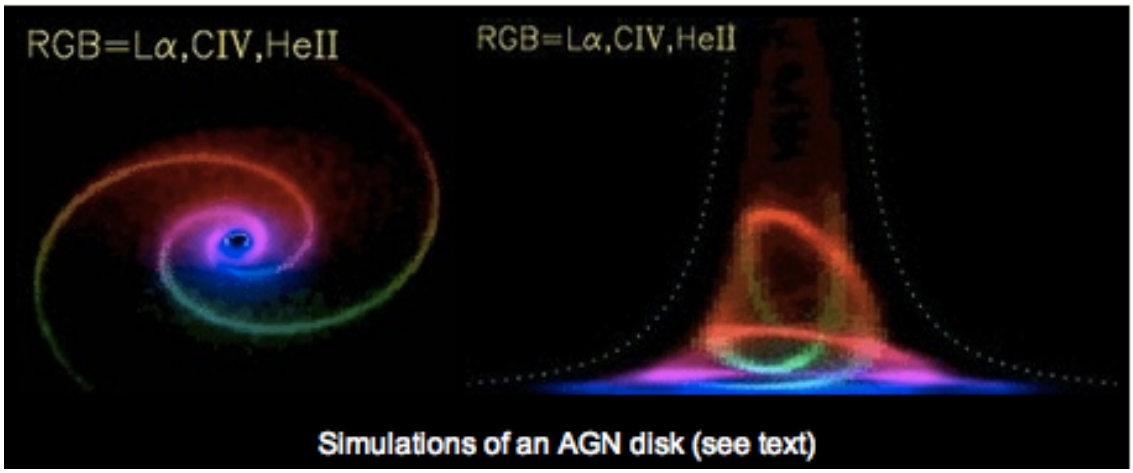

Figure 30: Left: An image of a quasar where the surrounding broad-line region structure is that of a disk with a spiral density wave. Right: Time delay vs. velocity map for the Lyα (red), C IV (green), and He II (blue) emission lines. When the continuum emission from the accretion disk varies, the gas giving rise to the broad emission lines responds similarly after a characteristic time delay. The spread of velocity components in each emission line is generated by different locations within the broad-line region, and therefore the line as a whole responds with a range of time delays. With sufficient S/N, time sampling, velocity resolution, and flux calibration, the velocity-delay map can be inverted to reconstruct the disk image. (Image credit: K. Horne [star-www.st-andrews.ac.uk/astronomy/research/agn.php])

DRAFT

Currently, only ~60 local, relatively low-luminosity AGN have RM-based measurements of their black hole masses (Bentz & Katz 2015), and only ~20% of these targets have high-quality data sufficient for producing velocity-delay maps. The largest optical mapping campaign to date is the ongoing (2 yrs to date) SDSS-BOSS program to monitor 849 $i < 21.7$ AGNs with the 2.5-m Apache Point Telescope in a single 7 deg^2 field (Shen et al. 2015). Dedicated time-intensive programs that monitor the rest-frame UV through optical of a *handful* of AGN are currently underway with e.g., HST COS (NGC 5548; PI Peterson) and the VLT X-Shooter (P.I. Denney). Though these programs will be foundational for taking the next step forward in RM science, MSE promises to go significantly further. Cosmological redshifting means that *optical* spectroscopic RM campaigns of quasars are fundamentally limited by a mismatch between the high quality data at low-*z* and what is accessible for high *z*. The lines sampled in these two regimes – e.g., Hβ and C IV for low and high *z*, respectively, arise from significantly different parts of the broad-line region, and there is large scatter in the black hole masses derived from these two lines in single epoch spectra as a result of their distinct characteristics (Denney 2012). Furthermore, local RM AGN occupy fundamentally different regions of parameter space than typical high-*z* quasars in terms of luminosity, the shape of their ionizing continua, and likely their host galaxy properties. *Accurate reverberation-mapping black hole mass measurements for a large sample of z~2 quasars would enable high-accuracy calibration of black hole masses from single-epoch spectra for the first time.*

The major advantages of MSE over other planned RM programs (e.g., SDSS, OzDES, or 4MOST) are sensitivity (~2–3 mags deeper in 1 hr) and near-IR capability because of the planned mirror size and instrumentation, and the exquisite Mauna Kea site. The only planned instrument that would be competitive with MSE on these terms is Subaru-PFS; however, the PFS wavelength

range only extends to 1.25 mm and there are no current plans to invest the requisite time to a mapping campaign as outlined in this proposal. *The inclusion of near-IR capability (to 1.8 mm) to reverberation-map the rest-frame UV-optical for ~5000 high-z quasars will make MSE a game-changer in this field (see* Figure 31*).*

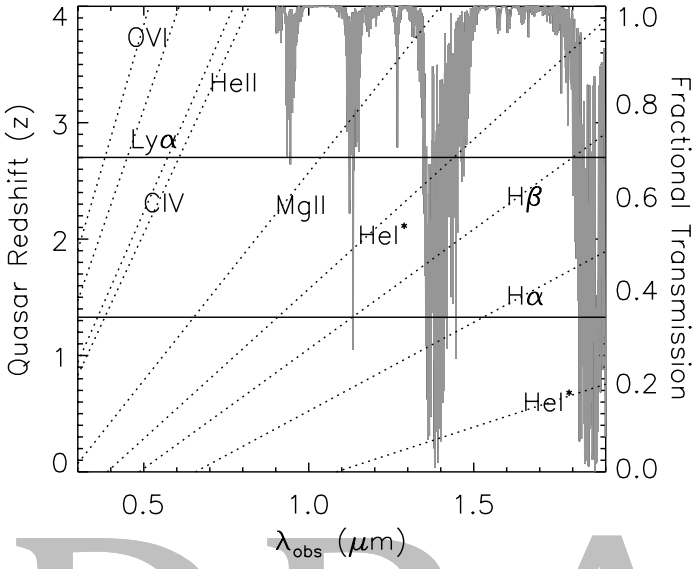

DRAFT

Figure 31: The observed wavelength of broad emission lines of interest overlaid on a representative atmospheric transmission spectrum for Mauna Kea. Across the peak of the quasar epoch (*z* = 1.3 – 2.7; bounded by horizontal lines) emission lines from O VI to Hα are accessible with wavelength coverage from 360 nm to 1.8 μm; at least one hydrogen line will be at a region of high atmospheric transparency. This range of lines probes size scales from the innermost broad-line region (of order light-days to light-weeks) to the dust sublimation radius (~10 times larger; Mor & Netzer 2012).

Ancillary Science: Though the demographics of the quasar population have changed remarkably since *z*~3, the structure of luminous quasars shows surprisingly little evolution in fundamentals such as metallicity and spectral energy distribution. They are thus promising objects for constructing a high-*z* Hubble diagram given an appropriate independent estimate of luminosity such as a well-calibrated $R_{line} - L_{cont}$ relation (Bentz et al. 2013). The size of a line-emitting region can be measured from reverberation; this then yields the average quasar luminosity. From the measured flux and the redshift, a Hubble diagram to *z*~3 can be made from the proposed MSE high-*z* quasar reverberation-mapping campaign, thus providing important constraints on general cosmological models (King et al. 2014).

Bentz, M. C., & Katz, S. 2015, PASP, 127, 67
Bentz, M. C., Denney, et al. 2013, ApJ, 767, 149
Blackburne, J. A., Pooley, D., Rappaport,S., & Schechter, P. L. 2011, ApJ, 729, 34
Blandford, R. D. & McKee, C. F. 1982, ApJ, 255, 419
Denney, K. D. et al. 2010, ApJ, 721, 715
Denney, K. D. 2012, ApJ, 759, 44
De Rosa, G. et al. 2015, ApJ, 806, 128
Edelson, R., et al. 2015, arXiv:1501.05951
Hopkins, P. F., Richards, G. T., & Hernquist, L. 2007, ApJ, 654, 731

Horne, K., et al. 2004, PASP, 116, 465
Jimenez-Vicente, J., et al. 2012, ApJ, 751, 106
King, A. L., et al. 2014, MNRAS, 441, 3454
King, A. L., et al. 2015, arXiv:1504.03031
Korista, K. T. & Goad, M. R. 2004, ApJ, 606, 749
Mor, R. & Netzer, H. 2012, MNRAS, 420, 526
Pancoast, A., Brewer, B. J., et al. 2014, MNRAS, 445, 3073
Peterson, B. M. 2011, ArXiv1109.4181P
Shakura, N. I. & Sunyaev, R. A. 1973, A&Ap, 24, 337
Shen, Y., et al. 2015, ApJS, 216, 4
Zu, Y., Kochanek, C. S., & Peterson, B. M. 2011, ApJ, 735, 80

K.3 Key astrophysical observables

The essential requirements for a successful reverberation mapping campaign are to accurately measure the time lag between continuum variability and the response of each emission line, and to obtain a root-mean-square (RMS) flux spectrum of the quasar. The time-lags provide the size scale of the emission-line region, while the RMS spectrum shows the velocity structure of the material responding to the continuum variability. Both of these are required to map the structure of the broad-line region and to obtain accurate black-hole masses.

The quality of these observables depends on the following parameters:

DRAFT

- *Accurate spectrophotometry:* To detect low-amplitude, short rest-frame timescale continuum and emission-line variations requires high S/N spectra (S/N~30 per resolution element at line centre). Accurate relative flux calibration across the wavelength range is critical to detect flux variability at the few percent level. The current state-of-the-art is <2% with long-slit programs, and 5% with the multi-fibre SDSS-RM campaign; we require a minimum of 4%. Accuracy of 3–4% will enable sensitivity to the low level variability needed to detect an RM signal, thereby increasing our success rate over what was predicted for and is currently being achieved with early results from the SDSS-RM program (Shen et al. 2015). Systematic errors come from uncertainties in modeling standard star spectra, telescope pointing, fibre-to-fibre differences, fibre placement errors, and seeing-dependent flux losses. Obtaining this goal may require allocating a larger fraction of standard star and sky fibres (200–500) than typical per field. We will build on lessons from the SDSS-RM and OzDES (King et al. 2015) multi-object spectrograph RM surveys in this regard.
- *Sensitivity:* Using the current MSE exposure-time calculator, we can achieve SNR~30 (the requirement for constructing velocity-delay maps) at C IVl1549 line centre for a typical z=2 quasar with i=21.8 in 1-hr integration times (seeing=0.6”; airmass=1.5; sky brightness=21.3). At the i=23.25 flux limit of the survey, 1-hr integration with the same conditions yields SNR~10 at line centre, sufficient for R_{line} (and thus black hole mass) measurements. Longer integration times compromise accurate spectrophotometry because of changing sky conditions.
- *Spectral resolution:* Quasar broad-emission lines have typical widths of 1000s of km s^{-1}. However, they are highly structured and often blended, and several resolution elements are required to adequately sample their velocity structure. Quasar narrow-emission

lines have widths of 100s of km s^{-1} and would ideally be resolved in an individual spectrum. This sets the minimum resolution requirement of 200 km s^{-1} (R∼1500) with 100 km s^{-1} (R∼3000) being ideal.

- *Wavelength range:* Continuous wavelength coverage in the regions of atmospheric transparency from 360 nm to 1.8 µm maximizes the science return on these time-intensive observations for quasars up to z∼3 (Figure 31). For z = 1.3 – 2.7, simultaneous coverage of C IV and Hβ will enable R_{line} measurements from the innermost regions to the dust-sublimation radius. Furthermore, including rest-frame optical emission lines is essential for tying the typical high-redshift quasar to the extensively calibrated local reverberation-mapped AGN. *Such broad-band spectral coverage with the proposed time cadence would enable accurate black hole mass measurements for the largest sample of quasars to date and unprecedented mapping of the central parsec.*

K.4 Target selection

Given the heroic efforts that have gone into building up large quasar samples with SDSS and follow-on surveys such as UKIDDS/DXS, several fields with known targets appropriate for the quasar variability program will be available prior to 2020. With sensitivity down to i = 23.25, the sky density of broad-line quasars is ∼450 deg^{-2} (from the Hopkins et al. 2007 luminosity function). Therefore, for a 1.8 deg^2 MSE field-of-view, we require 800 – 900 target fibres per pointing. The chosen fields should be within the LSST survey area to optimize the opportunity for improving spectrophotometric calibration and the increased time-sampling of continuum monitoring (a factor of 2 to 3; cf., Zu et al. 2011). If MSE is on-sky prior to LSST first-light, other facilities could be used for photometric monitoring both in preparation for and concurrently with this program. Our ideal sample size is ∼5000 quasars (approximately 6 fields) from which we anticipate approximately 50% will generate robust time-lag measurements. Such a large sample with this UV-optical spectral coverage will enable (1) proper calibration of the $R_{line} - L_{cont}$ relationship for all major emission lines of interest and (2) division of the sample by observed characteristics to study the scatter as a function of physical properties (e.g., luminosity, Eddington ratio, and shape of the ionizing continuum). *A robust understanding of the intrinsic $R_{line} - L_{cont}$ scatter across the AGN population is essential to improve the accuracy and reliability of the single epoch black hole masses used to map black hole growth over cosmic time. Furthermore, this sample size would make a high-z quasar Hubble diagram competitive with other methods for constraining dark energy (King et al. 2014).*

DRAFT

K.5 Cadence and temporal characteristics

Repeat observations to monitor continuum and emission-line variability are at the heart of our proposed science program. Quasar variability is a function of timescale (from days to years), luminosity (low luminosity quasars vary more), wavelength (quasars are more variable at shorter continuum wavelengths and in higher ionization-potential broad lines), and redshift (as a result of time dilation). In addition, measuring a reverberation time lag requires seeing at least one minimum or maximum in the continuum light curve that produces an associated feature in the emission-line light curve. In a given 6-month period of the SDSS-RM campaign, only ∼10% of

quasars are expected to have successfully measured lags (Shen et al. 2015). Multiple observing seasons are therefore necessary to achieve the science goals.

Horne et al. (2004) discuss the requirements for accurate reverberation mapping in detail. In brief, the peak emission-line time delay τ measured in a given RM campaign is the light-crossing time of the broad-line region in that line at that time. The delay resolution is $\Delta\tau \simeq 2\Delta t$ where Δt is the sampling time interval. Therefore, to sample both short lags (days) and long lags (years), we envision a multi-year program with a cadence of several days in the first year, and reduced cadence in each successive year, totaling ≃100 epochs per field over 3 – 5 years. The number of required spectroscopic epochs is based on the science goal of using time delay vs. velocity information to construct images of the broad-line region. Previous campaigns on individual objects have required 50 – 170 epochs for successful mapping (e.g., Denney et al. 2010; Pancoast et al. 2014; De Rosa et al. 2015). The mid-to-upper end of this range is required given the multi-object nature of this program. Based on experience with previous RM campaigns, we anticipate that such a program will yield 2000 – 3000 robust time lags.

In addition, we envision a dynamically allocated survey. As R_{line} values are measured for individual targets, they would be dropped from further observations, except for a small fraction used to constrain the intrinsic scatter in broad-line region distance measurements. Faint, low redshift targets require observations repeated at high cadence, but only until a sufficient number of lags are measured. Because of the time lag dependence, high redshift, high luminosity quasars require multi-year baselines at low cadence to yield RM lag measurements, and so over time the cadence can be reduced. Given that this program would require less than one-third of the available fibres per pointing, it could naturally be executed concurrently with programs that (1) require repeat observations of very faint targets to build-up S/N in individual spectra, and/or (2) require extremely dense sampling of objects in an extragalactic field. Furthermore, a deep galaxy survey in the RM fields with extremely high S/N quasar spectra would enable quasar absorption-line–galaxy correlation work to study the three-dimensional structure of baryonic gas and star formation.

DRAFT

K.6 Calibration requirements

- *Wavelength calibration:* As this program encompasses repeat and comparative observations of known targets, standard wavelength calibration should be sufficient.
- *Sky subtraction:* The main sky features will need to be well-subtracted to enable accurate flux calibration. This may require an additional allocation of sky fibres to adequately sample the field-of-view.
- *Flux (spectrophotometric calibration):* As mentioned in §3, the most stringent requirement for the success of the observing program is accurate (3–4%) absolute spectrophotometry. This could be achieved with accurate *relative* (across the wavelength range) spectrophotometry and concurrent, multi-band, high accuracy photometry (from a different facility). The ability to assign the same fibre to a target for all observations would remove one source of uncertainty arising from percent-level variations in transmission between different fibres. Fibre positioning accuracy will also contribute to the error budget depending on the fibre size; fibres larger by a factor of 2–

3 than the typical site seeing significantly improve the spectrophotometric calibration by mitigating systematics introduced by seeing-dependent flux losses.

- *Telluric absorption:* Accurate telluric absorption correction is important for obtaining the high quality broad-band spectra (particularly in the near-infrared) needed for this program. For this reason, it may be desirable to allocate a larger number of standard star fibres per pointing than in the typical survey program.
- *Other (e.g., stability):* Absolute flux and wavelength calibration are the primary concerns. As long as they are sufficient, instrument stability is not the focus. Fibre centroiding, pointing, and guiding must be accurate enough that they make negligible contributions to fibre light losses, relative to natural seeing, over the course of a 1-hr observation.

K.7 Data processing

- *Removal of instrumental signatures:* Instrumental signatures must be removed from the spectra for the proposed analysis.
- *Measurement of astronomical quantities:* For each quasar that varies sufficiently for reverberation mapping: (1) Available photometry, flux and wavelength-calibrated spectra from each epoch will be analyzed together to determine a reverberation lag for each broad line. (2) RMS spectra from each quasar will be constructed and analyzed to determine a black-hole mass. (3) For the best targets: time-delay vs. velocity data will be inverted to construct images of the broad-line region. (4) For each quasar in the survey: a high S/N composite spectrum will be constructed from the weighted average of individual spectra. These spectra will enable an unprecedented analysis of faint features in typical quasar spectra, such as structure in the broad emission lines, weak forbidden lines, host galaxy features, and absorption lines from associated and intervening gas.
- *Discussion of other data to be combined with MSE:* High quality photometry (e.g., from LSST or other facilities) would be used to improve the accuracy of the absolute spectrophotometry and increase the time baseline (in advance of MSE first light) and cadence for continuum variability monitoring. Quasars in this program with very high S/N spectra and well-measured black hole masses will be appealing targets for follow-up with other facilities, e.g., ALMA, TMT, and JWST.
- *Desired deliverables:* The minimum deliverables would be flux-calibrated spectra for each epoch and combined, average spectra for all the quasars. Higher level products such as reverberation lags for each broad line of successfully reverberation-mapped quasars and velocity-delay maps would require additional time and resources to provide.

K.8 Any other issues

None

DRAFT

Appendix L DSC – SRO – 12 Dynamics of the dark and luminous cosmic-web during the last three billions years

Authors: H. Courtois (IPNL, Lyon; SRO-5 PI), M. Colless (RSAA-ANU, Canberra), J. Comparat (Madrid), M. Fernandez-Lorenzo (IAA, Granada), M. Hudson (Waterloo), A. Johnson (CAS Swinburne), N. Kaiser (IfA Hawaii), J. Koda (INAF, Obs. Merate), A. Nusser (Technion, Haifa), C. Schimd (LAM, Marseille)

L.1 Abstract

This Science Reference Observation (SRO) proposes a galaxy redshift and peculiar velocity survey covering up to 24 000 square degrees, i.e., ¾ of the full sky apart from Milky Way. The goal is to measure both the cosmological redshift of about 2 million galaxies and for a subset to obtain the radial peculiar velocity (i.e., gravitational velocity). The survey will measure early- and late-type galaxies up to redshift $z \simeq 0.25$ using the Fundamental Plane and optical Luminosity-Linewidth (Tully-Fisher) techniques. The unprecedented depth of 1 Gpc is significantly deeper than surveys that will be completed in 2025, such as the two Australian southern surveys: the optical multi-fiber TAIPAN and the radio SKA Pathfinder WALLABY survey. This field of research is currently undergoing a revival, and this survey will achieve the same galaxy number density as in the contemporary pioneering proof-of-concept surveys as Cosmicflows-2 and 6DF catalogs, while multiplying the covered universe volume by a factor 150. Only these scales enable strong test of gravitation models.

Three major science goals define MSEv: (i) linear-growth rate of cosmic structures at low red-shift, obtained thru velocity-velocity comparison and the luminosity fluctuation method will be free of cosmic variance. This allows one to discriminate between modified theories of gravity at 1% level and provided a significant complement to the high-redshift constraints provided by the coeval spectroscopic surveys achieved e.g., by PFS-SuMIRe, MD-DESI, Euclid, and WFIRST; (ii) galaxy formation will be investigated in regard to unprecedented velocity-cosmic-web's 6D phase-space; (iii) dynamical tests probing the scale of homogeneity, and test for the backreaction conjecture in General Relativity, potentially providing terms dynamically equivalent to both dark matter and dark energy.

L.2 Science Justification

Galaxy peculiar velocities are direct signatures of the distribution of dark and luminous matter. This cosmological tool is presently the most reliable method for directly probing the structure and dynamics of density fluctuations on scales that have not yet collapsed. The other direct and complementary method is achieved by conducting dedicated weak lensing large surveys. The dynamics of large scale structures will bring insights on the dark-energy/dark-gravity sector and the geometry of the space-time (Sections 0, 0).

Gravitation is multi-scale. Galaxy formation processes can be studies in relation to the velocity cosmic-web as a pivotal application of such a survey (Section 0). The analysis of the extragalactic flows provided by MSEv will give unprecedented insights into the dark matter role on a large variety of scales, such as planes of dwarf galaxies, groups of galaxies, galaxy clusters, filaments,

voids and superclusters.

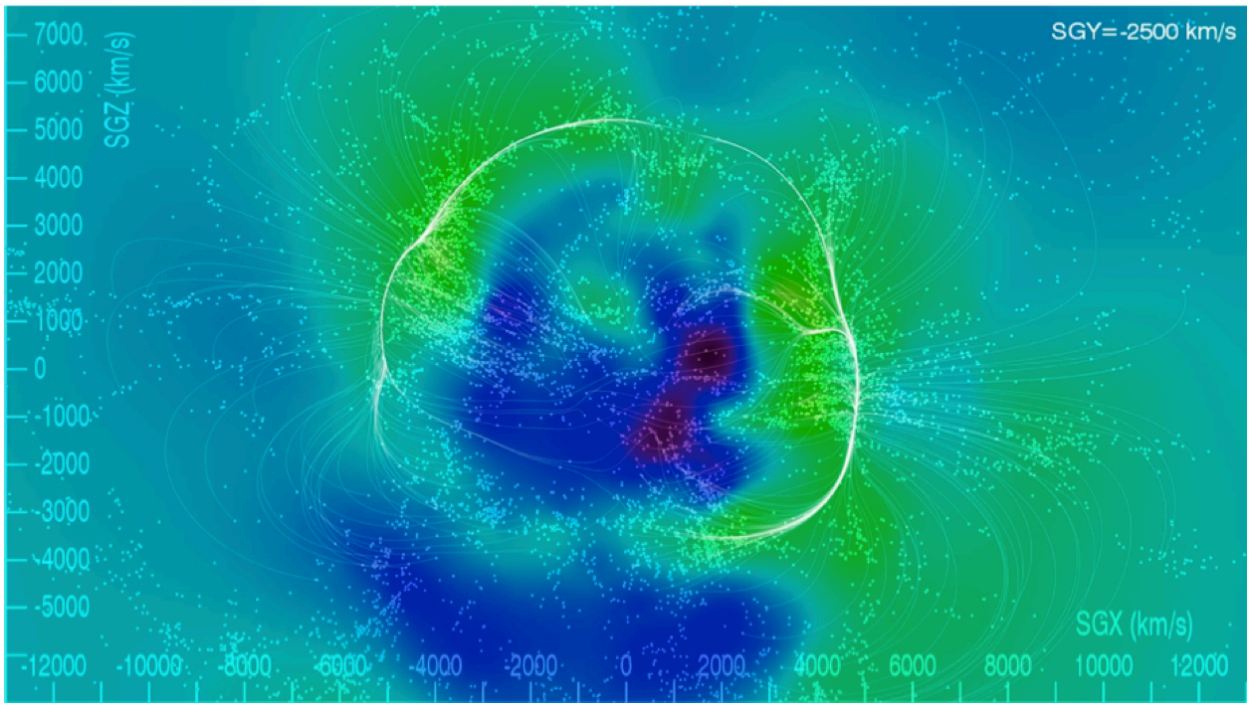

Figure 32: The matter overdensity field δ computed from the divergence field in Cosmic-flows-2 dataset is plotted in color. Galaxies identified by redshift surveys are plotted as white dots. The new technique of defining filaments using cosmic velocity fields give a new insight to the correlation length of galaxies. A filament of coherent motion of matter is half the "Arch" seen running from Perseus Pisces to Pavo-Indus structures in redshift surveys and in the cosmic V-web shear tensor. Only the analysis of watersheds allows one to identify the "splitting" zone of this structure.

L.2.1 Low-redshift growth-rate of structures: velocity-velocity and luminosity fluctuation methods

Redshift space distortions (RSD) are recognized as one of the most promising observable to investigate the theory of gravity, achieved by measuring the linear growth rate f ≡ d ln D+/d ln a of cosmic structures on cosmological scales to identify any departure from General Relativity (e.g. Linder & Jenkins 2003). Recent measurements have been obtained by WiggleZ and VIPERS teams (Blake et al. 2012, Contreras et al. 2013, de la Torre et al. 2013). Though, the standard measurement of RSD based on galaxy redshift surveys probes the power spectrum of the matter density field traced by a (single) biased population of sources and then it measures β = f/b, requiring therefore the knowledge of the luminosity bias of the tracers, b; this technique is further limited by sample variance, especially relevant when dealing with small (local) volumes. Multi-tracer techniques (McDonald & Seljak 2009) or higher-order statistics (Marín et al. 2013) must be used to overcome these problems.

Indeed, the theory of Gravitational Instability (GI) establishes a tight relation between the peculiar motions of galaxies and the underlying mass density fluctuations. The relation involves

the parameters determining the back- ground cosmology and the growth rate of fluctuations. Therefore, GI allows a reconstruction of the peculiar velocity field, which for the MSE redshift survey will be based on a redshift survey of 2 million galaxies. The outcome can be compared with the observed peculiar velocities in MSEv (velocity-velocity comparison). A huge advantage of this comparison is that it completely eliminates cosmic variance. Indeed, in the case of the hypothetical situation of perfect data, just a comparison of a few points suffices to determine the relevant parameters without any assumption about the galaxy bias. This comparison is at the heart of peculiar velocity studies (e.g. Davis et al. 2011), as it provides an assessment of gravity and dark energy theories; see Figure 33. In addition to not being affected by cosmic variance, peculiar velocity surveys are also the ideal framework to investigate primordial non-Gaussianities and general-relativistic (gauge) effects specific of large scales (Jeong, Schmidt & Hirata 2012; Villa, Verde & Matarrese 2014), and to test the scale-dependence of the growth rate of structure, a feature prevalent in modified theories of gravity and clustering dark-energy models (Parfrey, Hui & Sheth 2011; see also the review by Clifton et al. 2012).

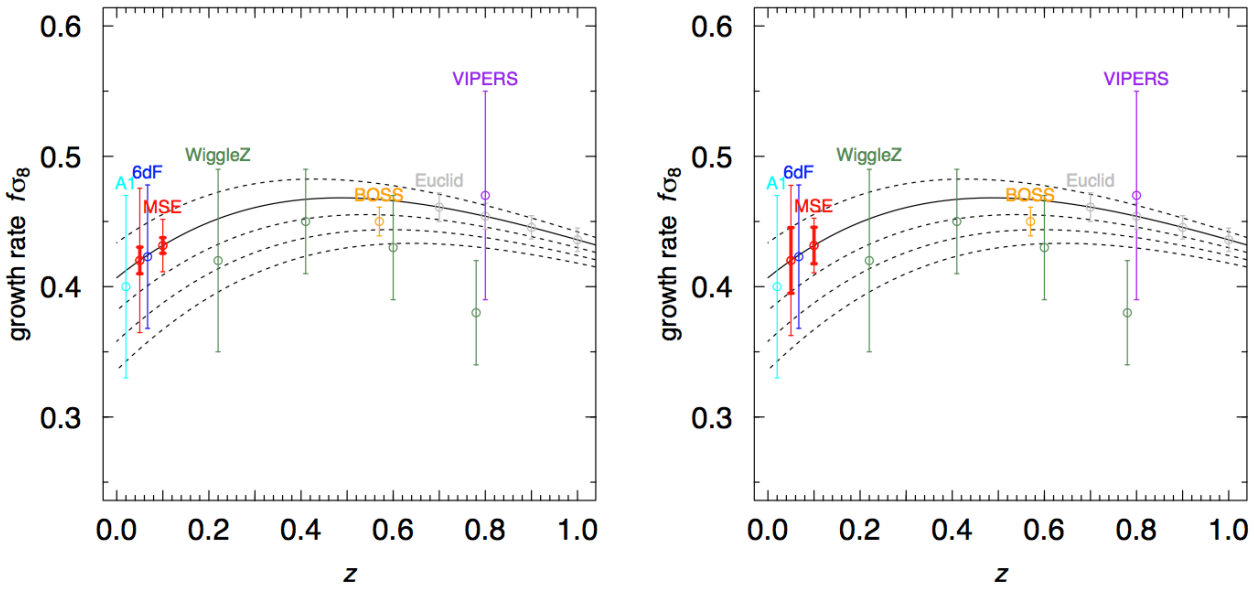

Figure 33: Linear growth rate at low redshift by velocity-velocity comparison — MSE Fisher matrix constraints around the fiducial ΛCDM Planck cosmology (solid line) at redshift z < 0.05 and z < 0.1 for 10,000 deg^2 and galaxy number density n = 0.03h^{3}Mpc^{-3} (left) and n = 0.003h^{3}Mpc^{-3} (right). Thick and thin (red) error bars account for density-only (RSD) and joint density-velocity MSE constraints, obtained using the same number of galaxies. Dashed (solid) lines correspond to f ≈ Ωγm with γ = 0.5, (0.55), 0.6, 0.65, 0.7 downward.

Following Koda et al. 2014 (see also Johnson et al. 2014) for a Fisher matrix forecast, the measurement of $f\sigma_8$ or β from angle-averaged auto- and cross-power spectra of galaxies' density and peculiar velocity can attain arbitrarily high precision; unlike constraints from RSD analysis by redshift surveys, the relative error of these parameters monotonically decreases with the mean number density of sources, n, yielding an improvement by a factor of ~ 5 on current constraints for MSEv. Figure 33 shows how a minimal MSE velocity survey covering 10 000 deg^2 provides the strongest constraint on the growth-rate f ≈ Ωγm, yielding one of the most stringent test of

General Relativity ($\gamma \approx 0.55$) at the level of $\delta\gamma \simeq 0.05$. Similar precision will be attained by future spectroscopic redshift surveys at high-redshift such as PFS-SuMIRe (not shown) and Euclid, which will benefit of a much larger volume but probe the growth-rate in a more challenging regime. **Error! Reference source not found.** shows the Fisher-analysis constraints that can be chieved by a MSE peculiar velocity survey with n = 0.003 h^3Mpc^{-3} and n = 0.03 h^3Mpc^{-3}; relative error can attain 1% level with a deep and large enough survey. It illustrates the benefit of the velocity-velocity comparison made possible by the knowledge of peculiar velocities (smaller, thick error bars in Figure 33) with respect to standard RSD predictions obtained based on the knowledge of the density only (larger, thin error bars).

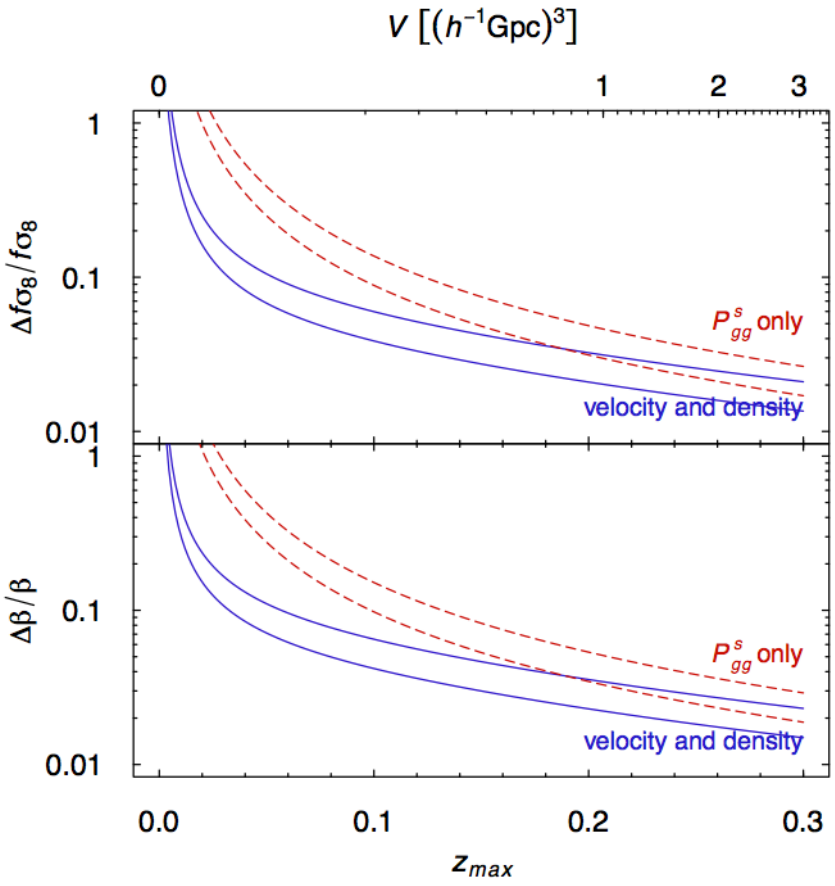

Figure 34: MSE Fisher matrix constraints. Relative error on the rescaled linear-growth-rate β = f/b and on the amplitude of matter fluctuations σ_8 as function of z_{max}, obtained using density-only (RSD; red dashed) and joint density-velocity power spectra (solid blue), for 10 000 deg^2 (upper curves) and 24 000 deg^2 (lower curves), and for galaxy number density n = 0.003 h^3Mpc^{-3}.

Table 4: Fisher matrix constraints on the rescaled linear growth-rate, β = f/b (where b is the linear bias parameter), and on the amplitude of matter fluctuations, σ_8, from density-only (RSD) and joint density-velocity (VEL) power spectra. Results for sky coverage of 10000 deg^2 (marginalization over the other parameters and using the WMAP-9 reference model). Values for the minimal and optimal setup for DSC-SRO-12 are boldfaced.

		$n = 0.003h^3Mpc^{-3}$		$n = 0.03h^3Mpc^{-3}$	
		$d\beta/\beta$	$d\sigma_8/\sigma_8$	$d\beta/\beta$	$d\sigma_8/\sigma_8$
$z < 0.1$	RSD	0.151	0.137	0.145	0.132
	VEL	0.065	0.06	0.024	0.024
$z<0.20$	RSD	0.054	0.049	0.051	0.047
	VEL	0.036	0.032	0.015	0.014
$z<0.25$	RSD	0.038	0.035	0.037	0.033
	VEL	0.028	0.026	0.013	0.012
$z<0.30$	RSD	0.029	0.026	0.028	0.025
	VEL	0.023	0.021	0.011	0.01

One method to obtain tight constraints on the combination fσ8 is to compare the predicted peculiar velocities derived from a galaxy redshift survey with observed peculiar velocities. The comparison gives β = f/b, where b is the bias parameter. Carrick et al 15 show that, with appropriate smoothing, the method is unbiased. If one measures σ8,g from the galaxy redshift survey itself, this can be combined with β to obtain $f\sigma_8$. In Carrick et al. 15, the measurement of fσ8, based on ~ 5000 peculiar velocities with a typical depth of z ~ 0.02, has a precision of 5%. With a much deeper and more comprehensive peculiar velocity and redshift survey from MSE, one might expect to reduce this uncertainty by a factor of ~ 5, yielding a precision of 1%.

MSEv would also allow the application of the luminosity fluctuation method. Spatial variations in the luminosity function of galaxies, with luminosities estimated from redshifts instead of distances, are correlated with the peculiar velocity field. Comparing these variations with the peculiar velocities inferred from the MSE redshift surveys could also be a powerful test of our fundamental cosmological paradigm on cosmological scales. The method has been successfully applied (Feix, Nusser & Branchini 2015, PRL) to the SDSS Data Release 7. An application to MSE with its larger sky coverage and larger number of galaxies should yield results that could be competitive to RSD analysis.

L.2.2 Homogeneity, isotropy, and backreaction conjecture

The cosmological standard model relies on the hypothesis that the Universe is homogeneous and isotropic on large scale, without giving any information about this scale. The theory of primordial inflation (which is incorporated into the ΛCDM model) actually predicts a certain level of density fluctuations on all scales, with a power spectrum of scalar fluctuations which is not scale invariant (ns ≠ 1) but colored (ns) as confirmed by the recent Planck measurements. As a consequence, the transition to the large-scale homogeneity and isotropy is expected to be gradual, attaining the level δΦ/c2 ≃ 10−5 at the epoch of last scattering, as inferred from the cosmic microwave background (CMB) radiation. At redshift z ≃ 1100 the large-scale homogeneity is well supported by the high degree of isotropy of the CMB (Fixsen et al. 1996), under the hypothesis of the cosmological Copernican principle.

At low redshift such symmetries are less evident. As for the isotropy, using hard X-ray data from the HEAO-1 A-2 experiment, Scharf et al. (2000) demonstrated how the dipole anisotropy of the distant X-ray frame (z ≃ 1) can constrain the amplitude of bulk motions of the universe, probing evidence for a mild anisotropy that indeed could be of Galactic origin. In the local universe, the recent analysis of peculiar velocity data (Hoffman, Courtois & Tully 2015) estimated the bulk flow of the local flow field probing that it is dominated by the data out to $200h^{-1}$Mpc and that it is consistent in the X-Y supergalactic plane with the CMB dipole velocity down to a very few km/s, as recovered by the Wiener filter velocity field reconstructed from the radial velocity data. With a volume 150 times larger than that currently probed, thus largely encompassing the homogeneity scale, the MSEv survey will be unique in answering the question of whether the cosmological bulk flow exists on 800 Mpc scales, as found by some of the cluster studies.

Isotropy itself is not sufficient to deduce homogeneity, unless probing it as a function of flux or redshift. Based on simple counting of sources in three-dimensional regions in order to estimate the fractal (Minkowski-Bouligand) dimension and its departure from the Euclidean value D2 = 3, Hogg. et al (2004) assessed the homogeneity scale for the LRG sample from the SDSS at ~ $70h^{-1}$ Mpc in the redshift range 0.2 < z < 0.4. This value has been confirmed by WiggleZ data (Scrimgeour et al. 2012), proving the transition to the large-scale homogeneity around ~ 70 − $80h^{-1}$ Mpc at redshift z = 0.2 − 0.8, with un upper bound around $300h^{-1}$ Mpc. This value is consistent with fractal analysis, anomalous diffusion and Shannon entropy methods based numerical-simulation-based studies (e.g. Yadav, Bagla & Khandai 2010, Kraljic 2014, Pandey 2013). The most important implication of inhomogeneity is the long-standing “averaging problem” in General Relativity (Ellis 1962), accounting for the role of (small-scale) perturbations on the expansion rate of the spacetime once they enter the nonlinear regime. Whilst in Newtonian cosmology, at the linear order, their effect vanishes on average by construction, in full GR the density fluctuations potentially should have some backreaction effect on averaged quantities; according to the Buchert formalism (Buchert 2000, Ellis & Buchert 2005) they drive new effective source terms in the Friedmann-like equations accounting for the expansion rate of every domain D over which averaged quantities are calculated. A unique cosmological application of peculiar velocity surveys is the direct measurement of the so-called kinematical backreaction term, QD = Var[div v] − 2/3⟨σ2⟩, the mean and variance being calculated over the domain D (here σ2 is the amplitude of the shear velocity tensor); depending on its sign, this

term is dynamically equivalent to dark matter (on small/galactic scales) or to dark energy (on large/cosmological scales). In the era of precision cosmology, aiming at validating or disproving the cosmological standard model and the theory of General Relativity, a quantitative measurement of this quantity is mandatory; a not-vanishing value would definitely indicate the necessity to revisit the standard FLRW model. A peculiar velocity survey provide the genuine key ingredient to probe this concept; as long as the velocity field in redshift space is irrotational, and so may be derived from a velocity potential (e.g. Nusser & Davis 1994), one can directly infer the kinematical backreaction term by measuring the Minkowski functionals of the velocity fronts defined by the excursion-set of the velocity potential (Buchert 2008). Because of the limited size of existing velocity surveys, this program has not been addressed on real data. Instead, with a velocity survey such as MSEv, owing to its large volume, the calculation is expected to yield robust enough results to assess the backreaction conjecture.

L.2.3 Cosmic-web dynamics and galaxy formation

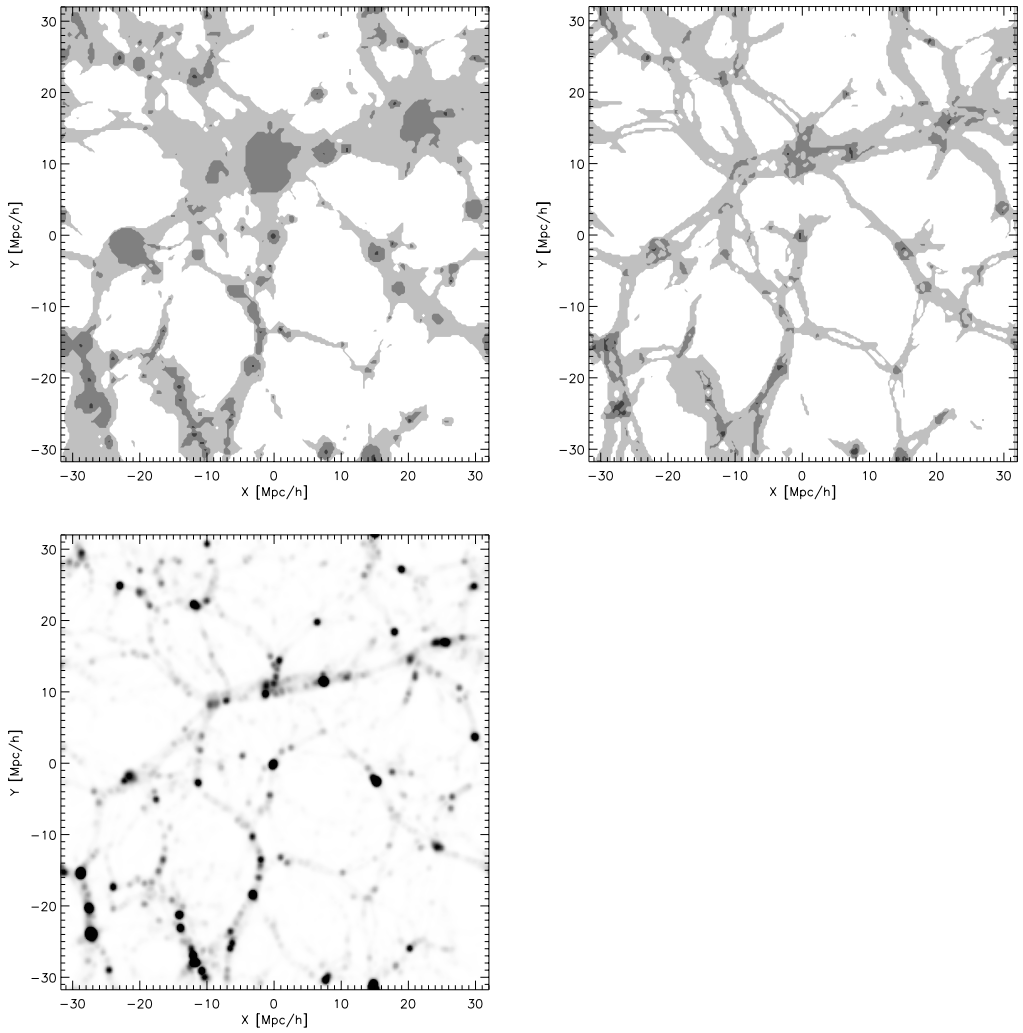

Figure 35: Cosmic-web components (voids, filaments, sheets, and knots in white, light gray, dark gray, and black, respectively) obtained from the velocity shear tensor (top left, the V-web) and gravitational tidal tensor (top right, the T-web). The latter, reconstructed from the density field (bottom panel), allows ~ 10 times lower resolution scale. *(Figure adapted from Hoffman et al. 2012).*

With an accurate measurement of the peculiar velocities, one could apply the method devised by Hoffman and collaborators (2012) to reconstruct the velocity-based cosmic web, or V-web, whose components (sheets, filaments, knots, and voids) are cinematically identified by the local value of the eigenvalues of the velocity shear tensor. Based on N-body simulations (see figure 1), this technique has been proven to resolve cosmic structures down to $<\sim 0.1h^{-1}$ Mpc, providing much more details than a similar classification algorithm based on the gravitational tidal tensor obtained from the density field (dubbed T-web; Hahn et al. 2007, Forero-Romero et al. 2009), which allows one to achieve only ~ $1h^{-1}$ Mpc resolution scale. The higher resolution can be explained by the slower evolution of the velocity field away from the linear-regime than

the density field, which retains less memory of the initial conditions.

Exploiting the high-resolution spectroscopic capabilities of MSE, the knowledge of the V-web further provides a platform to investigate the tidal torque theory, the alignment of the galaxy spin to the cosmic-web filaments, and the segregation of galaxies and halos with respect to their environment and dynamics.

L.2.4 Comparison with competitive optical-NIR fibre-fed MOS

The table hereafter shows what instrumental capacities are currently or will be available before MSE. No adequate setup exist or is planned that satisfy the requested large field-of-view, large mirror, multi-target and mini-IFU high resolution spectroscopy.

Project	Hemisphere	Telescope M1 diameter (m)	FoV	Fibres (fibres/deg^2) [#IFU×# fibres]	Spectroscopic resolution	First light
Subaru/FMOS	N^+	8.2	?	?	2000	ongoing
Keck-II/DEIMOS	N^+	10.4	?	?	?	ongoing
VLT/FLAMES...	S	8.2	25 arcmin^2			ongoing
...GIRAFFE				$\leq$ 130 (18720)	10000 or 25000	
...UVES				$\leq$ 8 (1150)	47000	ongoing
Mayall/DESI	S	3.8	8.04 deg^2	5000 (621)	2000-5500	2018
Subaru/PFS-SuMIRe	N^+	8.2	1.78 deg^2	5000 (621)	2000-5000	2017
VISTA/4MOST	S	4	7.1 deg^2	3000 (423)	3000-5000	2017-18
VLT/MOONS	S	8.2	0.14 deg^2	500 (5371)	3000-20000	2017
WHT/WEAVES	S	4.2	3.14 deg^2	1000 (318)	5000-20000	2018
GTC/MEGARA	N	10.4	12.24 arcmin^2	94 bundles (?)	5000-17000	-
HET/VIRUS	N	10	19.63 deg^2	34944(1780) [78 IFU×448 f.]	700	2015
HET/HETDEX	N	9	0.108 deg^2	33350(309,000) [145 IFU× 230 f.]	1000	2011
WFIRST-AFTA	space/deep	2.4	3 × 3.15 arcmin^2	IFU ?	70	-
WFIRST-AFTA	space/wide	2.4	0.281 deg^2	?	?	-
MSE	N^+	11.6	1.5 deg^2	4000(2666) [571 IFU×7 f.(lin)] [800 IFU×5 f.(lin)] [72 IFU ×37 f.(hex)] [140 IFU×19 f.(hex)]	2000-6500-40000	2025

L.2.5 Comparison with other modern galaxy velocity surveys

Future peculiar velocity surveys include the Transforming Astronomical Imaging surveys through Polychromatic Analysis of Nebulae (TAIPAN), a successor survey of 6dFGSv planned to begin in 2015 and using the UK Schmidt Telescope with upgraded fiber-fed spectrograph to improve the velocity dispersion measurements. It is expected to extend the upper limit of 6dFGSv up to z ≃ 0.1 and increasing the number density by a factor of ∼ 20 by decreasing the velocity dispersion

from 116 kms^{-1} for 6dFGSv to 70 kms^{-1}, collecting 500 000 redshifts over about ¾ of the sky with magnitude r < 17 and K < 14, of which 50 000 early-type galaxies peculiar velocities with magnitude J < 15.15.

At about a similar depth but in the radio domain, a planned HI survey with the Australian SKA Pathfinder (ASKAP), WALLABY (Johnston et al. 2008, Koribalski & Stavely-Smith 2009, Duffy et al. 2012), will probe the mass and dynamics of over 600,000 emission-line galaxies over 3π steradians up to z ≃ 0.15, and is expected to yield the peculiar velocities of 50 000 spiral galaxies. A similar HI survey is currently discussed in the northern hemisphere named WNSHS (Duffy et al. 2012). It would cover π steradians and achieving slightly deeper magnitude, and is expected to produce ~ 0.8 millions redshifts and 32 000 velocities.

MSE would supersede even the ensemble of all these surveys in the size of the surveyed volume of universe, and in the number of galaxies measured. Its large redshift extent allows one to measure not only a cosmological parameters (for example the growth rate of structures), but the variation of these during the last 3 billion years. This will allow real physical understanding of the forces at play.

L.3 Key astrophysical observables

Successful fundamental plane measurements are demonstrated for galaxies up to redshift z > 1 (Van DoKkum and Stanford 2002) with typically a total of 4 exposures of 1800 seconds with the LRIS Double Spectrograph on the Keck I Telescope, using a 1 arcsec slit. More recently, the fundamental plane of EDisCS galaxies was studied for galaxies in groups, clusters and in the field up to z = 0.9 (Saglia et al. 2010 A&A 524,A6) achieving an accuracy on the internal effective velocity dispersion σ_e of 10%. The spectra were obtained with multi-object mask spectroscopy using the FORS2 instrument at the VLT. The central wavelength was 6780 with resolution FWHM ≈ 6).

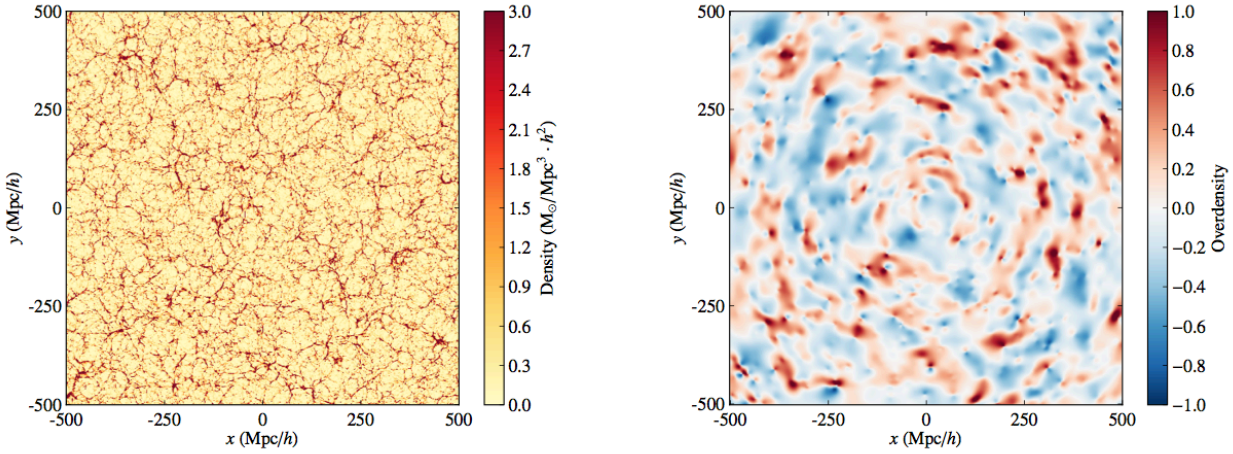

Figure 36: Multidark cosmological simulation used here as a mock MSEv survey. Left: L = $1h^{-1}$ Gpc (38403 particles, Planck 1 cosmology). Right: test of the density reconstruction by Wiener filtering method, based on 40 000 radial peculiar velocities with 10% accuracy.

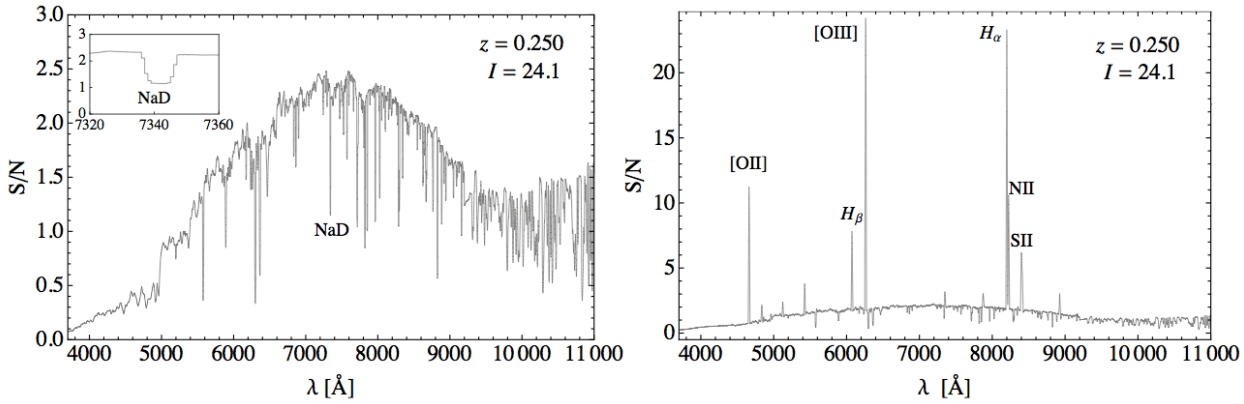

Figure 37: Synthetics spectra of an elliptical galaxy (left panel; centered on the NaD absorption line) and for a spiral galaxy (right panel; centered on Hα and [OIII] lines) at z ≃ 0.25 with apparent magnitude I = 24.1, as computed with the MSE exposure time calculator setting one hour exposure-time at mid-resolution and for effective 11.4 m primary mirror.

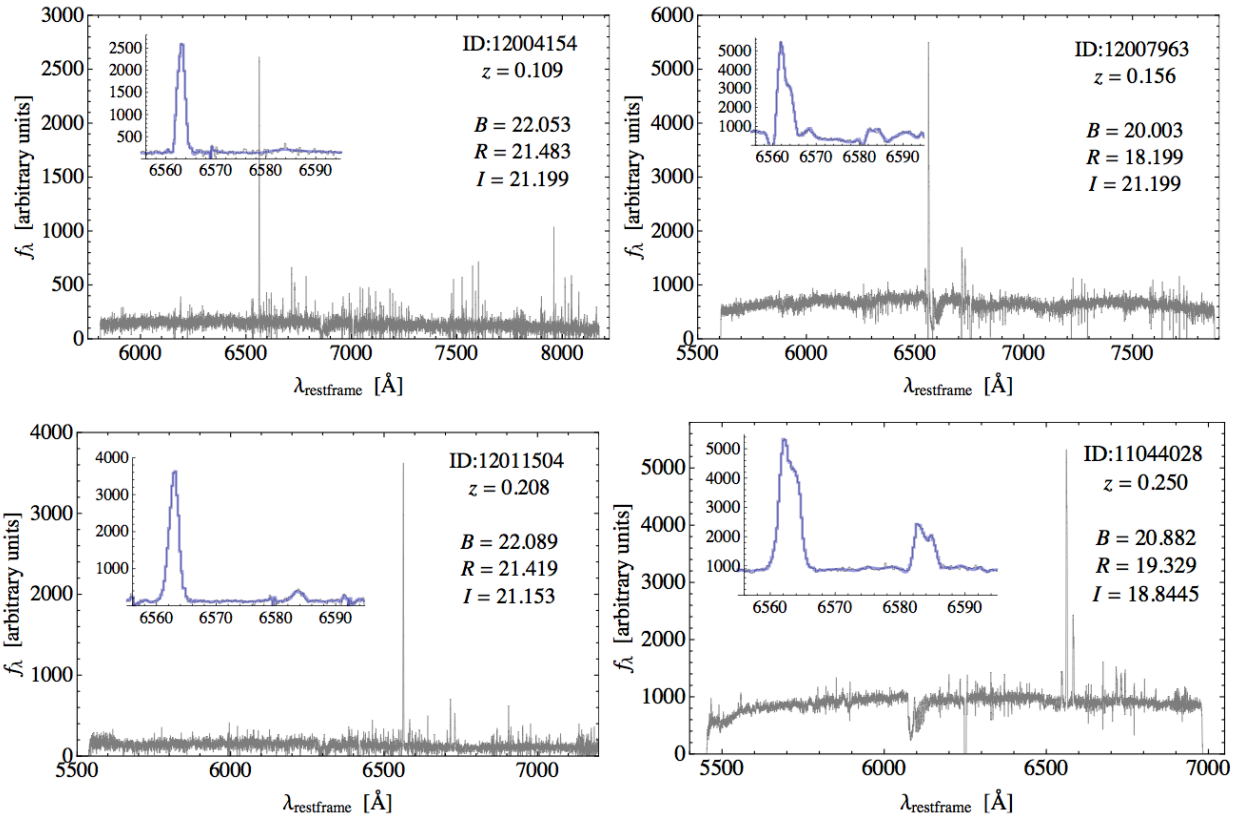

Figure 38: Keck-II (Deep 2) spectra of galaxies for TF distance measurement at z = 0.11, 0.16, 0.21, 0.25 obtained with long slits DEIMOS spectrograph (resolution λ/Δλ = 4000, one-hour exposure-time). The zoom panels show Hα (λ6563) and [NeII] (λλ6583-6585) emission lines.

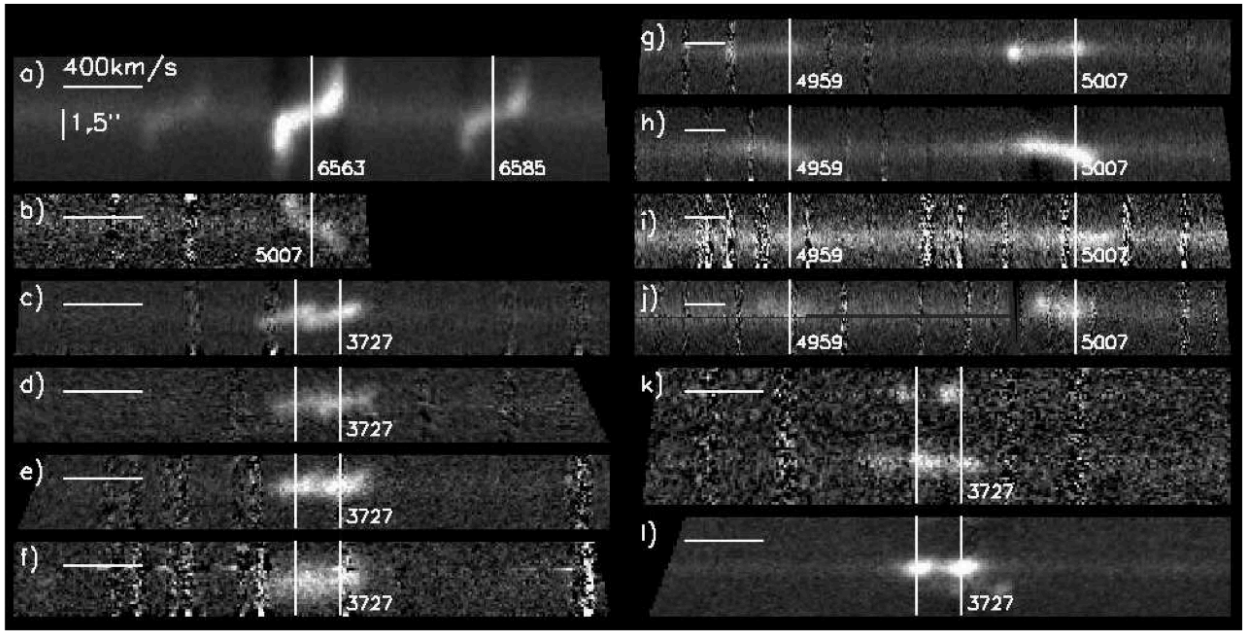

Figure 39: Keck-II Deep 2 interesting or unusual two-dimensional spectra obtained measured with DEIMOS at λ/Δλ ~ 6000 spectral resolution. The horizontal line corresponds to a rest-frame velocity of 400 km s−1 in all cases. Spectra (a)-(f) show rotation curves and/or broadened spectral lines ; objects like (a) would represent the optimal target for MSEv

Kinematics of nearby early-type galaxies are usually determined from the spectral region containing the strong Mg b line at 5172 Å (e.g., Davies et al. 1987; Lucey et al. 1991; Jørgensen, Franx, Kjærgaard 1995b; Mehlert et al. 2000).

- Required key measurement of the source spectrum:
  Redshift and Width of some principal emission and absorption lines from optical-NIR (3900-8600 Å: Hα, [OIII], [OII], [NII], Hβ, [SII]; NaD).
- Accuracy of the measurement:
  - FP method: similar spectral resolution as TAIPAN, i.e. 30 km/s rest-frame (still viable option is < ~60 km/s rest-frame).
  - Optical TF methods (see below): as in radio surveys, i.e. 4 km/s rest-frame (still viable option is < ~30km/s rest-frame).
- Standard or envisioned technique for extracting the information from the data:
  - Standard technique: FP method, based on measurement of stellar radius and velocity dispersion of early-type galaxies; it requires mid-resolution spectra and precision photometry (see section 4). This technique could be applied with single-fibre spectrograph, although a mini-IFU is preferred.
  - Envisioned technique: baryonic Tully-Fisher (bTF; Zaritsky, Courtois et al. 2014) and optical Tully-Fisher (oTF, to be implemented), allowing the use of late-type galaxies. The successful measurement depends on signal-to-noise > ~5. TF techniques are traditionally applied using long-slit spectrographs; alternatively, fibre- fed multi-IFUs may provide the necessary setup. For instance, linear fibre-

bundles with 5 (minimal requirement) or 7 fibres can simulate long-slits, to be further aligned on the major kinematical axis of each pointed galaxy in the field-of-view. A better option would be provided by hexagonal 19-fibre bundles (minimal requirement) or 37-fibre bundles (optimal requirement; see figure 9), which do not require any alignment while assuring an optimal measurement of the velocity dispersion. This technology is developed for instance by Thorlabs Inc. (http://www.thorlabs.com), including round-to-round, round-to-linear, and linear-to-linear multimode fibre bunldes as long as 19-fibres bundles with common end mapped to a 10-fiber leg and a 9-fiber leg; see figure 10. The accurate determination of inclination of late-type galaxies will be of capital importance for the determination of rotational velocity. A standard approach is based on photometry. Alternatively, assuming that the emission comes from a thin planar disk in circular motion around the galaxy center, we can select the deprojection angles that minimize the departures from such a flow, eventually apply the so-called kinemetry technique (Krajnovic 2006; MNRAS 366, 787). This method is particularly well adapted for HI kinematics, which covers the whole galaxy disk. We foresee to use the same technique with optical mini-IFU, in order to obtain better estimates than the one measured with photometric data as demonstrated by recent surveys like Atlas3D (Cappellari 2008, MNRAS 390, 71).

L.4 Target selection

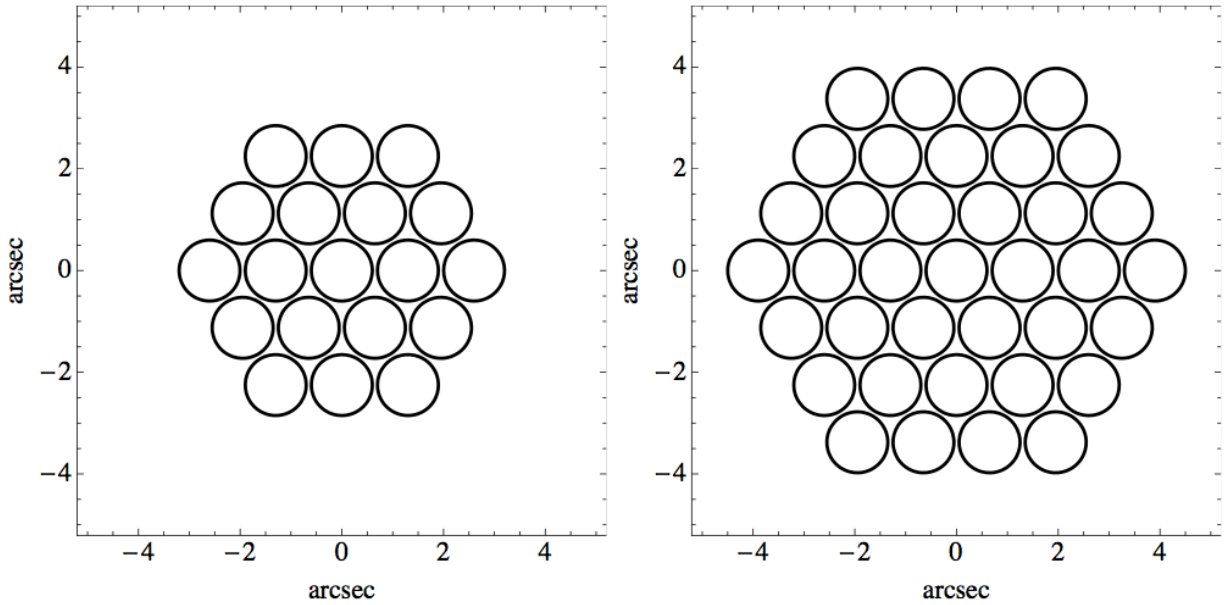

Figure 40: Hexagonal 19-fibre bundles (minimal requirement) or 37-fibre bundles (optimal requirement;with single fibres of diameter less than 1.2" (1.3" with cartridge). Linear fibre-bundles with 5 or 7 fibres would require a dedicated, object-by-object alignment along the photometric maximum axis of galaxies.

Figure 41: Multimode fibre bundles by Thorlabs Inc.

Pre-imaging data for target selection will be likely provided by Pan-STARRS, CFIS, and Euclid (all sky wide survey), and by LSST and DES for Dec < 30 degrees. Photometric zero-points must be controlled at the level of millimags. Photometry in i band is preferred.

The recommended magnitude limit are r < 24.5, i < 24.5, J < 15.2 (J-band similar to TAIPAN). Though, to estimate the number of targets we used the same numbers as in the SRO lead by Aaron Robotham (z < 0.25; covered area 24,000 deg2; absolute magnitude Mi < −21.3, i.e. M_* galaxies and brighter): i < 24.1: 2.3M galaxies , i < 25.3: 2.7M galaxies. And compared also to number counts as in SDSS (see **Figure 42** and **Table 5**).

A M_* galaxy at z = 0.25 with typical size of 30 kpc subtends an angle of 7.7”, corresponding to 8 fibers of 0.9” along the major kinematical axis (optimal), 7 fibres of 1.1” (minimum), or 6 fibres of 1.2” (worst). Using 19- or -37-fibre bundles (corresponding to 5 and 7 fibres along the major axis, respectively) on both spirals and ellipticals, one can reach for the full mapping of the dynamics of the galaxy and measure the velocity dis- persion at the effective radius for ellipticals, allowing for an excellent measurement of bTF for spirals and fast rotators.

The best option (24 000 deg^2) will give 96 galaxies/deg^2, or 144 galaxies/MSE-FoV. This corresponds to 144 × 19 = 2736 (144 × 37 = 5328) fibres per MSE FoV, or 43 millions (85 millions) spectra over the full coverage.

As seen with **Figure 37**, 1 hour exposure time leads to a Signal to noise ratio of about 20 in emission line late-type galaxies and SNR of about 2 in absorption line early type galaxies. 16,000 pointings are necessary to cover the 24,000 deg2. A ratio 4:1 is acceptable in terms of redshift and peculiar velocity share of measurements respectively. Redshifts can be measured in 15 minutes exposure time.

Total survey time: 12,000 × 15 minutes + 4,000 × 1 hour = 7000 hours = 875 nights = 4 years of dark and grey time.

24000/1.5= 16,000 FOV. 77 spirals : 10 minutes (S/N=20 in 1 hour) 77 ellipticals : 1 hour (S/N=2 in NaD)

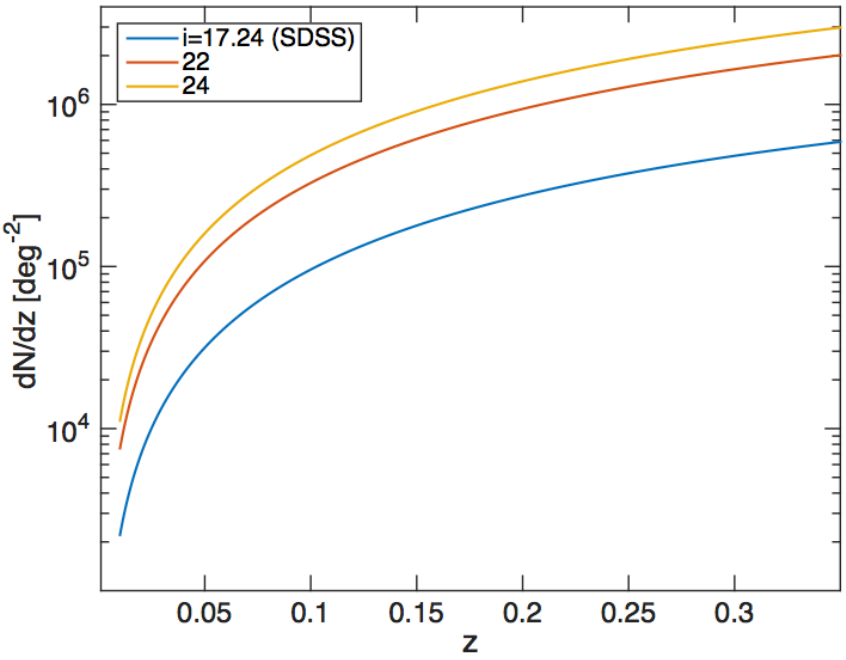

Figure 42: Number of galaxies from a Schechter function, no K-correction applied. For an SDSS type survey and for MSEv survey.

Table 5: Number of galaxies from a Schechter function, no K-correction applied. For an SDSS type survey and for MSEv survey, see Figure 11.

Mag limit	N ($z \leq 0.1$)/deg^2	N ($z \leq 0.25$)/deg^2
i=24	2 x 10^4	2 x 10^5
i=22	1.3 x 10^4	1.4 x 10^5
i=17	3799	3.4 x 10^4

- Source density: Best option: mean number density of peculiar velocities n ≈ 0.03h3Mpc−3 (2500 gal/deg2 for 24,000 deg2) allowing an improvement by a factor ≈ 3 on cosmological parameters (see table 1). Minimal viable option: mean number density of peculiar velocities n ≈ 0.003h3Mpc−3, with even distribution across sky, covering

10,000 deg2 (1000 gal/deg2 for 10,000 deg2).

- Total number of science targets required to be observed to enable science goal: Best option: about 2.5M L* galaxies over 24,000 deg2 with i < 24.1.

L.5 Cadence and temporal characteristics

- Repeat observations are required only for "high value objects". A spectroscopic success rate as large as 80% should be achieved by adequate exposure time for each field of view. Largest possible sky coverage is preferred in order to minimize the cosmic variance impact on cosmology measurements.
- There are no specific issues relating to the timing of the observations.

L.6 Calibration requirements

- Wavelength calibration: standard.
- Sky subtraction: standard (using fibres on sky).
- Flux (spectro-photometric) calibration: using standard stars.
- Telluric absorption: standard.
- The removal of instrumental signatures can be done using standard procedure.
- From standard spectra the following astrophysical quantities will be measured: redshift from emission lines and continuum (Balmer break), velocity dispersion from width of absorption and emission lines.
- Pan-STARRS, CFIS, Euclid, WISE, LSST would assure the necessary high-precision photometry of MSE sources; TMT could also assure the follow-up of the faintest MSE targets.

L.7 Data processing requirements

- The desired deliverables to the science team includes raw data and wavelength calibrated spectra.

L.8 Any other issues

This proposal is an ongoing and evolving piece of work. We are aware of some studies and tests that are currently missing.

- Reducing the error on peculiar velocities:
  Errors are proportional to distance from the observer, a 15% error at z=0.15 (45,000 km/s) translates into an error of 6750 km/s on a measurement of the order of 500 km/s. Innovative data grouping procedures are currently devised in the literature. Grouping an ensemble of 100 galaxies lying at a similar distance would decrease the error by a factor 10. This could be tested with mock catalogs from a cosmological simulation.
- 3D reconstruction of density and velocity fields:
  In this document, as a preliminary test we tried to simulate a mock MSEv 3D reconstruction using 40,000 peculiar velocities at 10% accuracy, randomly located

within the 1 Gpc volume. This is our current computation limit. The input capacity of the analysis code will be enlarged in the coming months, enabling more realistic realizations of MSEv mock studies.

- Accurate number of targets and observational strategy:
  The survey is bimodal with short exposure times and low signal to noise required for redshift measurements, and long exposures of typically 1 hour for peculiar velocity line-width measurements. Short exposures can be accommodated by single fiber spectroscopy. Line-width 3D spectroscopy require mini-IFU setups. The observational strategy needs to be think through in more depth and also devised in regard to the other proposed SRO's, with possible "piggy-back" strategy.
- Continue discussing upcoming possible facilities for this type of survey (none that we know at the moment):
  - MANGA (SDSS) goes to z=0.03, they will do 4,000 square degrees. 17 bundles of fibers in 7 square degrees, they will do R 2000, 3 hour with dithering S/N per fiber : 5-10 at 1.5 Re. Dates of survey : 2015-2020. 10,000 galaxies resolution primary targets : only M > 109 for very nearby peculiar velocity.
  - PFS will do 0.8 < z < 2.4 : redshifts for BAO 8.2m Subaru telescope, for a few million of galaxies. 2,000 galaxies at once per field for a total 1400 square degrees. No peculiar velocity survey.
- First light or second light survey:
  (1) main goal = pec vel survey with fiber bundles + redshift survey from single fibers, (2) if not possible for the first light, let use first-light facilities to measure redshifts, identify sources to be followed-up with fiber bundles during second-light, (3) if first-light capabilities include too few mini-IFU, use them as benchmark as validation of method.